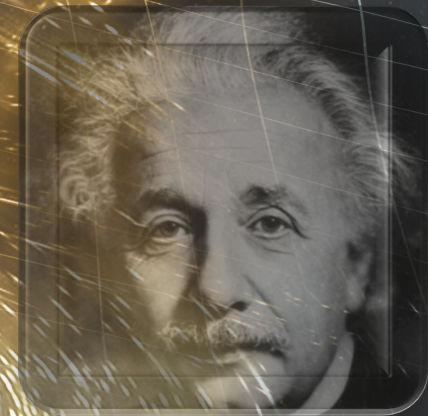


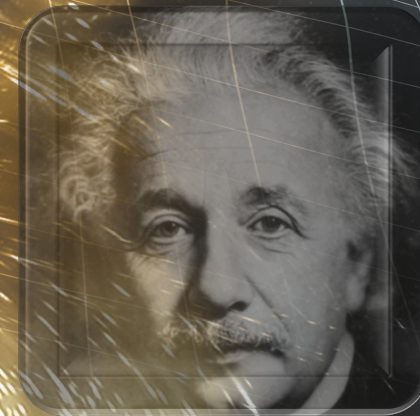
GW Astronomy results to date and prospects, Current and future GW detectors – sensitivity they achieve and how they do it, Astrophysical requirements and benefits of calibration accuracy



Prof Stefan Hild,
University of Glasgow, UK



GW Astronomy results to date and prospects, Current and future GW detectors – sensitivity they achieve and how they do it, Astrophysical requirements and benefits of calibration accuracy

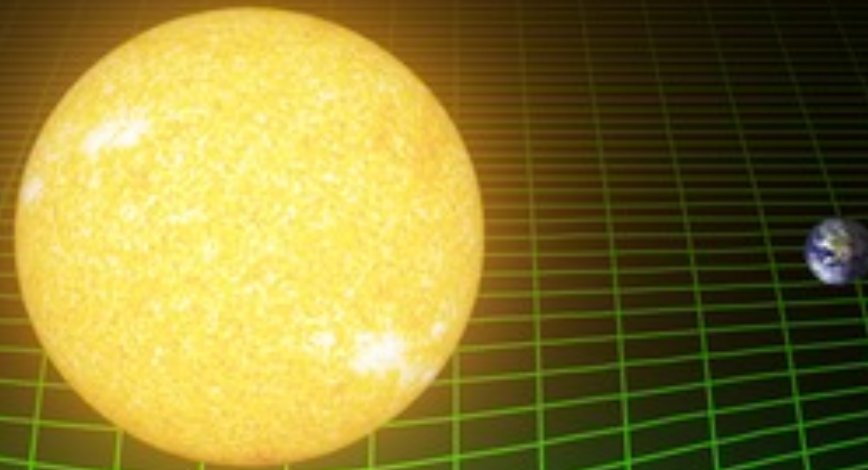


Prof Stefan Hild,
University of Glasgow, UK



Theory of General Relativity

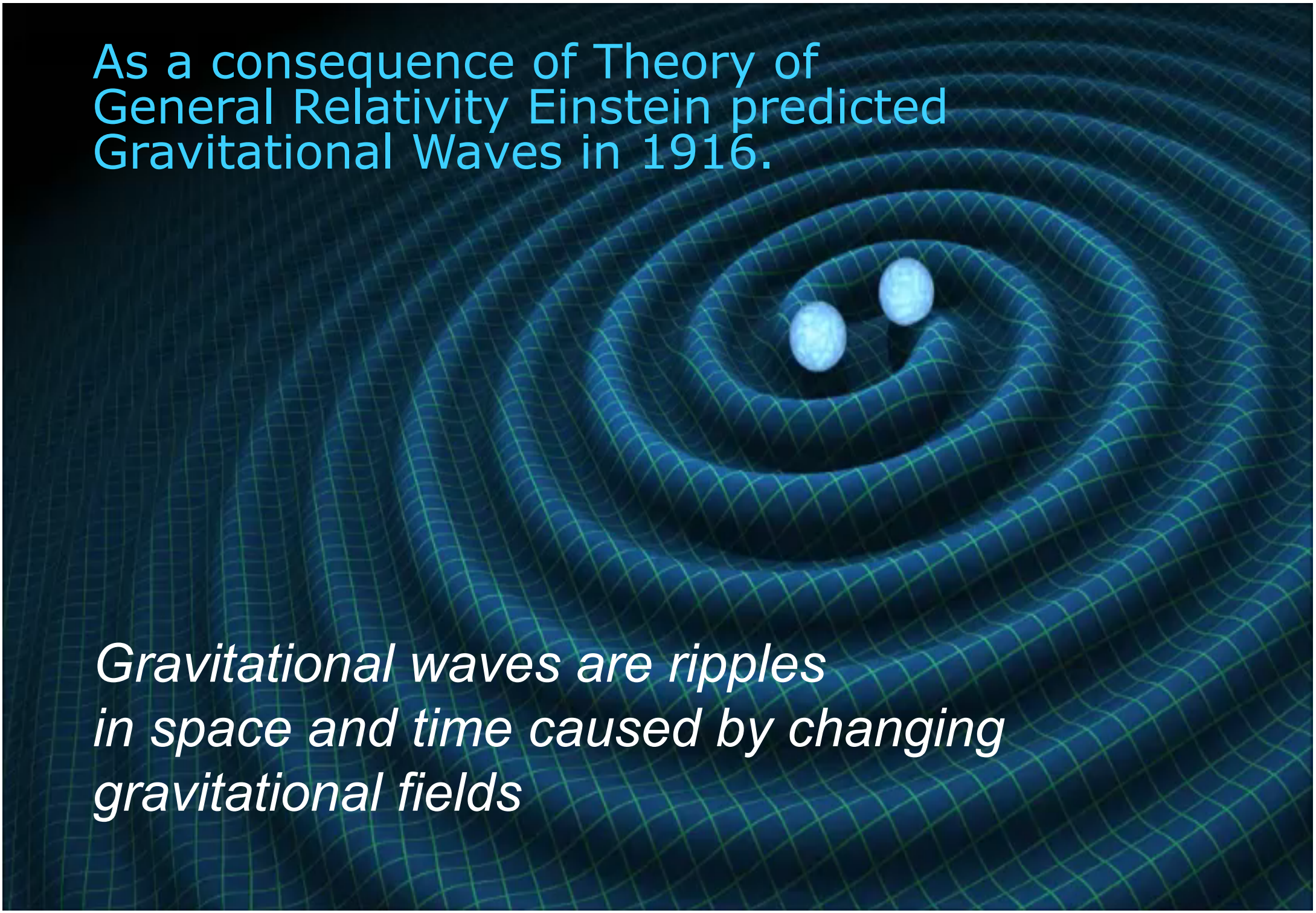
*Newton described Gravity quite well, but
But how does the Earth know to orbit the Sun?
How does gravity act at a distance across space?*



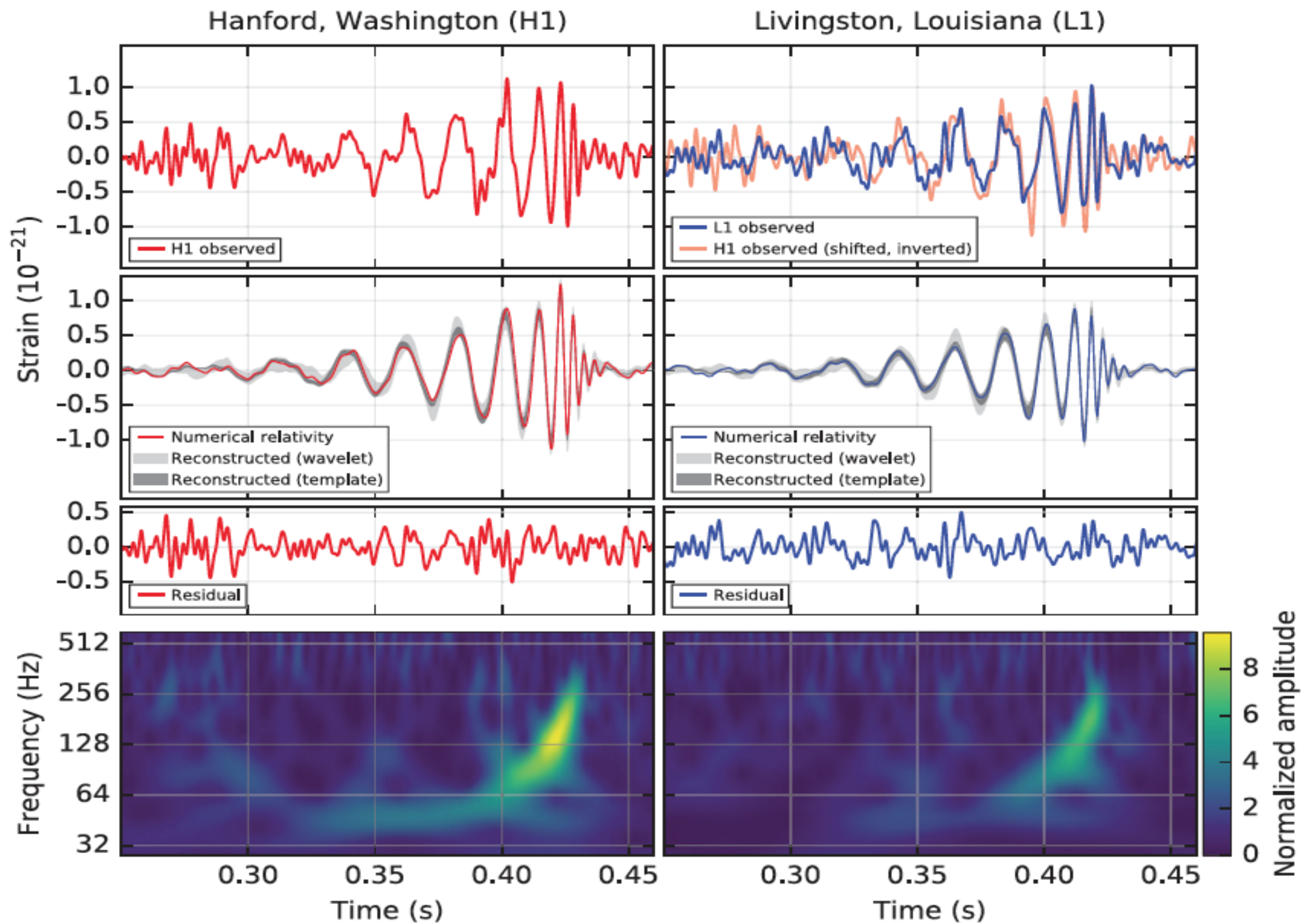
*“Spacetime tells matter how to move,
and matter tells spacetime how to curve”*

As a consequence of Theory of General Relativity Einstein predicted Gravitational Waves in 1916.

Gravitational waves are ripples in space and time caused by changing gravitational fields



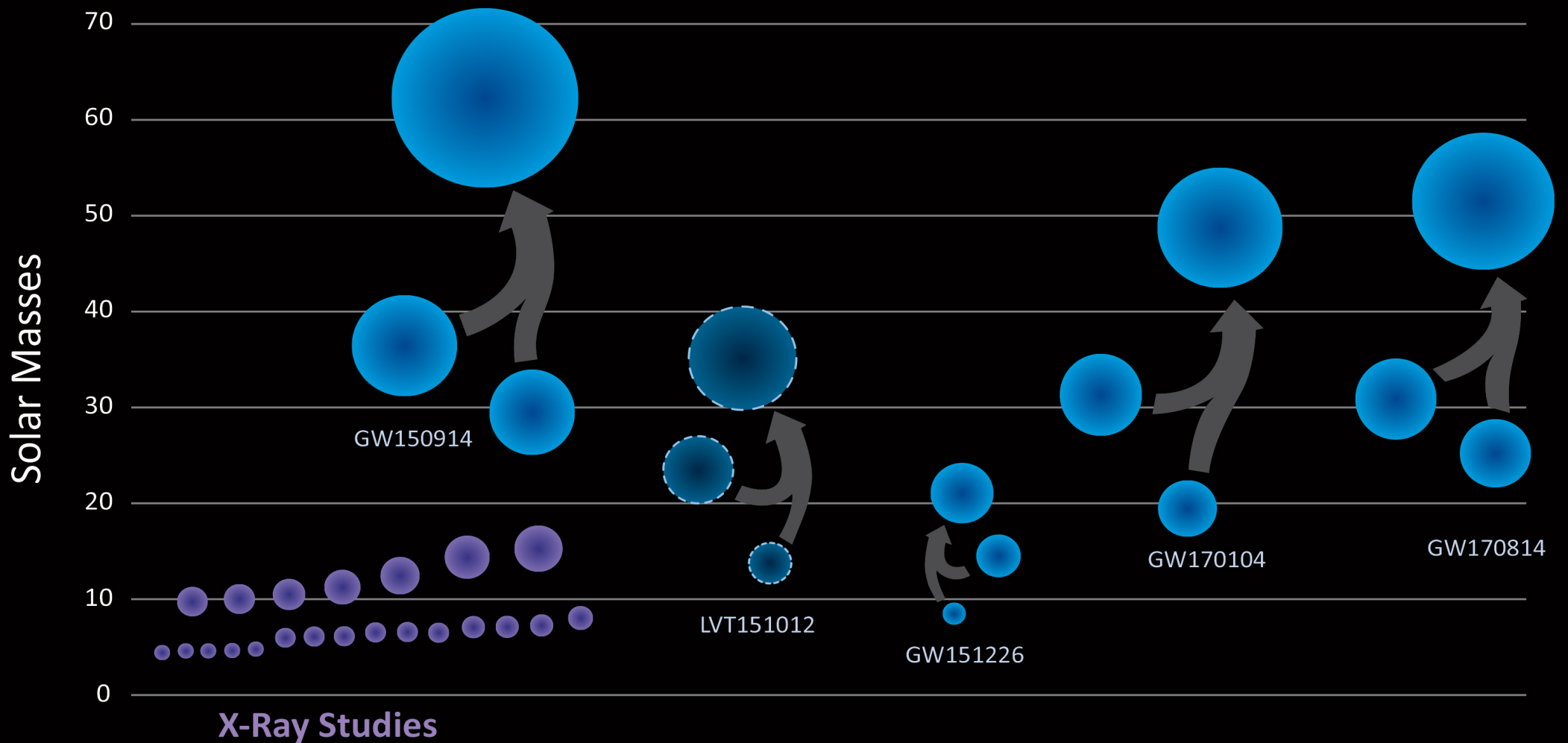
**A LONG TIME AGO
IN A GALAXY FAR,
FAR AWAY**



The Discovery

- First direct detection of Gravitational Waves
 - First indirect confirmation by Hulse-Taylor binary system (1993 Noble prize)
- First direct measurement of a black hole
 - Inferred from ringdown signal [and not from observing gas (X-ray binary) / stars (galactic center) around a blackhole]
- First direct measurement of a binary black hole
 - Only possible with GW observation
- First observation of heavy stellar mass black holes
 - So far no evidence for blackholes with mass between 20 and millions of solar masses
- Most luminous event ever observed:
 - For short period 50 more energy emitted than the observable Universe

Black Holes of Known Mass





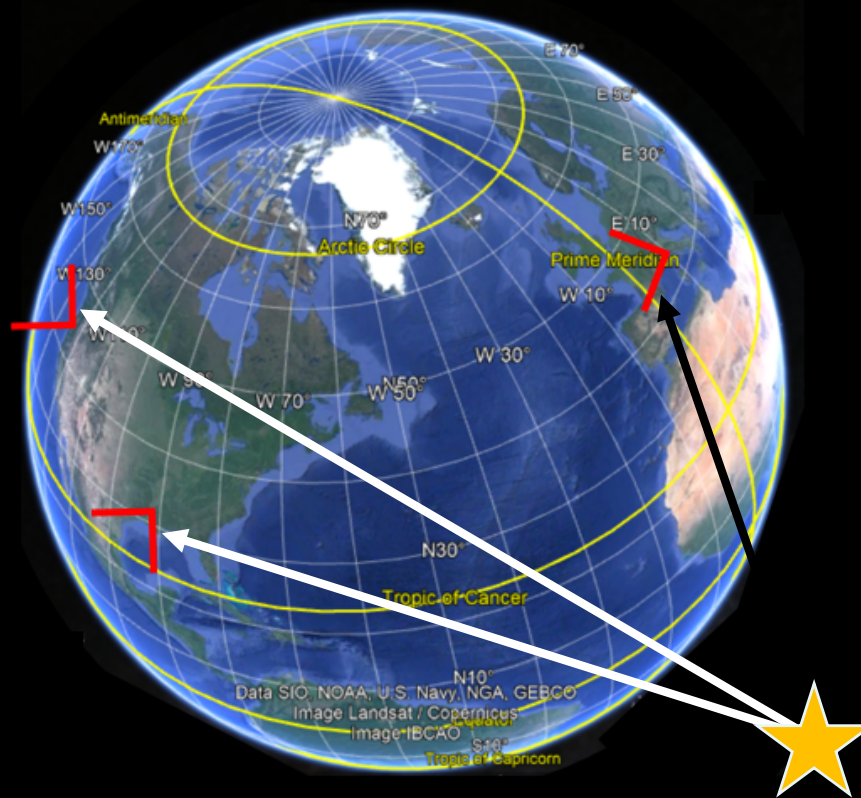
Virgo, Cascina, Italy



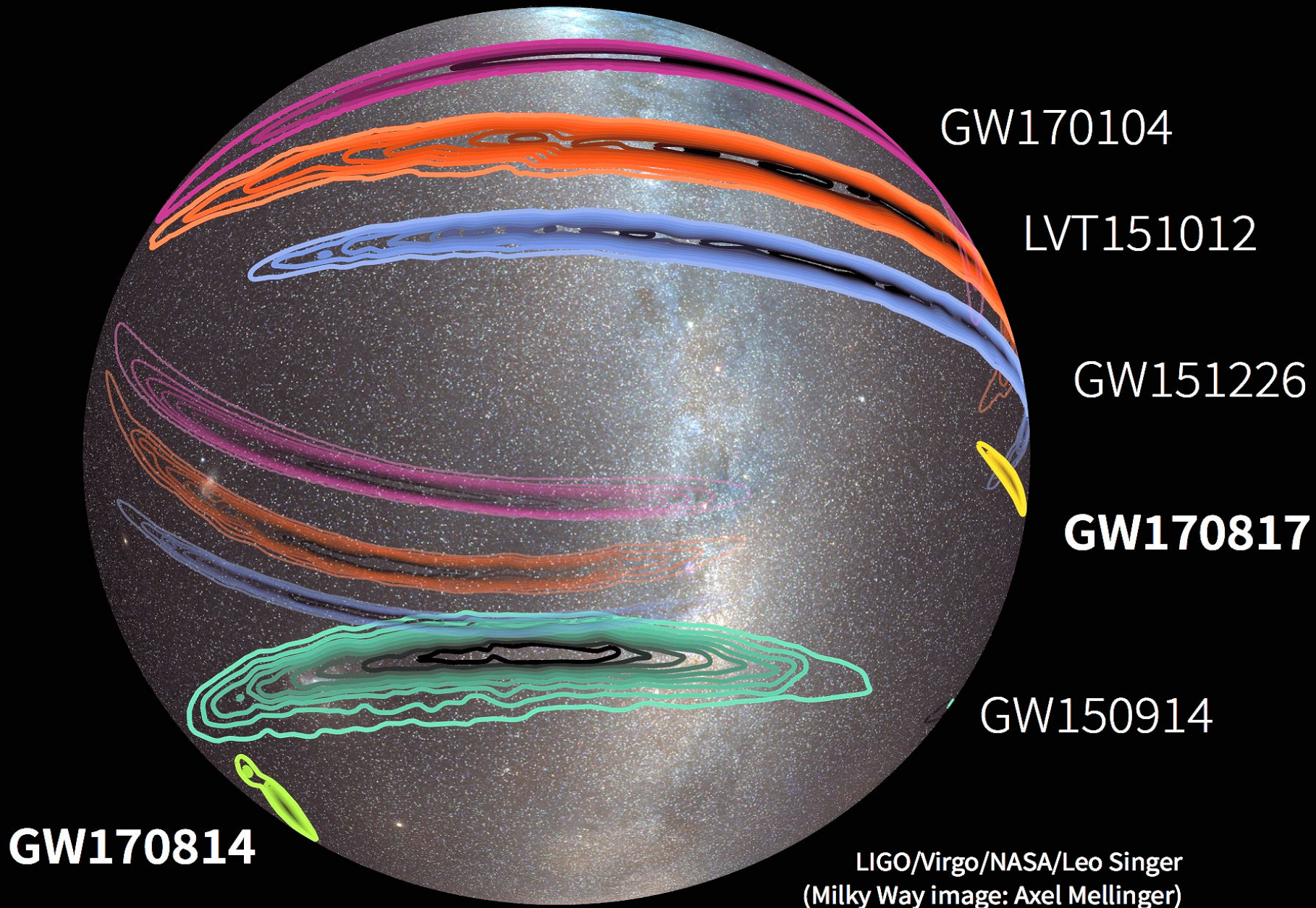
LIGO, Livingston, LA

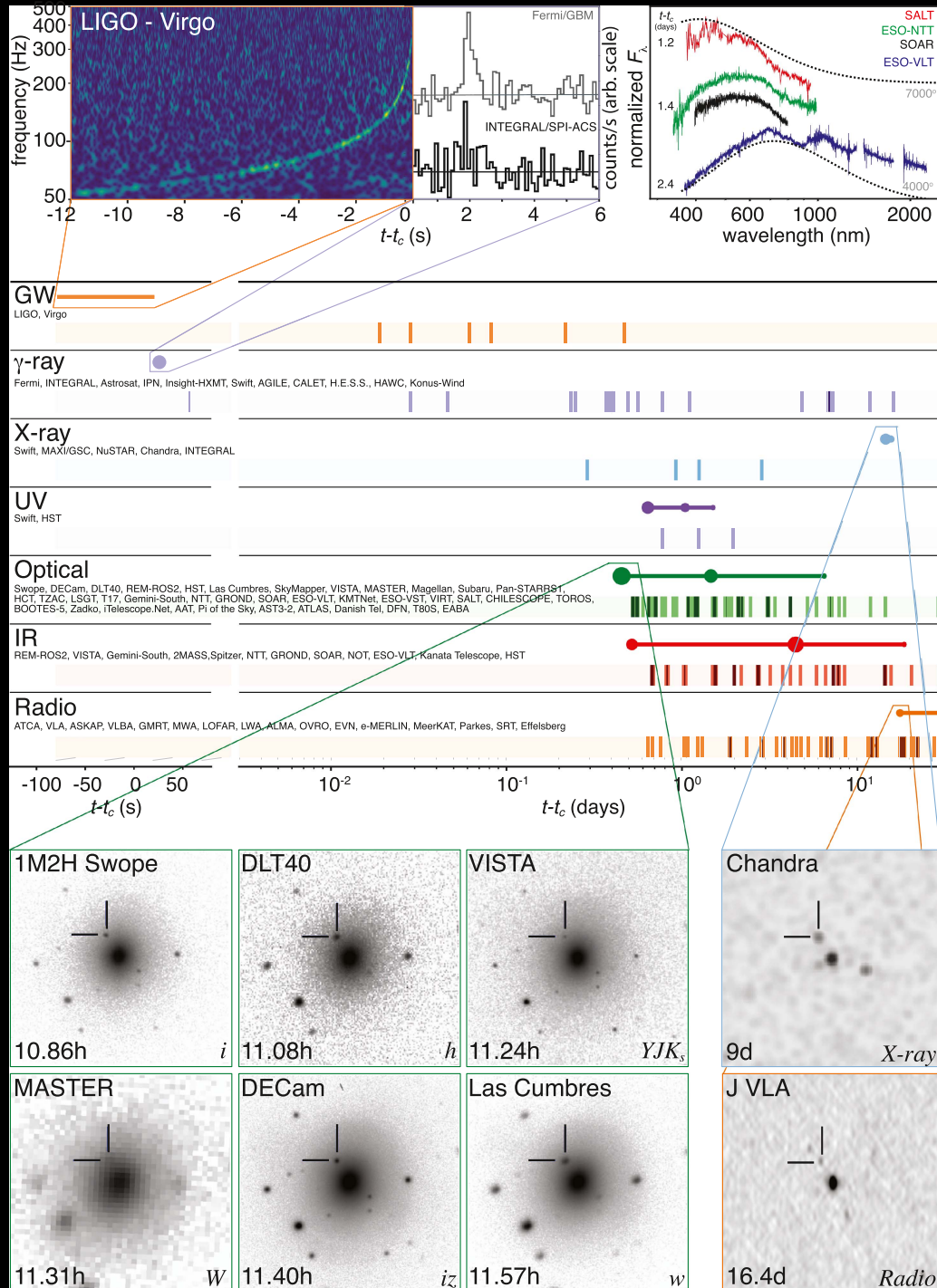


LIGO, Hanford, WA



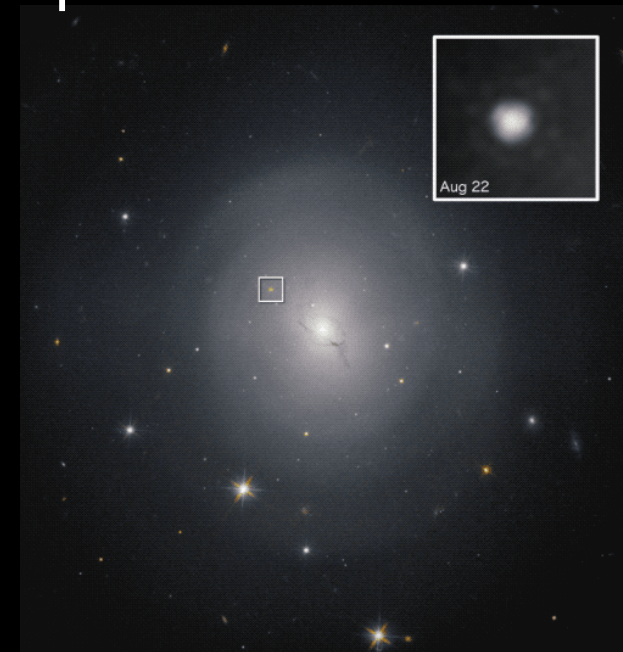
Getting a 3rd GW observatory online

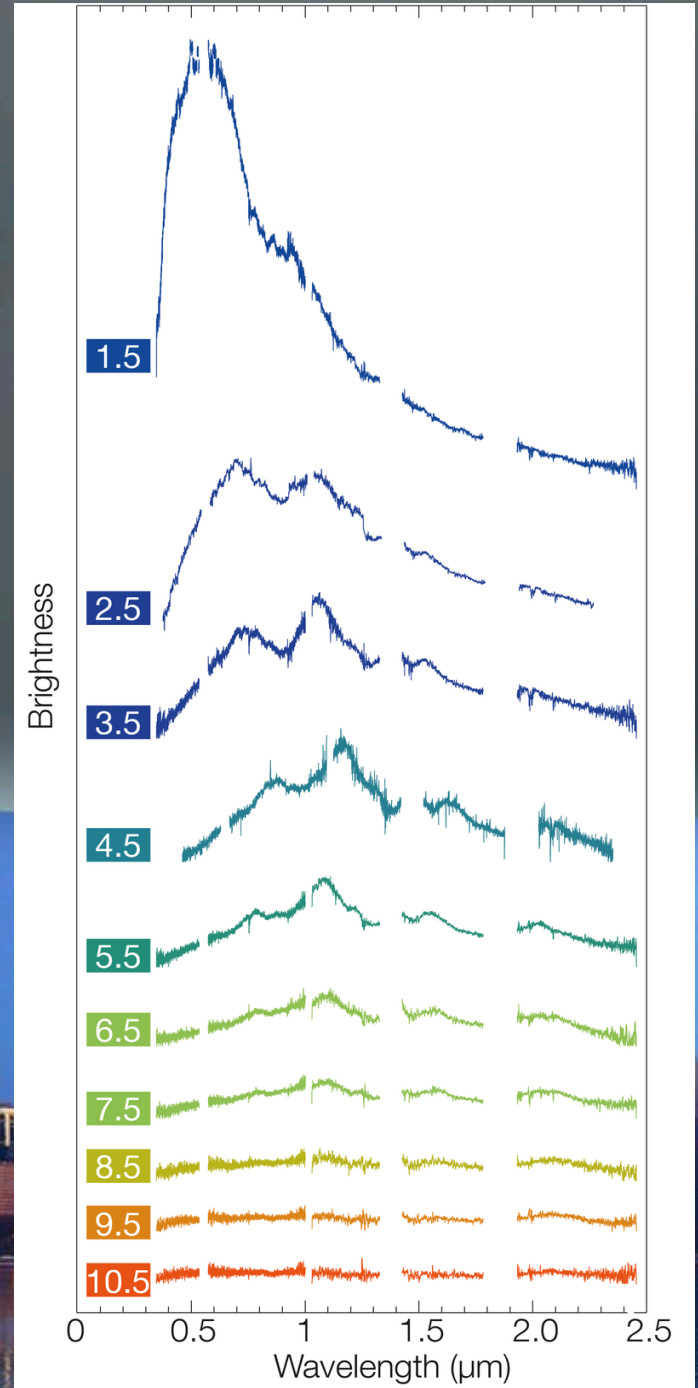
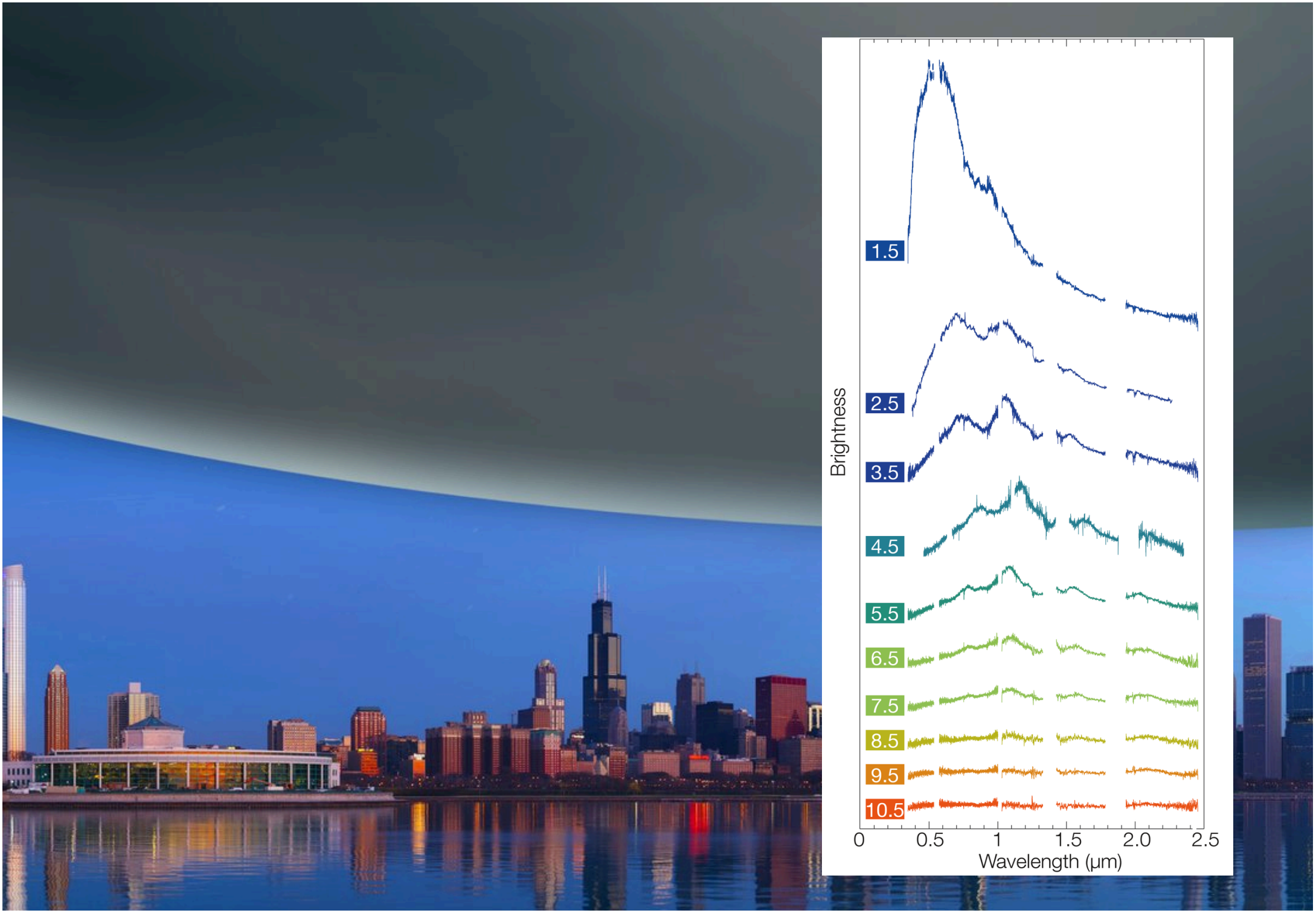




Link between BNS and one class of GRB.

Measurement of speed of GW





The 'Gold-Factory'

Element origins

1 H																	2 He	
3 Li	4 Be											5 B	6 C	7 N	8 O	9 F	10 Ne	
11 Na	12 Mg											13 Al	14 Si	15 P	16 S	17 Cl	18 Ar	
19 K	20 Ca	21 Sc	22 Ti	23 V	24 Cr	25 Mn	26 Fe	27 Co	28 Ni	29 Cu	30 Zn	31 Ga	32 Ge	33 As	34 Se	35 Br	36 Kr	
37 Rb	38 Sr	39 Y	40 Zr	41 Nb	42 Mo	43 Tc	44 Ru	45 Rh	46 Pd	47 Ag	48 Cd	49 In	50 Sn	51 Sb	52 Te	53 I	54 Xe	
55 Cs	56 Ba			72 Hf	73 Ta	74 W	75 Re	76 Os	77 Ir	78 Pt	79 Au	80 Hg	81 Tl	82 Pb	83 Bi	84 Po	85 At	86 Rn
87 Fr	88 Ra																	
		57 La	58 Ce	59 Pr	60 Nd	61 Pm	62 Sm	63 Eu	64 Gd	65 Tb	66 Dy	67 Ho	68 Er	69 Tm	70 Yb	71 Lu		
		89 Ac	90 Th	91 Pa	92 U													

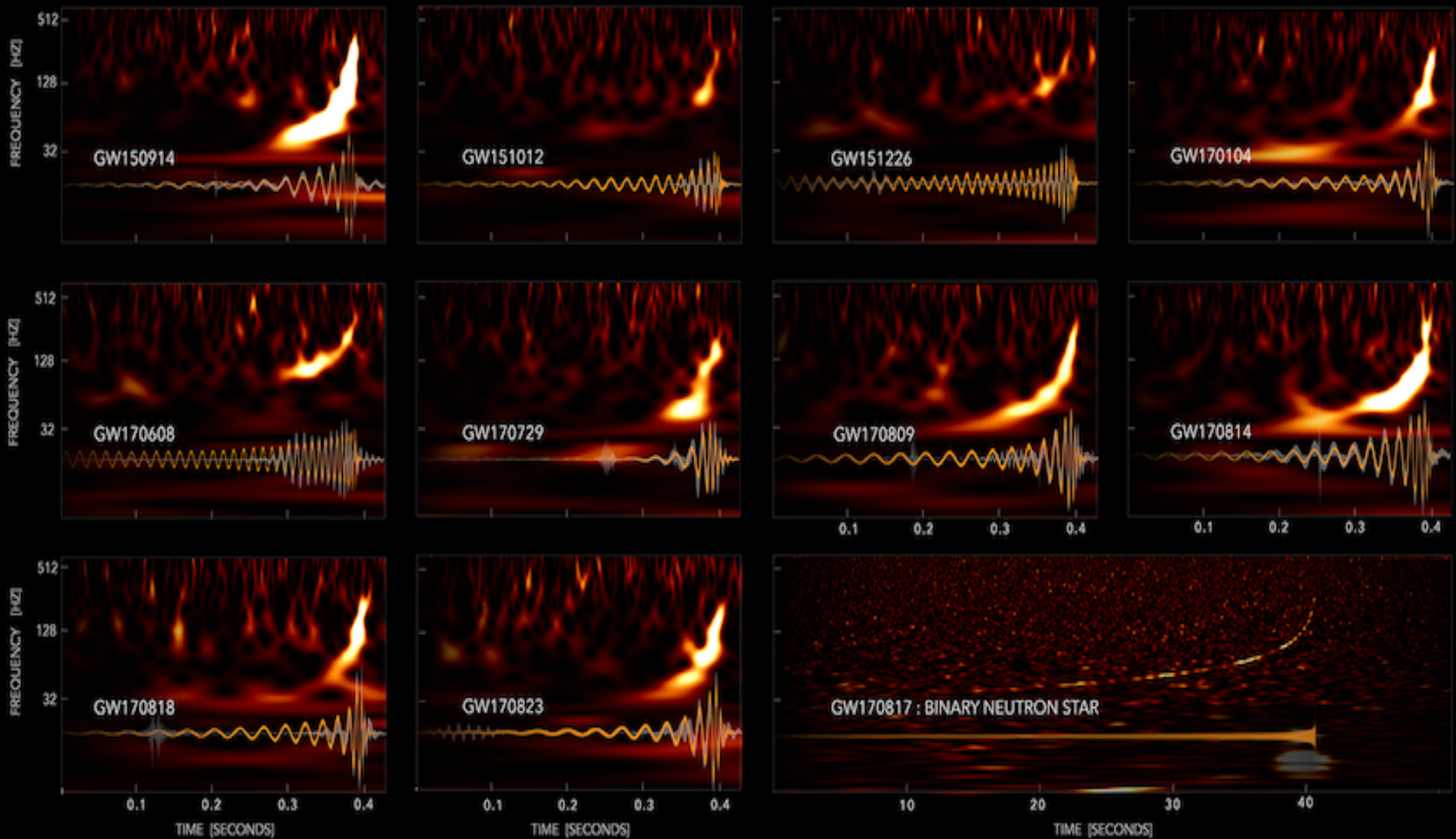


Merging neutron stars
Dying low mass stars

Exploding massive stars
Exploding white dwarfs

Big Bang
Cosmic Ray Fission

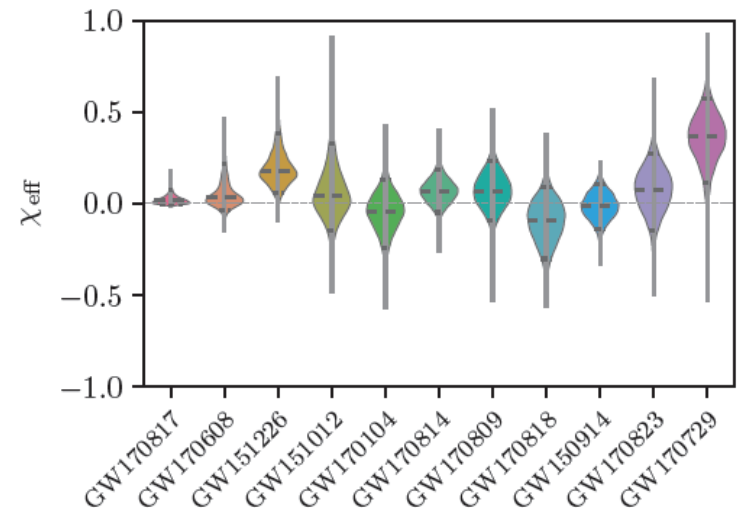
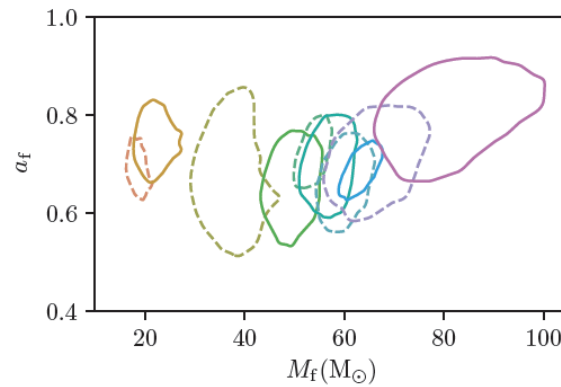
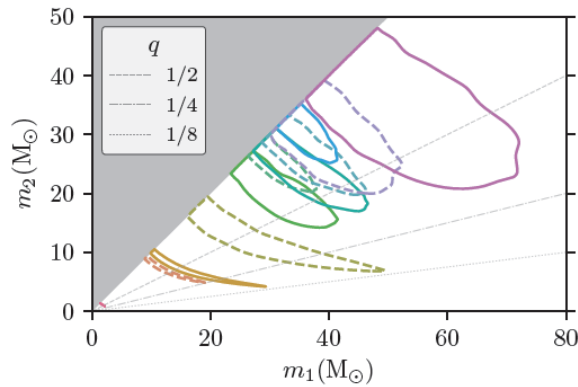
GRAVITATIONAL-WAVE TRANSIENT CATALOG-1



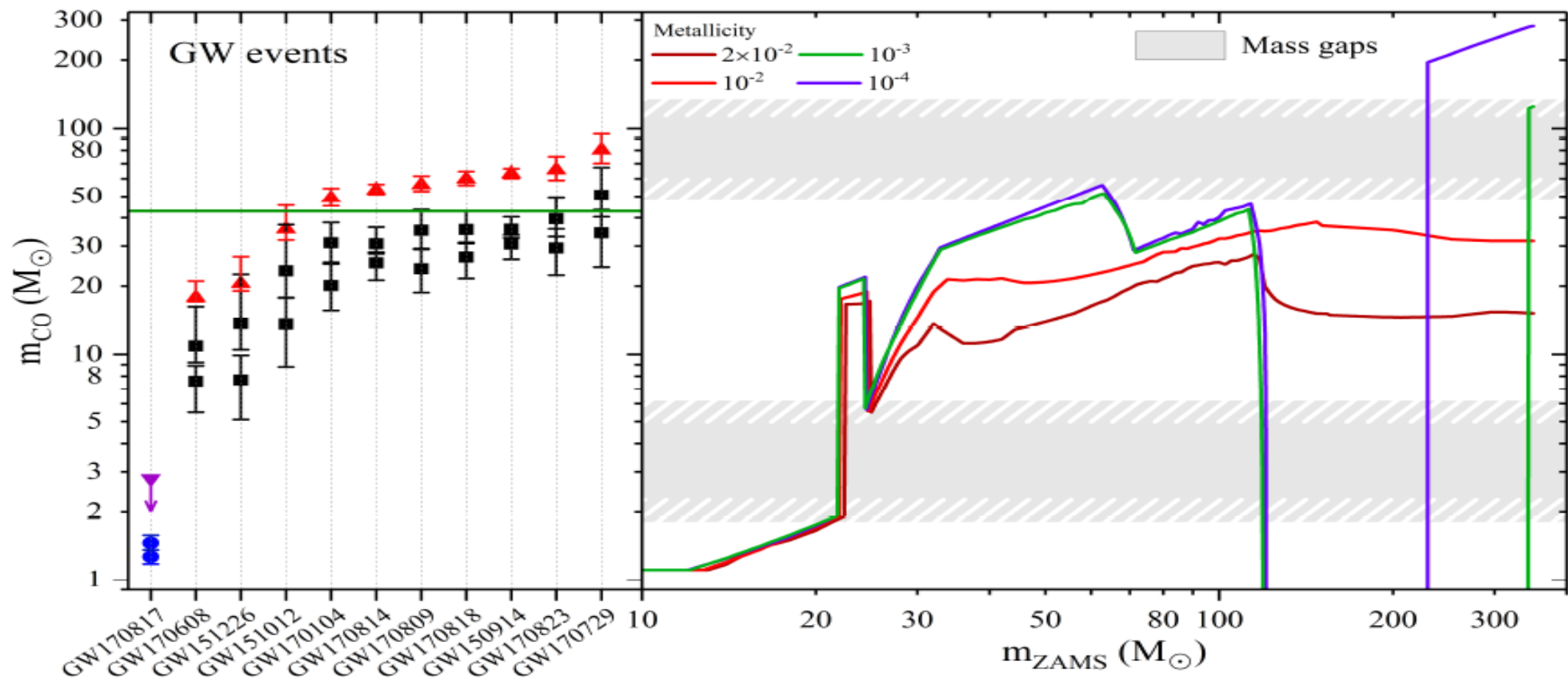
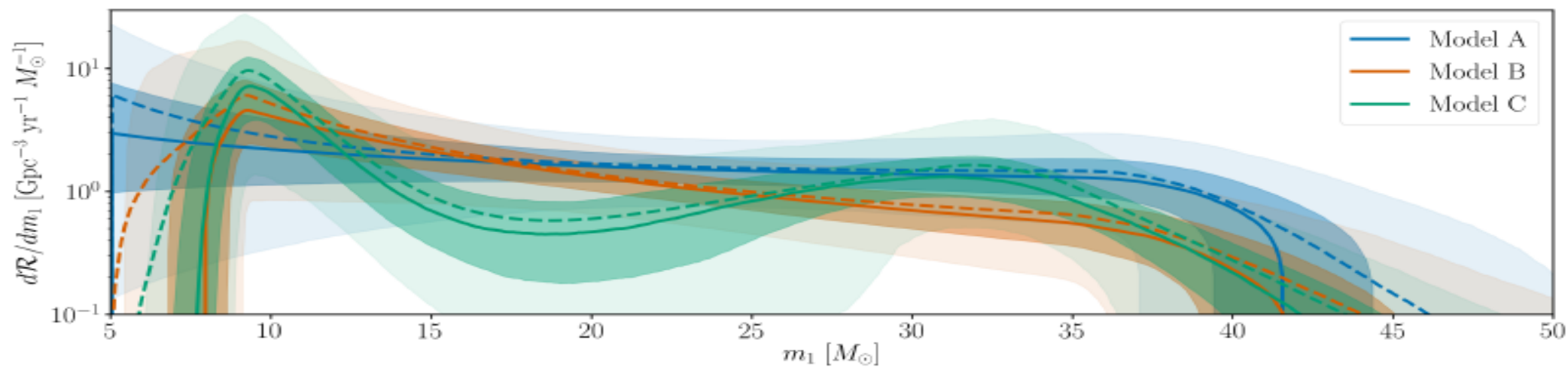


First GW catalog: GWTC-1

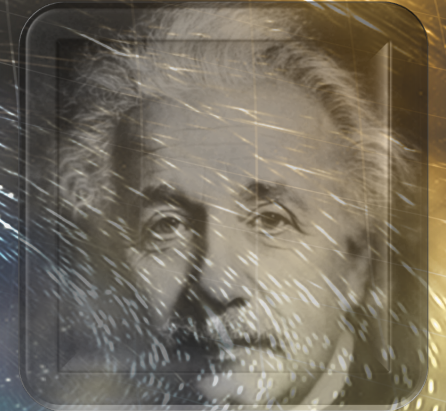
Event	m_1/M_\odot	m_2/M_\odot	M/M_\odot	χ_{eff}	M_f/M_\odot	a_f	$E_{\text{rad}}/(M_\odot c^2)$	$\ell_{\text{peak}}/(\text{erg s}^{-1})$	d_L/Mpc	z	$\Delta\Omega/\text{deg}^2$
GW150914	$35.6^{+4.8}_{-3.0}$	$30.6^{+3.0}_{-4.4}$	$28.6^{+1.6}_{-1.5}$	$-0.01^{+0.12}_{-0.13}$	$63.1^{+3.3}_{-3.0}$	$0.69^{+0.05}_{-0.04}$	$3.1^{+0.4}_{-0.4}$	$3.6^{+0.4}_{-0.4} \times 10^{56}$	430^{+150}_{-170}	$0.09^{+0.03}_{-0.03}$	179
GW151012	$23.3^{+14.0}_{-5.5}$	$13.6^{+4.1}_{-4.8}$	$15.2^{+2.0}_{-1.1}$	$0.04^{+0.28}_{-0.19}$	$35.7^{+9.9}_{-3.8}$	$0.67^{+0.13}_{-0.11}$	$1.5^{+0.5}_{-0.5}$	$3.2^{+0.8}_{-1.7} \times 10^{56}$	1060^{+540}_{-480}	$0.21^{+0.09}_{-0.09}$	1555
GW151226	$13.7^{+8.8}_{-3.2}$	$7.7^{+2.2}_{-2.6}$	$8.9^{+0.3}_{-0.3}$	$0.18^{+0.20}_{-0.12}$	$20.5^{+6.4}_{-1.5}$	$0.74^{+0.07}_{-0.05}$	$1.0^{+0.1}_{-0.2}$	$3.4^{+0.7}_{-1.7} \times 10^{56}$	440^{+180}_{-190}	$0.09^{+0.04}_{-0.04}$	1033
GW170104	$31.0^{+7.2}_{-5.6}$	$20.1^{+4.9}_{-4.5}$	$21.5^{+2.1}_{-1.7}$	$-0.04^{+0.17}_{-0.20}$	$49.1^{+5.2}_{-3.9}$	$0.66^{+0.08}_{-0.10}$	$2.2^{+0.5}_{-0.5}$	$3.3^{+0.6}_{-0.9} \times 10^{56}$	960^{+430}_{-410}	$0.19^{+0.07}_{-0.08}$	924
GW170608	$10.9^{+5.3}_{-1.7}$	$7.6^{+1.3}_{-2.1}$	$7.9^{+0.2}_{-0.2}$	$0.03^{+0.19}_{-0.07}$	$17.8^{+3.2}_{-0.7}$	$0.69^{+0.04}_{-0.04}$	$0.9^{+0.0}_{-0.1}$	$3.5^{+0.4}_{-1.3} \times 10^{56}$	320^{+120}_{-110}	$0.07^{+0.02}_{-0.02}$	396
GW170729	$50.6^{+16.6}_{-10.2}$	$34.3^{+9.1}_{-10.1}$	$35.7^{+6.5}_{-4.7}$	$0.36^{+0.21}_{-0.25}$	$80.3^{+14.6}_{-10.2}$	$0.81^{+0.07}_{-0.13}$	$4.8^{+1.7}_{-1.7}$	$4.2^{+0.9}_{-1.5} \times 10^{56}$	2750^{+1350}_{-1320}	$0.48^{+0.19}_{-0.20}$	1033
GW170809	$35.2^{+8.3}_{-6.0}$	$23.8^{+5.2}_{-5.1}$	$25.0^{+2.1}_{-1.6}$	$0.07^{+0.16}_{-0.16}$	$56.4^{+5.2}_{-3.7}$	$0.70^{+0.08}_{-0.09}$	$2.7^{+0.6}_{-0.6}$	$3.5^{+0.6}_{-0.9} \times 10^{56}$	990^{+320}_{-380}	$0.20^{+0.05}_{-0.07}$	340
GW170814	$30.7^{+5.7}_{-3.0}$	$25.3^{+2.9}_{-4.1}$	$24.2^{+1.4}_{-1.1}$	$0.07^{+0.12}_{-0.11}$	$53.4^{+3.2}_{-2.4}$	$0.72^{+0.07}_{-0.05}$	$2.7^{+0.4}_{-0.3}$	$3.7^{+0.4}_{-0.5} \times 10^{56}$	580^{+160}_{-210}	$0.12^{+0.03}_{-0.04}$	87
GW170817	$1.46^{+0.12}_{-0.10}$	$1.27^{+0.09}_{-0.09}$	$1.186^{+0.001}_{-0.001}$	$0.00^{+0.02}_{-0.01}$	≤ 2.8	≤ 0.89	≥ 0.04	$\geq 0.1 \times 10^{56}$	40^{+10}_{-10}	$0.01^{+0.00}_{-0.00}$	16
GW170818	$35.5^{+7.5}_{-4.7}$	$26.8^{+4.3}_{-5.2}$	$26.7^{+2.1}_{-1.7}$	$-0.09^{+0.18}_{-0.21}$	$59.8^{+4.8}_{-3.8}$	$0.67^{+0.07}_{-0.08}$	$2.7^{+0.5}_{-0.5}$	$3.4^{+0.5}_{-0.7} \times 10^{56}$	1020^{+430}_{-360}	$0.20^{+0.07}_{-0.07}$	39
GW170823	$39.6^{+10.0}_{-6.6}$	$29.4^{+6.3}_{-7.1}$	$29.3^{+4.2}_{-3.2}$	$0.08^{+0.20}_{-0.22}$	$65.6^{+9.4}_{-6.6}$	$0.71^{+0.08}_{-0.10}$	$3.3^{+0.9}_{-0.8}$	$3.6^{+0.6}_{-0.9} \times 10^{56}$	1850^{+840}_{-840}	$0.34^{+0.13}_{-0.14}$	1651



■ GW170817 ■ GW151226 ■ GW170104 ■ GW170809 ■ GW150914 ■ GW170729
■ GW170608 ■ GW151012 ■ GW170814 ■ GW170818 ■ GW170823



GW Astronomy results to date and pro-spects, Current and future GW detectors – sensitivity they achieve and how they do it, Astrophysical requirements and benefits of calibration accuracy



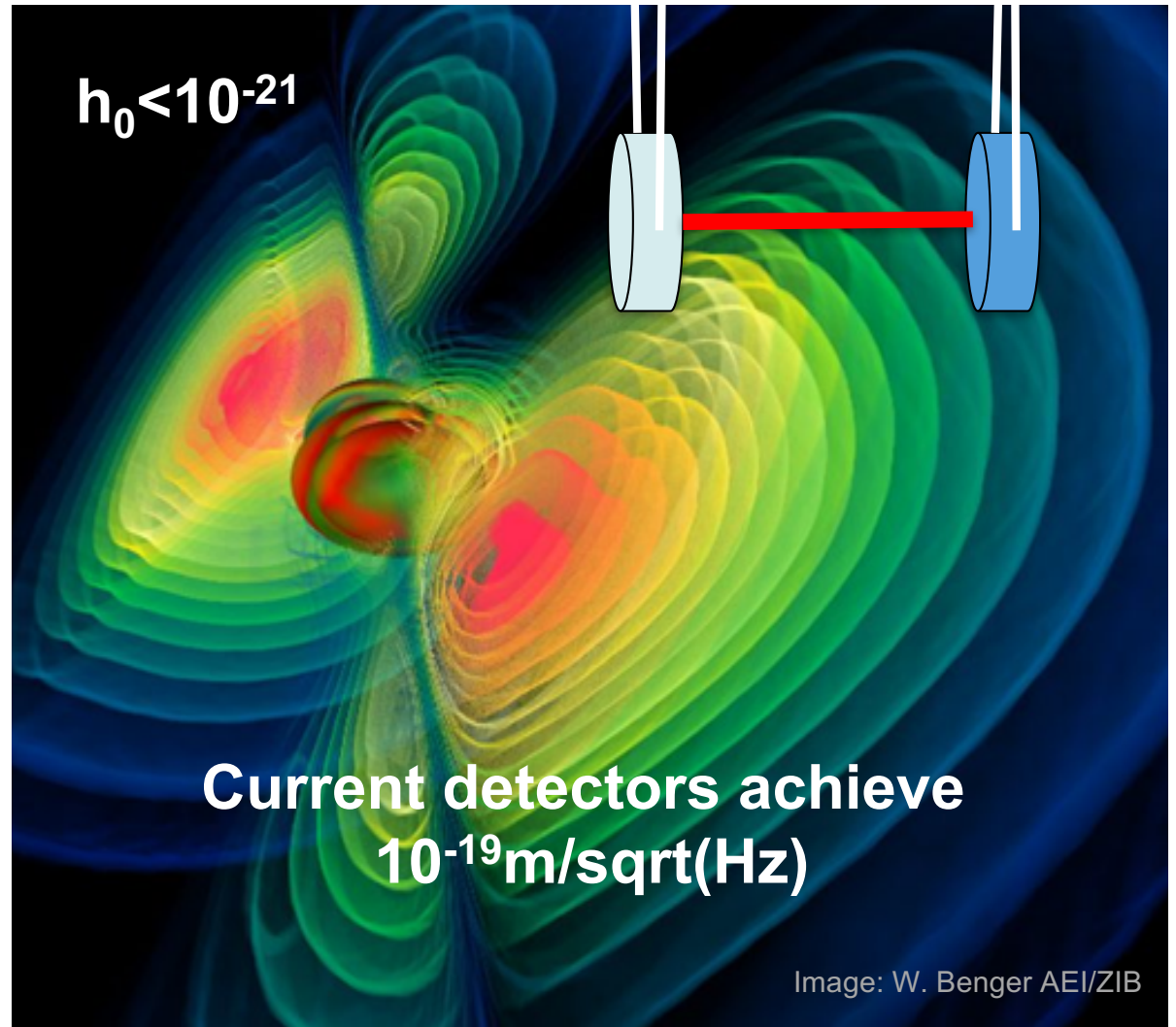
Prof Stefan Hild,
University of Glasgow, UK

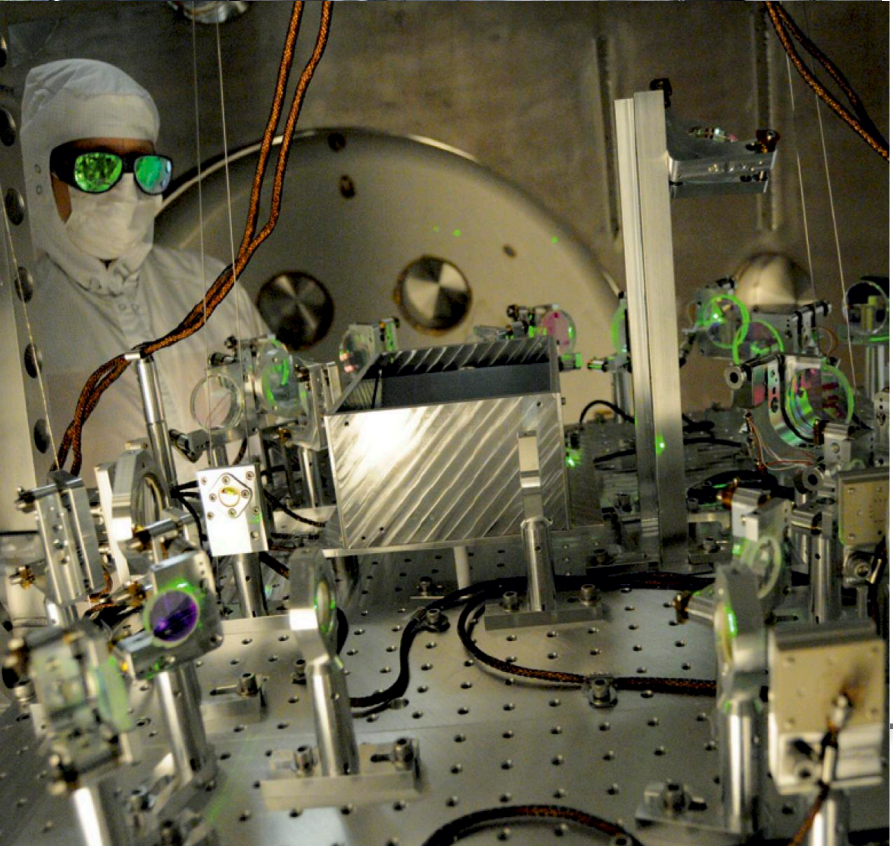
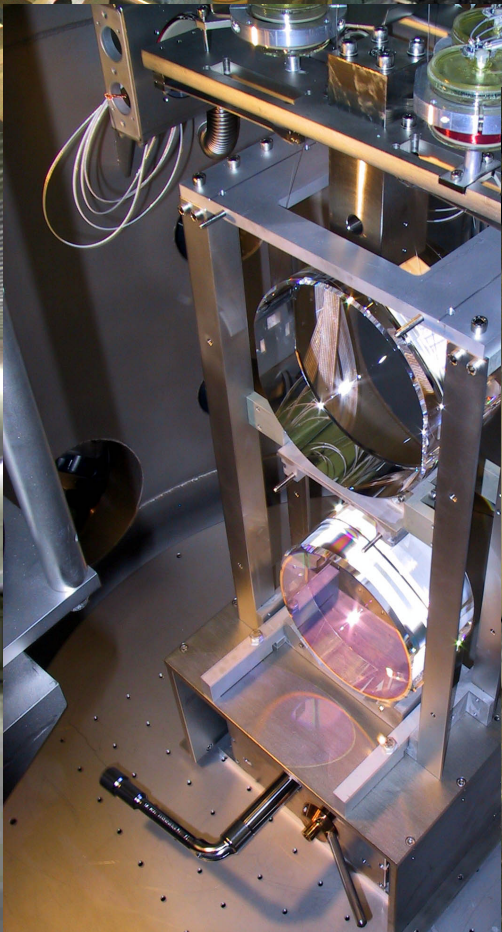
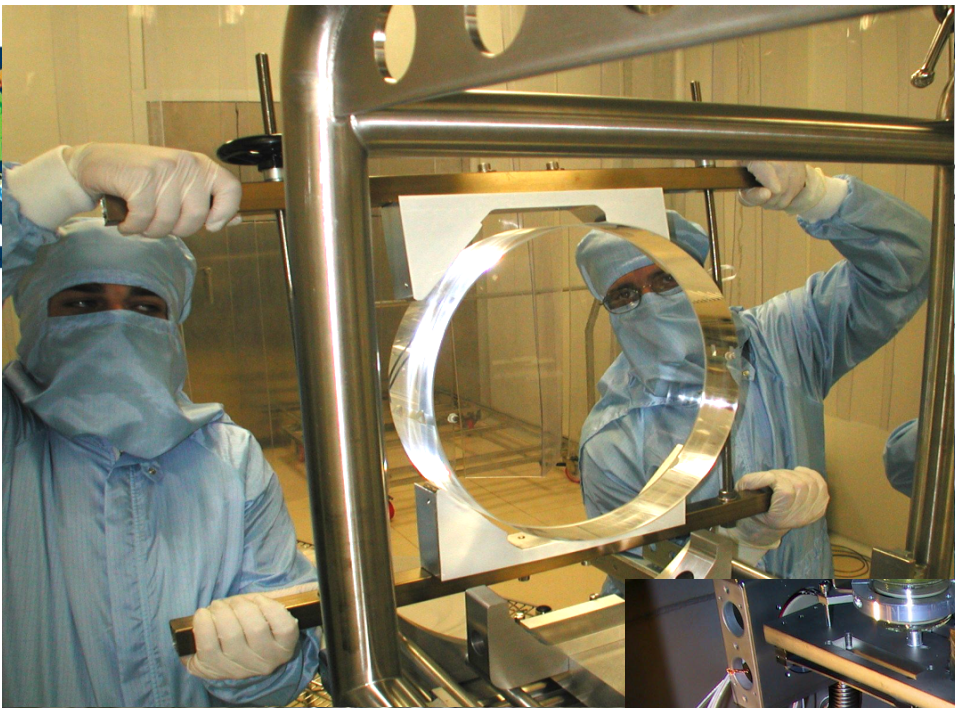




Detecting Gravitational Waves

- In order to detect GW you need to very accurately measure the position of test masses.
- First you need to make your test masses quieter than what you want to measure.
- Secondly, you need to readout the strain to the required precision without (!) introducing 'too much' additional noise.







Detecting Gravitational Waves

Travel time in x-arm

$$\tau_x = \frac{2L}{c} + \frac{1}{2} \int_{t-2\frac{L}{c}}^t h_+(t') dt',$$

Phase

Laser freq

$$-\varphi = \omega_0 \tau_x$$

$$h_+(t) = h_0 \cos \omega_g t$$

Assumption of GW signal

GW amplitude

GW freq

Phase shift
Produced by
GW

$$\Delta\varphi(t) = h_0 \frac{\omega_0}{\omega_g} \sin\left(\omega_g \frac{\tau}{2}\right) \cos\left(\omega_g \left(t - \frac{\tau}{2}\right)\right).$$

Geometry term

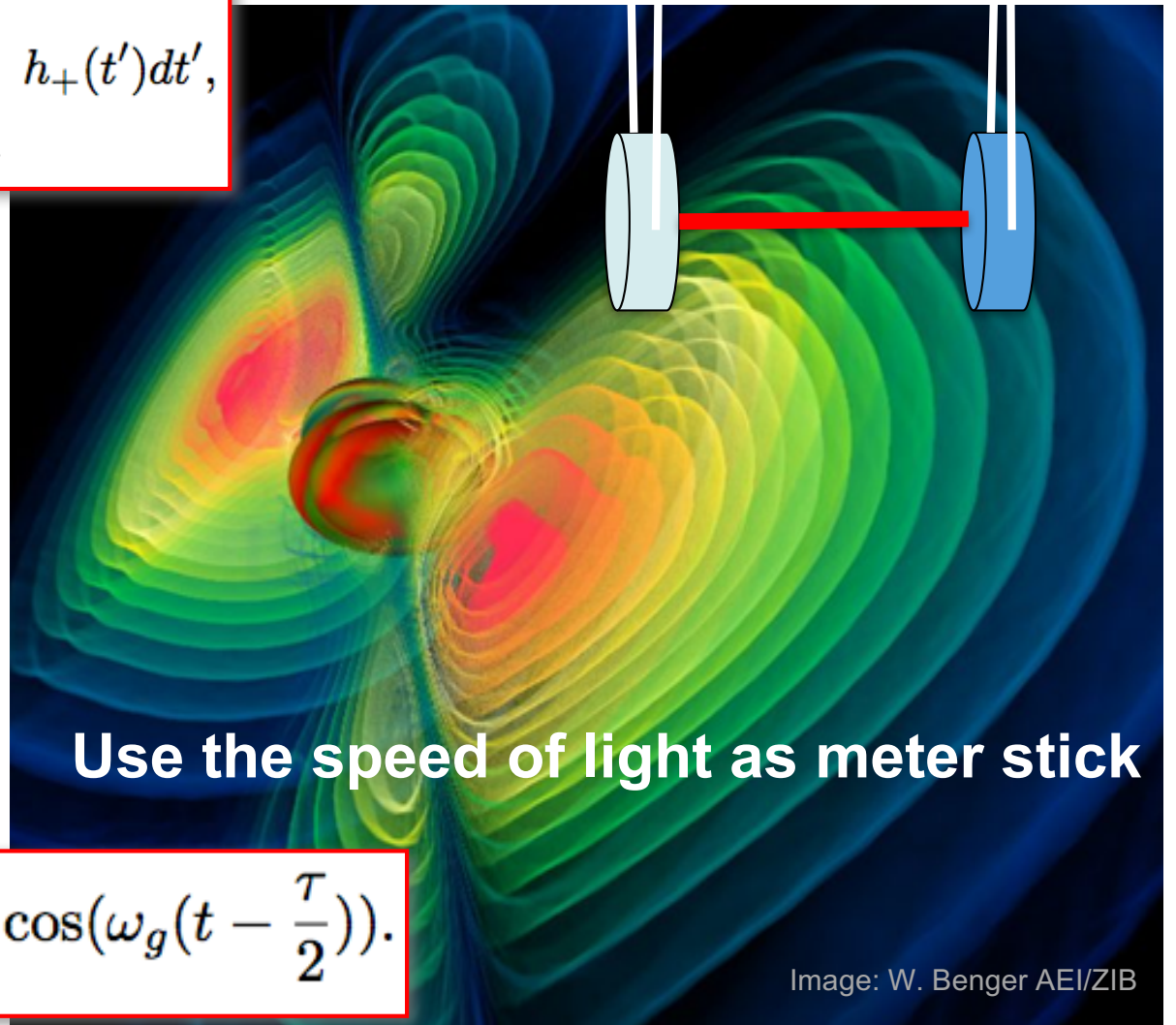
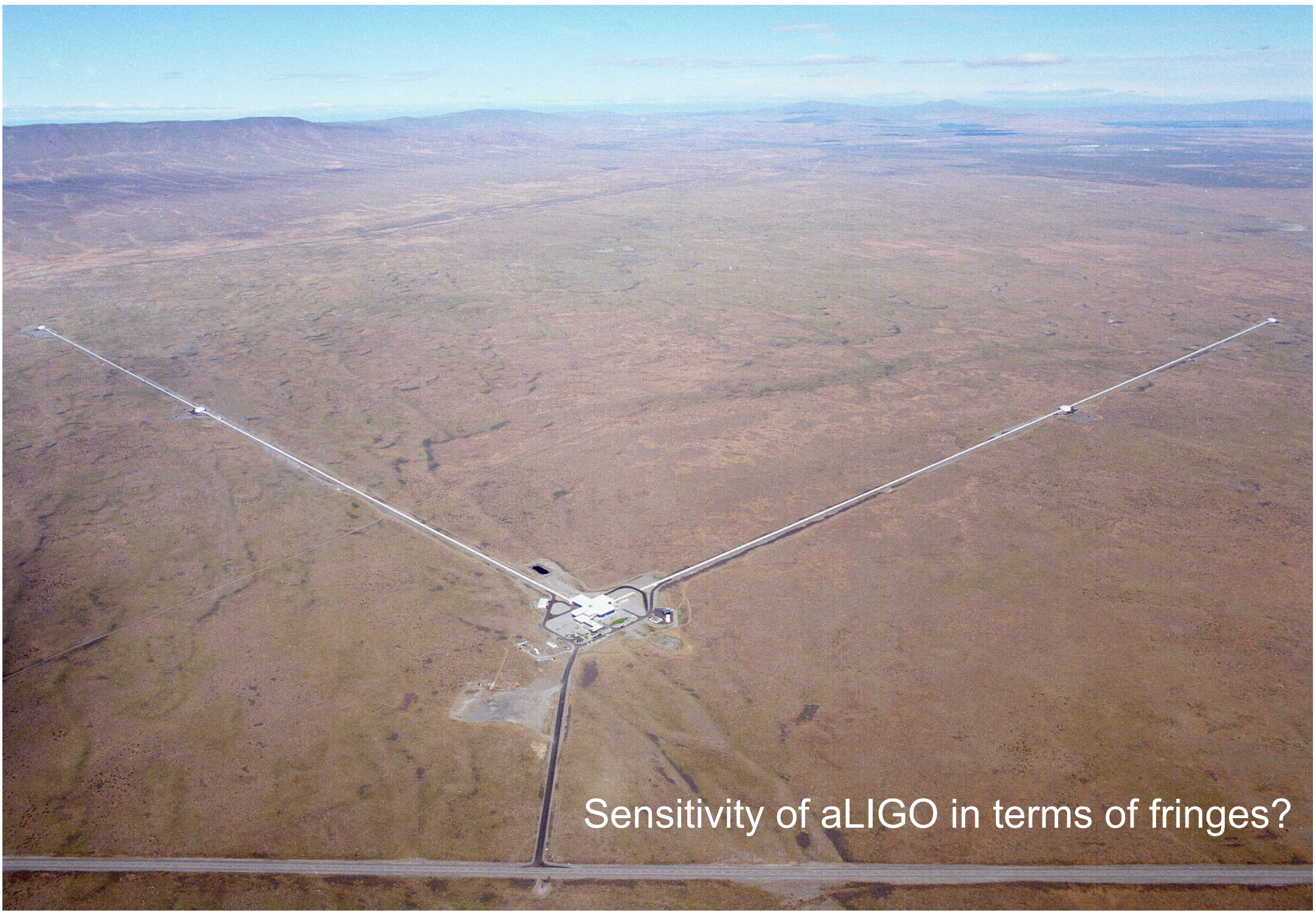


Image: W. Benger AEI/ZIB

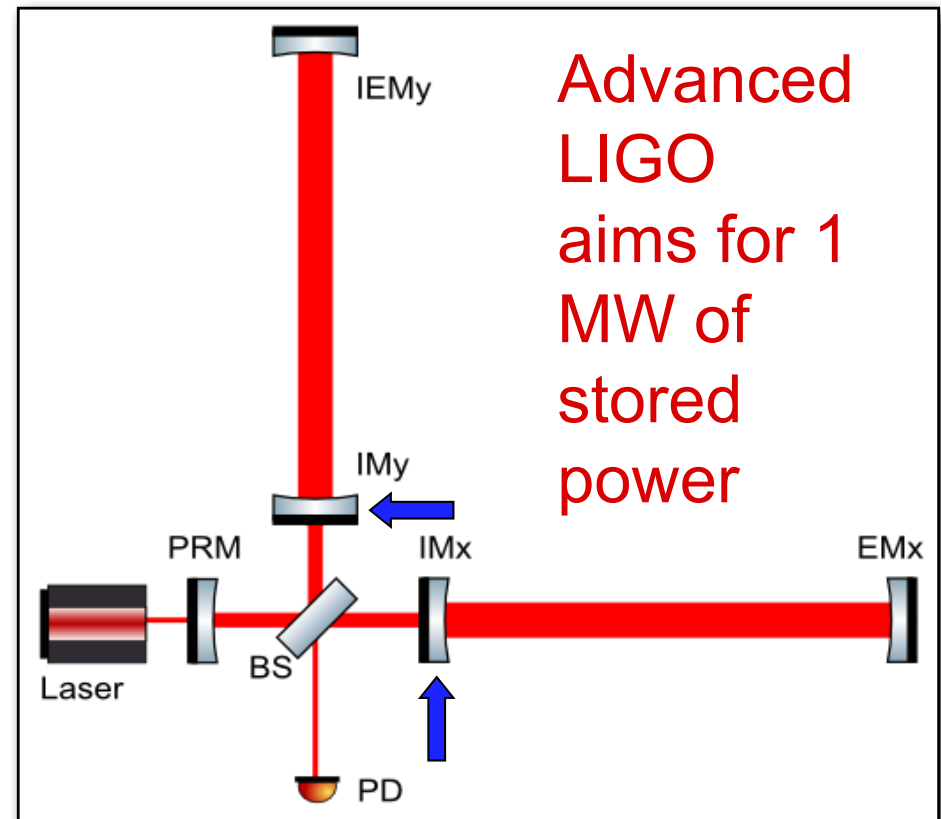
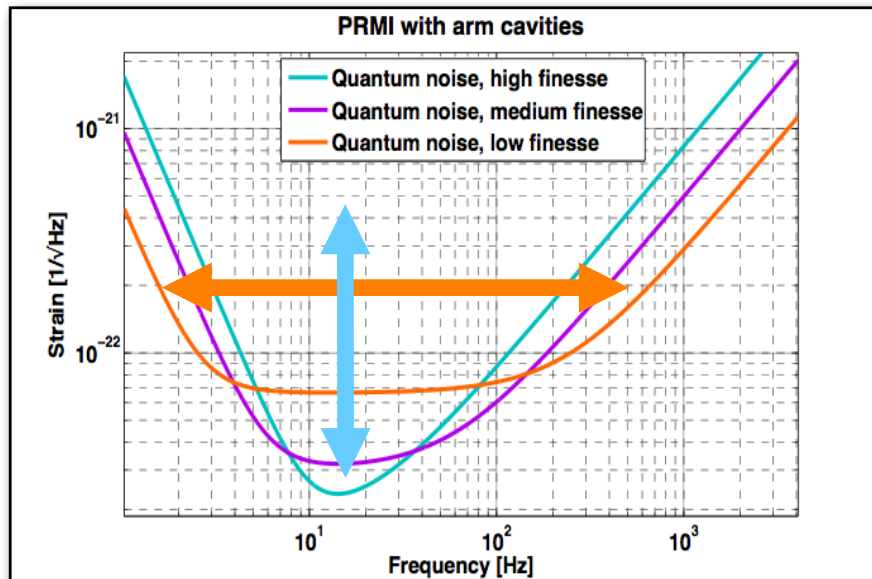


Sensitivity of aLIGO in terms of fringes?



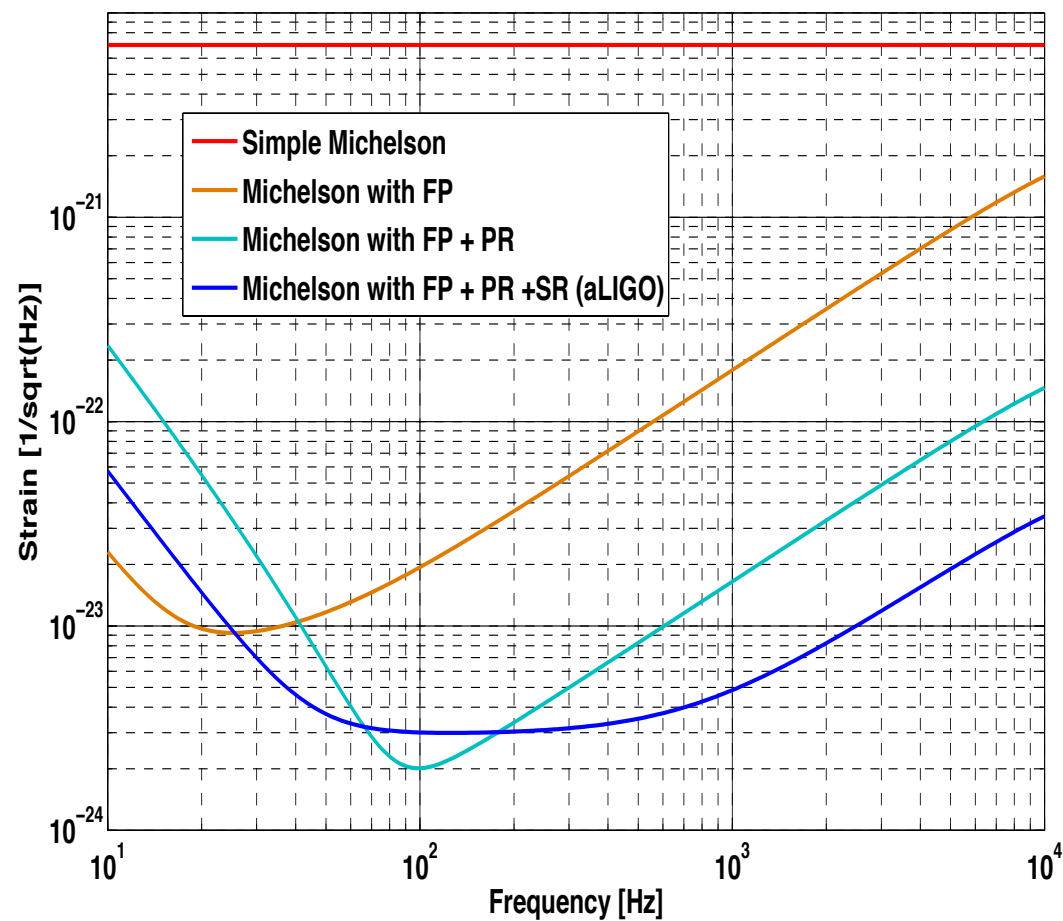
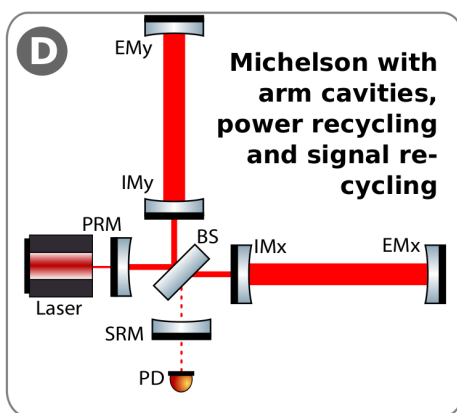
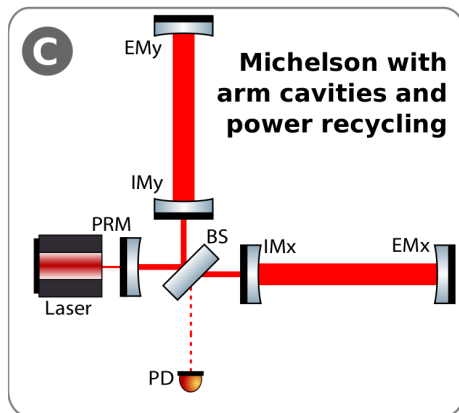
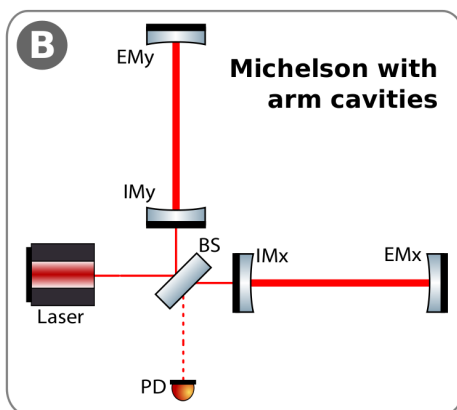
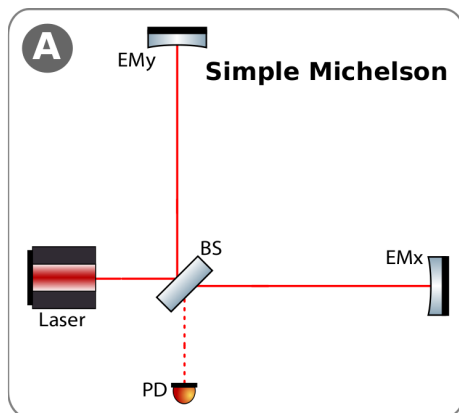
Interferometry: Arm cavities

- ➔ Increasing the storage time in the arms by using arm cavities.
- ➔ Finesse of the arm cavities determines bandwidth of GW detector.





ALIGO Example



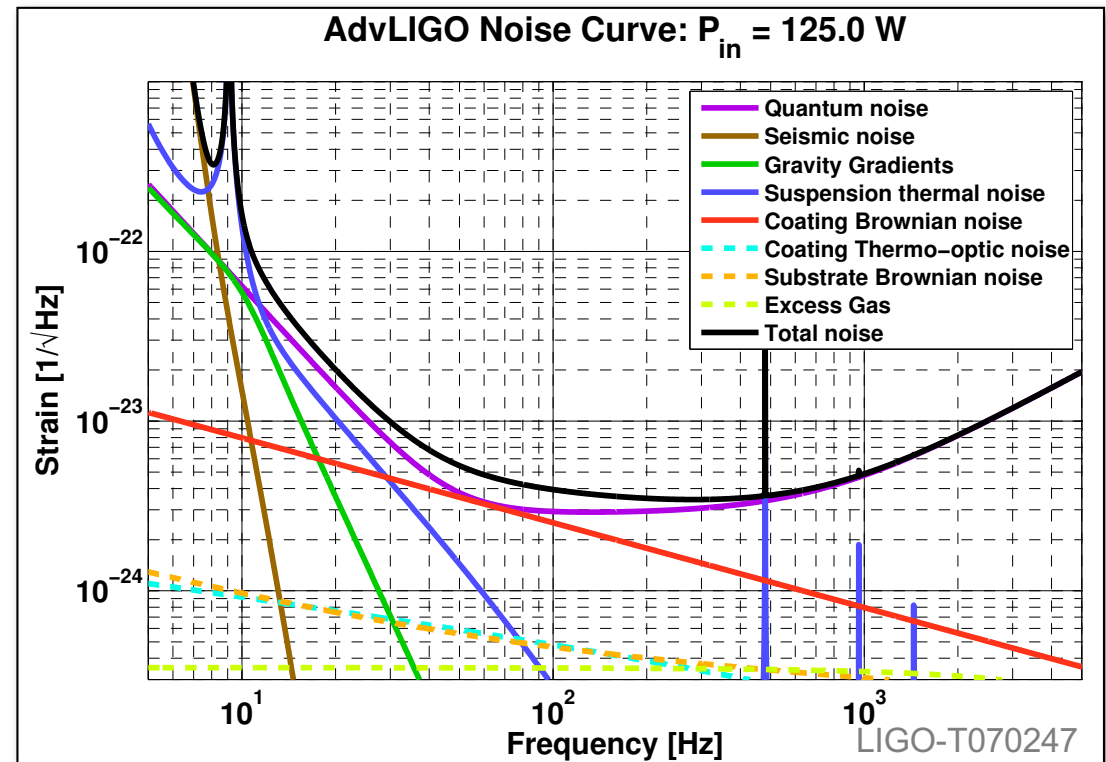


Noise Sources limiting the aLIGO



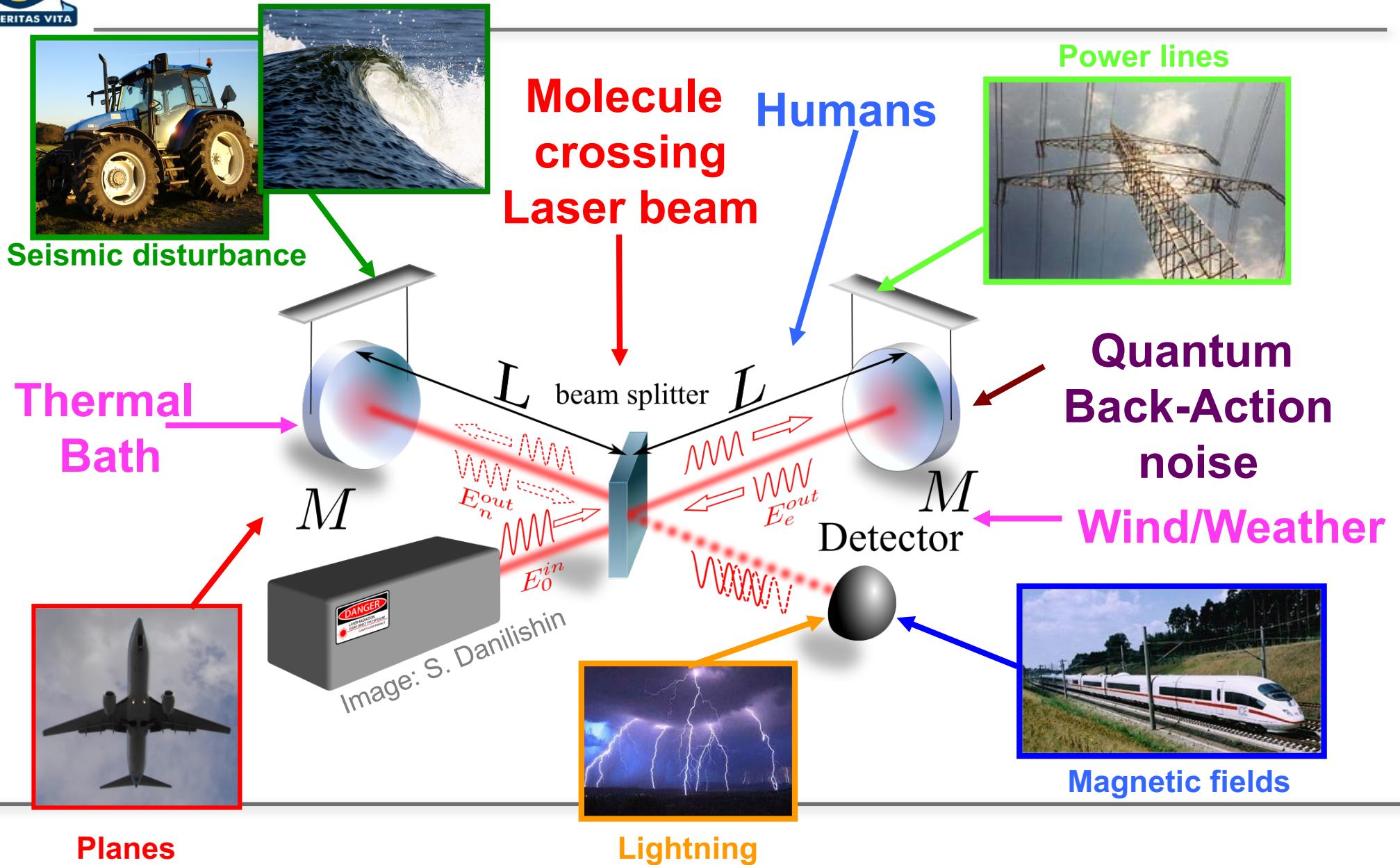
➔ In order to understand how we can potentially improve Advanced LIGO, we need to see what is limiting:

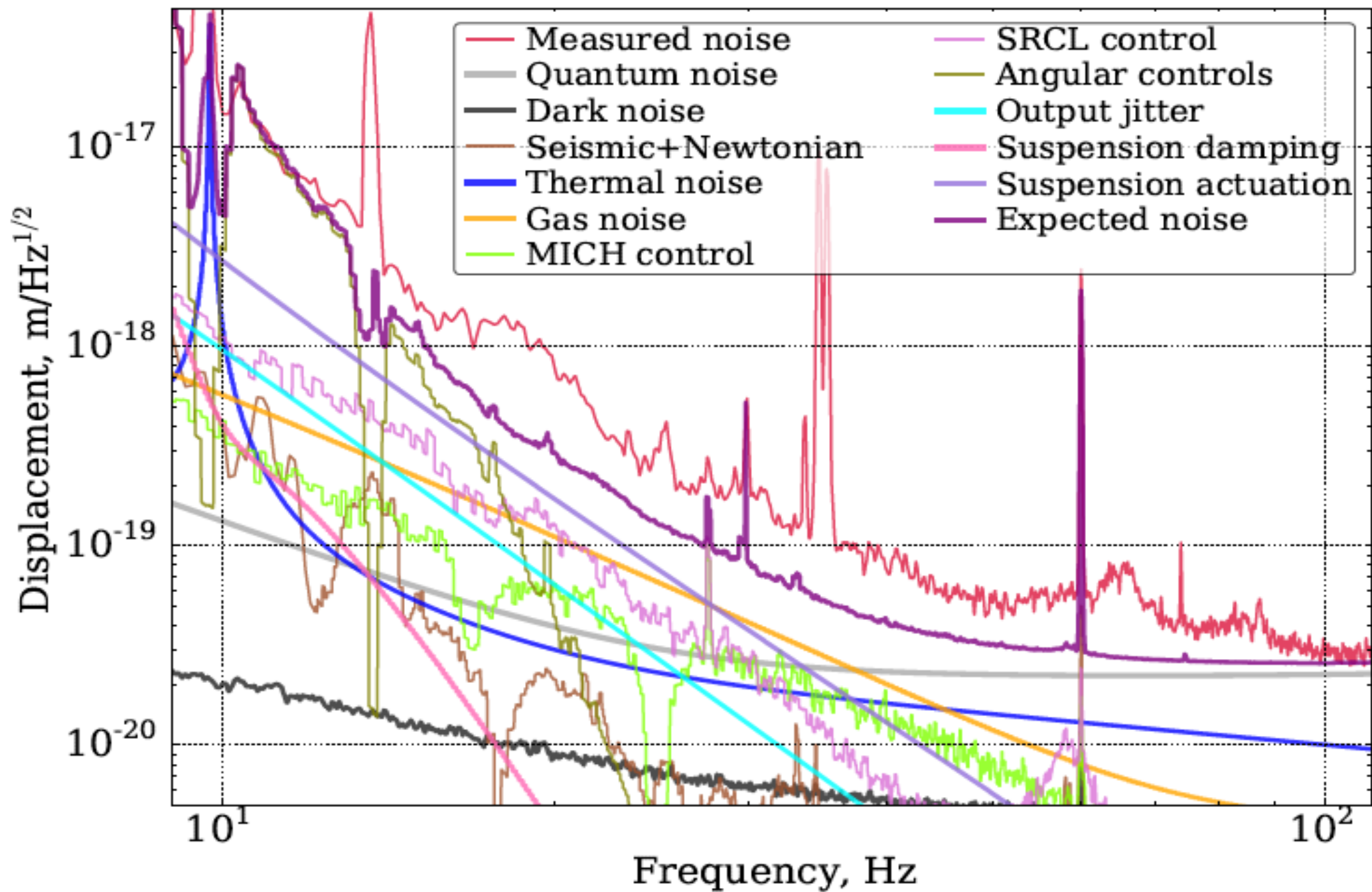
- **Quantum Noise** limits most of the frequency range.
- **Coating Brownian** limits (or is close) in the range from 50 to 100Hz.
- Below 50Hz we are limited by 'walls' made of **Suspension Thermal**, **Gravity Gradient** and **Seismic noise**.





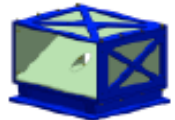
Myriad of Disturbances



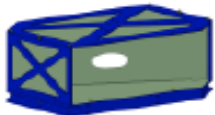


(a) LIGO Livingston Observatory

LAYOUT OF SCATTERED LIGHT BAFFLES IN ADVANCED LIGO



HWS2 ALL SCRAPE BAFFLE (HWS2)
 D1400027
 2. BAR IN COATED 304L SUPERINVAR SPACER AND BRKT. BAR IN COATED AL. 20% SCRAPE. 2-PC COATED.



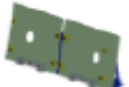
SR2 SCRAFER BAFFLE
 D1400028
 COATED SHORT BEAM FLARE. MC, 2PC & 1PC.
 1PC: 2. BAR IN COATED 304L SUPERINVAR SPACER AND BRKT. 2. BAR IN COATED AL. 20% SCRAPE. 2-PC COATED.



HWS2 ALL SCRAPE BAFFLE (HWS2)
 D1400027
 2. BAR IN COATED 304L SUPERINVAR SPACER AND BRKT. BAR IN COATED AL. 20% SCRAPE. 2-PC COATED.



SR2 SCRAFER BAFFLE
 D1400028
 COATED SHORT BEAM FLARE. MC, 2PC & 1PC.
 1PC: 2. BAR IN COATED 304L SUPERINVAR SPACER AND BRKT. 2. BAR IN COATED AL. 20% SCRAPE. 2-PC COATED.



HWS2 ALL SCRAPE BAFFLE (HWS2)
 D1400027
 2. BAR IN COATED 304L SUPERINVAR SPACER AND BRKT. BAR IN COATED AL. 20% SCRAPE. 2-PC COATED.



SR2 SCRAFER BAFFLE
 D1400028
 COATED SHORT BEAM FLARE. MC, 2PC & 1PC.
 1PC: 2. BAR IN COATED 304L SUPERINVAR SPACER AND BRKT. 2. BAR IN COATED AL. 20% SCRAPE. 2-PC COATED.



HWS2 ALL SCRAPE BAFFLE (HWS2)
 D1400027
 2. BAR IN COATED 304L SUPERINVAR SPACER AND BRKT. BAR IN COATED AL. 20% SCRAPE. 2-PC COATED.



SR2 SCRAFER BAFFLE
 D1400028
 COATED SHORT BEAM FLARE. MC, 2PC & 1PC.
 1PC: 2. BAR IN COATED 304L SUPERINVAR SPACER AND BRKT. 2. BAR IN COATED AL. 20% SCRAPE. 2-PC COATED.



HWS2 ALL SCRAPE BAFFLE (HWS2)
 D1400027
 2. BAR IN COATED 304L SUPERINVAR SPACER AND BRKT. BAR IN COATED AL. 20% SCRAPE. 2-PC COATED.

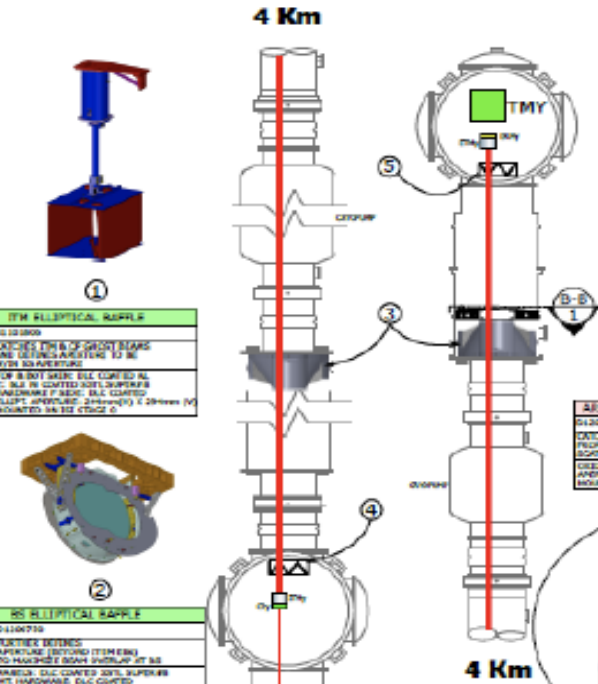


SR2 SCRAFER BAFFLE
 D1400028
 COATED SHORT BEAM FLARE. MC, 2PC & 1PC.
 1PC: 2. BAR IN COATED 304L SUPERINVAR SPACER AND BRKT. 2. BAR IN COATED AL. 20% SCRAPE. 2-PC COATED.

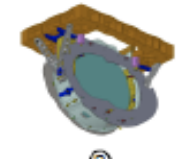
HWS2 ALL SCRAPE BAFFLE (HWS2)
 D1400027
 2. BAR IN COATED 304L SUPERINVAR SPACER AND BRKT. BAR IN COATED AL. 20% SCRAPE. 2-PC COATED.



HWS2 ALL SCRAPE BAFFLE (HWS2)
 D1400027
 2. BAR IN COATED 304L SUPERINVAR SPACER AND BRKT. BAR IN COATED AL. 20% SCRAPE. 2-PC COATED.

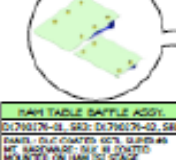


TM ELLIPTICAL BAFFLE
 D1400029
 COATED TOP & BOTTOM BEAMS AND COATED ANGLE TO BE WITH SCAPATURE.
 TOP & BOT BEAMS: 2-PC COATED AL. 2. BAR IN COATED 304L SUPERINVAR SPACER AND BRKT. 2. BAR IN COATED AL. 20% SCRAPE. 2-PC COATED.

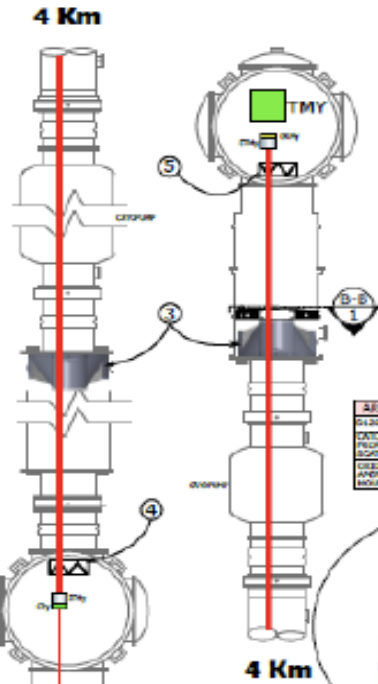


TM ELLIPTICAL BAFFLE
 D1400029
 COATED TOP & BOTTOM BEAMS AND COATED ANGLE TO BE WITH SCAPATURE.
 TOP & BOT BEAMS: 2-PC COATED AL. 2. BAR IN COATED 304L SUPERINVAR SPACER AND BRKT. 2. BAR IN COATED AL. 20% SCRAPE. 2-PC COATED.

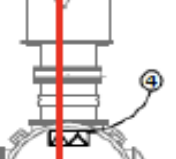
SR2 SCRAFER BAFFLE
 D1400028
 COATED SHORT BEAM FLARE. MC, 2PC & 1PC.
 1PC: 2. BAR IN COATED 304L SUPERINVAR SPACER AND BRKT. 2. BAR IN COATED AL. 20% SCRAPE. 2-PC COATED.



SR2 SCRAFER BAFFLE
 D1400028
 COATED SHORT BEAM FLARE. MC, 2PC & 1PC.
 1PC: 2. BAR IN COATED 304L SUPERINVAR SPACER AND BRKT. 2. BAR IN COATED AL. 20% SCRAPE. 2-PC COATED.

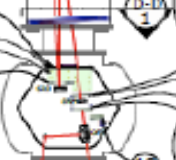


TM ELLIPTICAL BAFFLE
 D1400029
 COATED TOP & BOTTOM BEAMS AND COATED ANGLE TO BE WITH SCAPATURE.
 TOP & BOT BEAMS: 2-PC COATED AL. 2. BAR IN COATED 304L SUPERINVAR SPACER AND BRKT. 2. BAR IN COATED AL. 20% SCRAPE. 2-PC COATED.

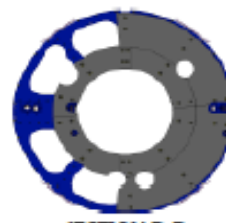


TM ELLIPTICAL BAFFLE
 D1400029
 COATED TOP & BOTTOM BEAMS AND COATED ANGLE TO BE WITH SCAPATURE.
 TOP & BOT BEAMS: 2-PC COATED AL. 2. BAR IN COATED 304L SUPERINVAR SPACER AND BRKT. 2. BAR IN COATED AL. 20% SCRAPE. 2-PC COATED.

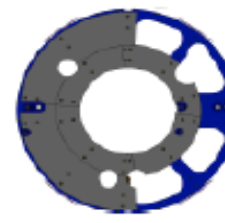
SR2 SCRAFER BAFFLE
 D1400028
 COATED SHORT BEAM FLARE. MC, 2PC & 1PC.
 1PC: 2. BAR IN COATED 304L SUPERINVAR SPACER AND BRKT. 2. BAR IN COATED AL. 20% SCRAPE. 2-PC COATED.



SR2 SCRAFER BAFFLE
 D1400028
 COATED SHORT BEAM FLARE. MC, 2PC & 1PC.
 1PC: 2. BAR IN COATED 304L SUPERINVAR SPACER AND BRKT. 2. BAR IN COATED AL. 20% SCRAPE. 2-PC COATED.



SECTION B-B

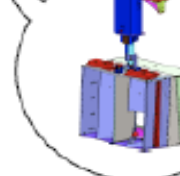
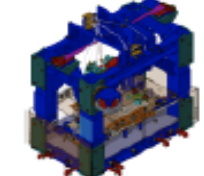
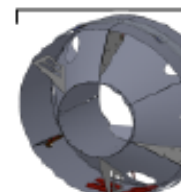
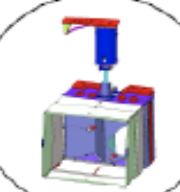


SECTION A-A

LOCAL SHIELD 4 BARREL BAFFLE ASSY
 D1400030, 1PC, 2-PC COATED, 1PC
 COATED 304L SUPERINVAR SPACER AND BRKT. COATED AL. 20% SCRAPE. 2-PC COATED.

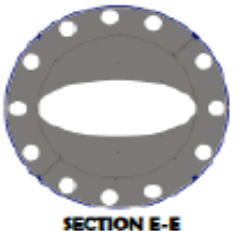
ARM CAVITY BAFFLE, STM
 D1400031, 1PC, 2-PC COATED, 1PC
 COATED 304L SUPERINVAR SPACER AND BRKT. COATED AL. 20% SCRAPE. 2-PC COATED.

TRANSFOLD / OPTOPREP BAFFLE, STM
 D1400032, 1PC, 2-PC COATED, 1PC
 COATED 304L SUPERINVAR SPACER AND BRKT. COATED AL. 20% SCRAPE. 2-PC COATED.



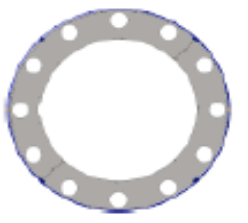
ARM CAVITY BAFFLE, STM
 D1400031, 1PC, 2-PC COATED, 1PC
 COATED 304L SUPERINVAR SPACER AND BRKT. COATED AL. 20% SCRAPE. 2-PC COATED.

TRANSFOLD / OPTOPREP BAFFLE, STM
 D1400032, 1PC, 2-PC COATED, 1PC
 COATED 304L SUPERINVAR SPACER AND BRKT. COATED AL. 20% SCRAPE. 2-PC COATED.



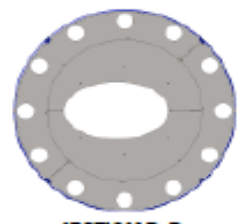
SECTION E-E

MODE CLEANER TUBE BAFFLE HEAD
 D1400033, 1PC, 2-PC COATED, 1PC
 COATED 304L SUPERINVAR SPACER AND BRKT. COATED AL. 20% SCRAPE. 2-PC COATED.



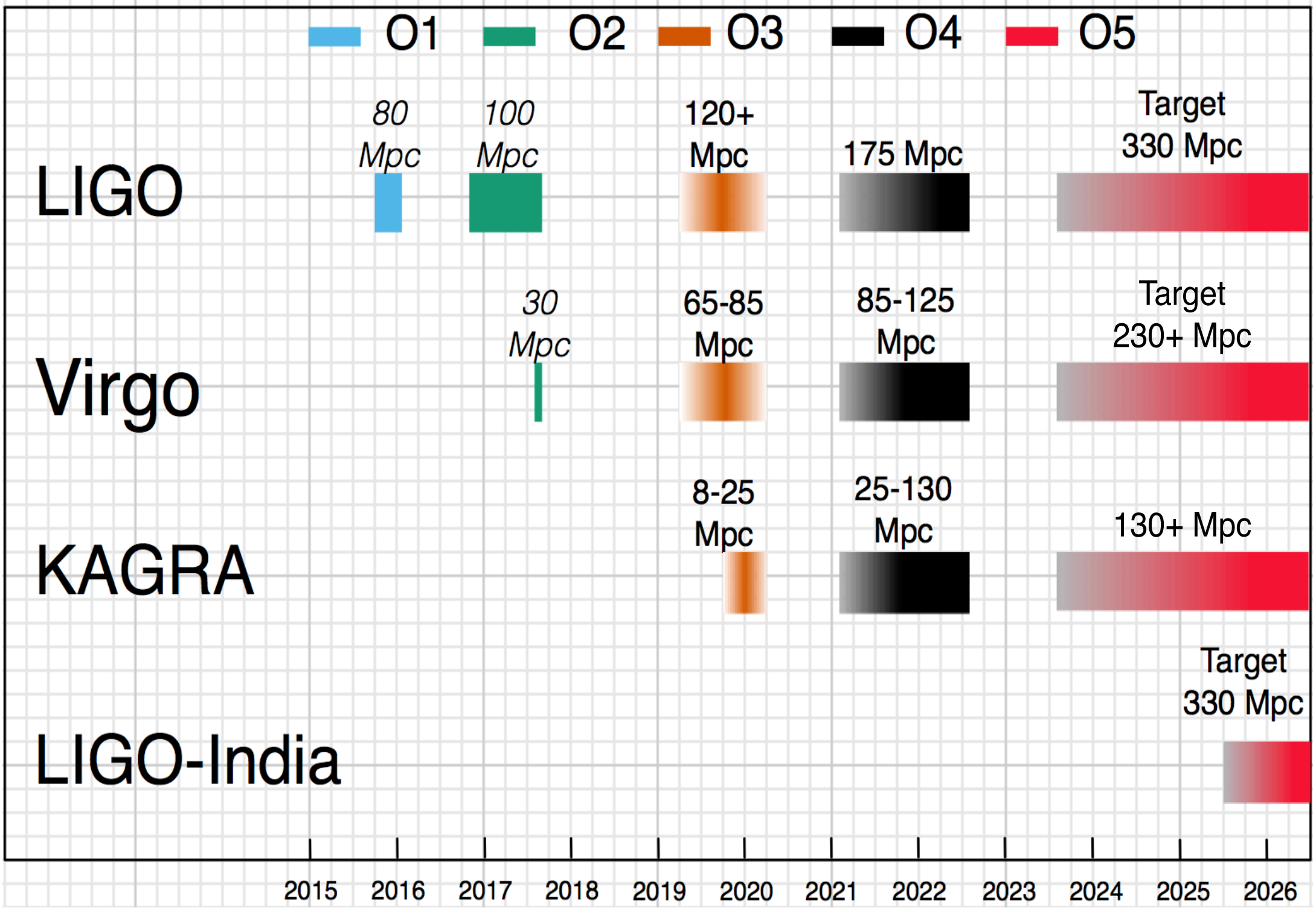
SECTION C-C

MODE CLEANER TUBE BAFFLE HEAD
 D1400033, 1PC, 2-PC COATED, 1PC
 COATED 304L SUPERINVAR SPACER AND BRKT. COATED AL. 20% SCRAPE. 2-PC COATED.



SECTION D-D

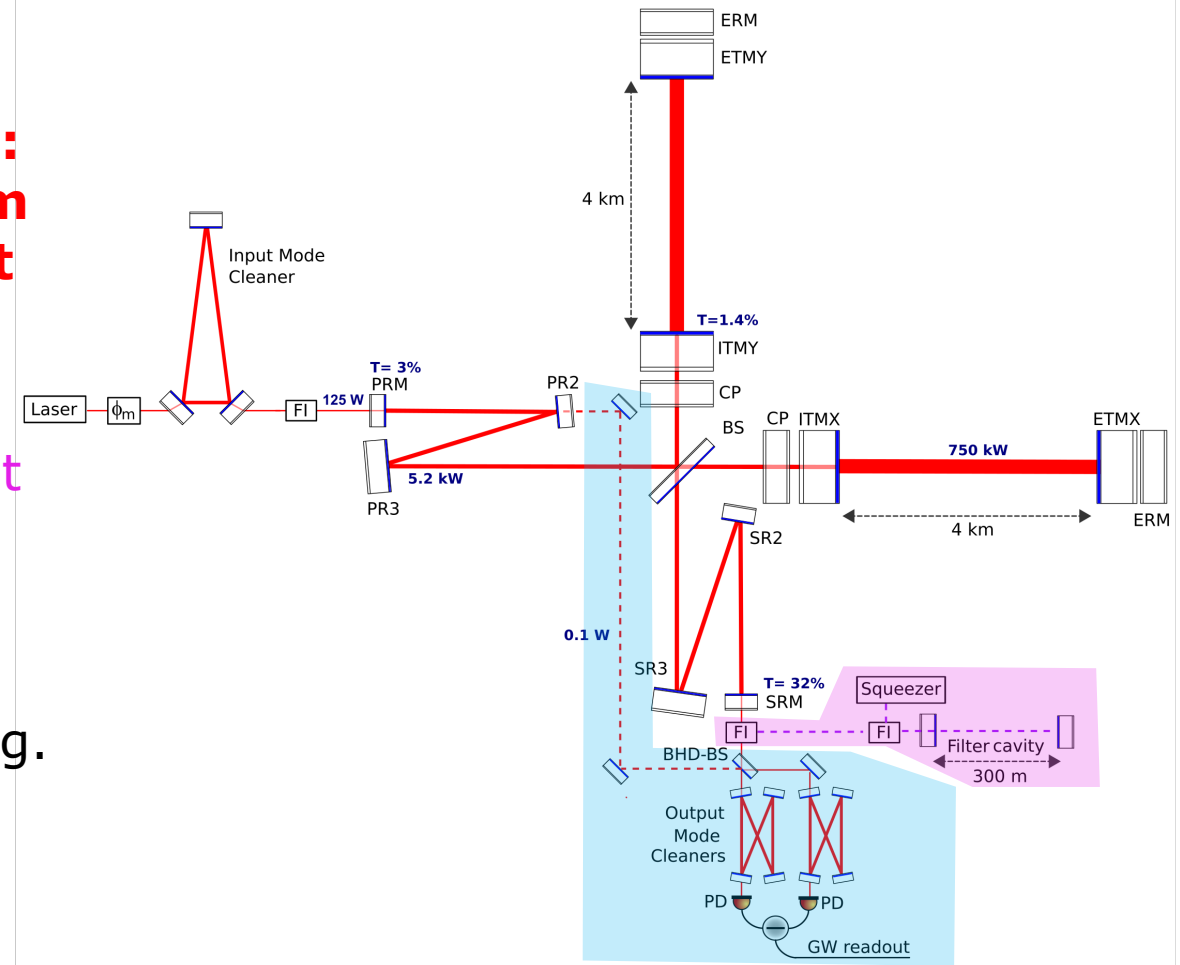
MODE CLEANER TUBE BAFFLE HEAD
 D1400033, 1PC, 2-PC COATED, 1PC
 COATED 304L SUPERINVAR SPACER AND BRKT. COATED AL. 20% SCRAPE. 2-PC COATED.





aLIGO+

- ➔ **US/UK linked proposals + in-kind contribution from AU: 20M\$ from NSF + £10M from STFC. US project started Oct 1st.**
- ➔ 2nd upgrade: 300m filter cavity to provide frequency dependent squeezing
- ➔ Aim: obtain squeezing at high frequency without spoiling low frequency due to anti-squeezing. Short cavity sufficient.
- ➔ In order to get full squeezing benefit will have to switch to **balanced homodyne readout**.





aLIGO+

Becoming available ~2024

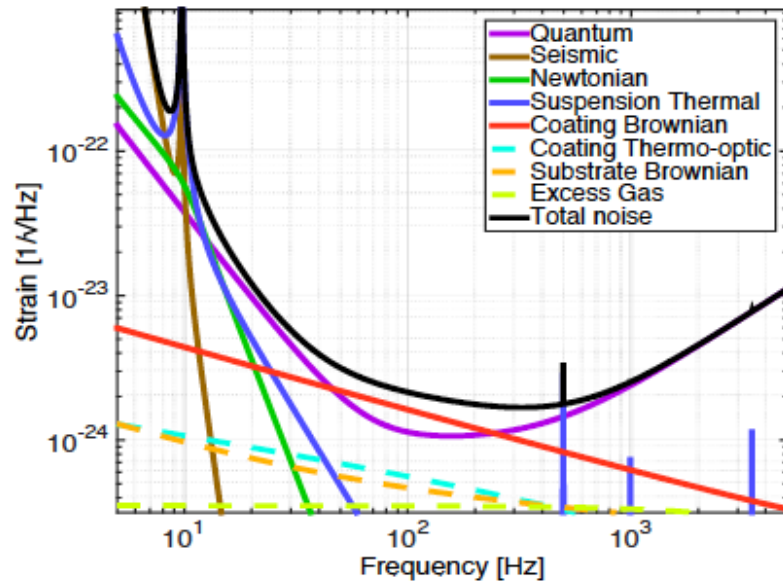
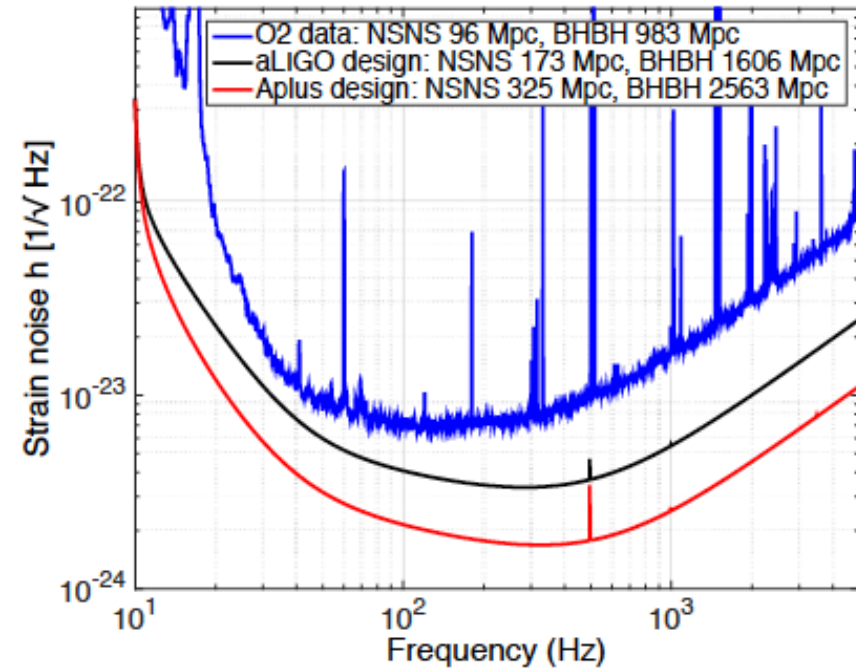


Figure 10: Target A+ strain spectral density (black) with dominant contributing factors [56]. Coating Brownian and quantum noise are targeted in the upgrade; other noise terms are unchanged with respect to aLIGO (Figure 8).



- ➔ In addition to quantum noise improvements aLIGO+ assumes factor 2 reduction in coating noise.
- ➔ Overall improvement will yield **increase in detection rate of 4-7.**

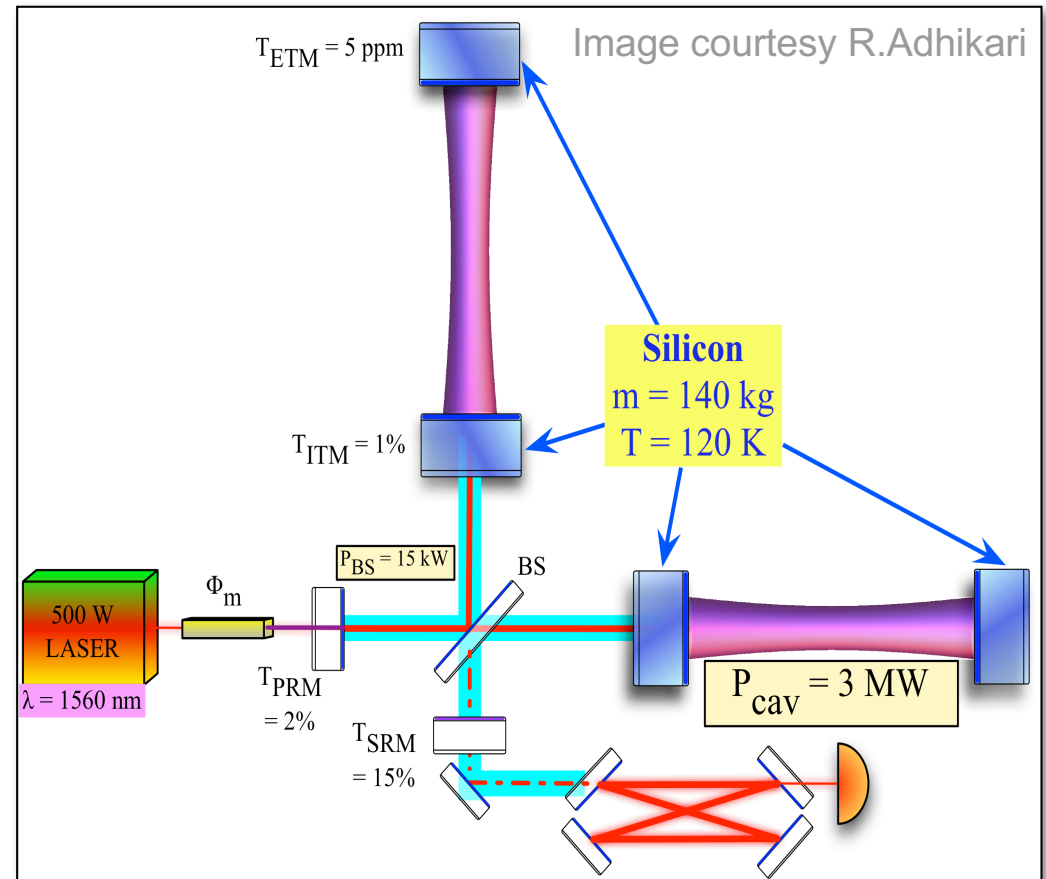


Voyager (1)

- ➔ Based on **cryogenic (120K) silicon test masses** and suspensions to reduce thermal noise.
- ➔ Good properties of silicon:
 - Thermal expansion has a zero-crossing at 120K.
 - High thermal conductivity => smaller thermal gradients.

Winkler et al, Phys. Rev. A 44, 7022–7036 (1991)

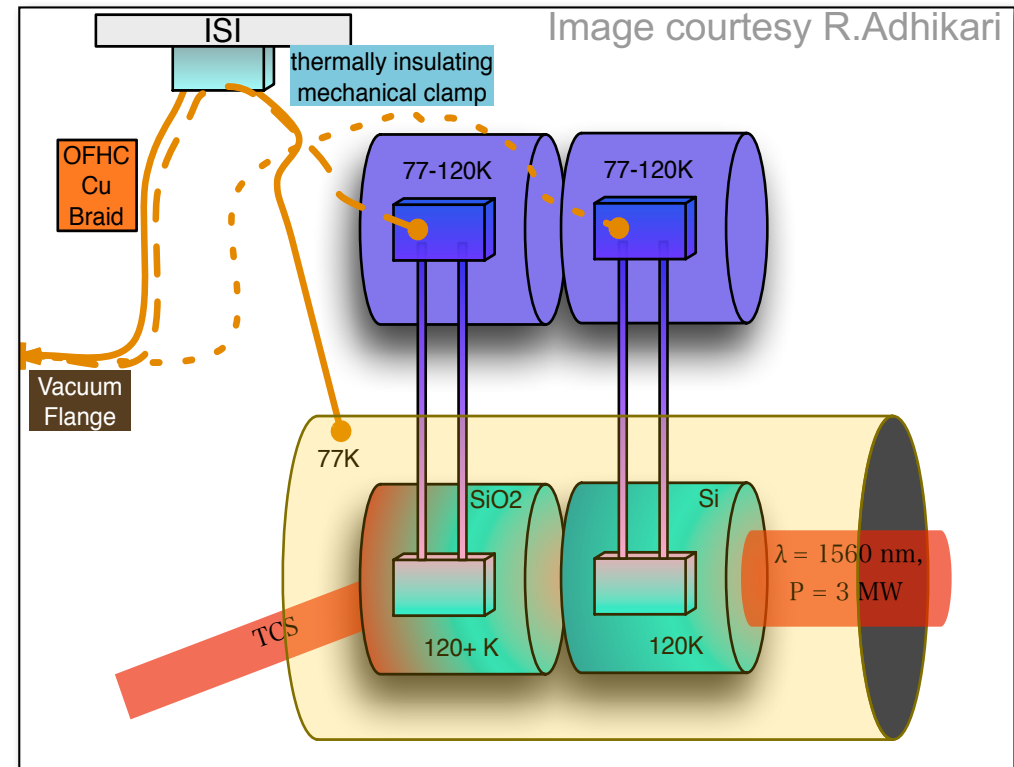
- ➔ **Purpose of going cryogenic is to enable high power operation.**





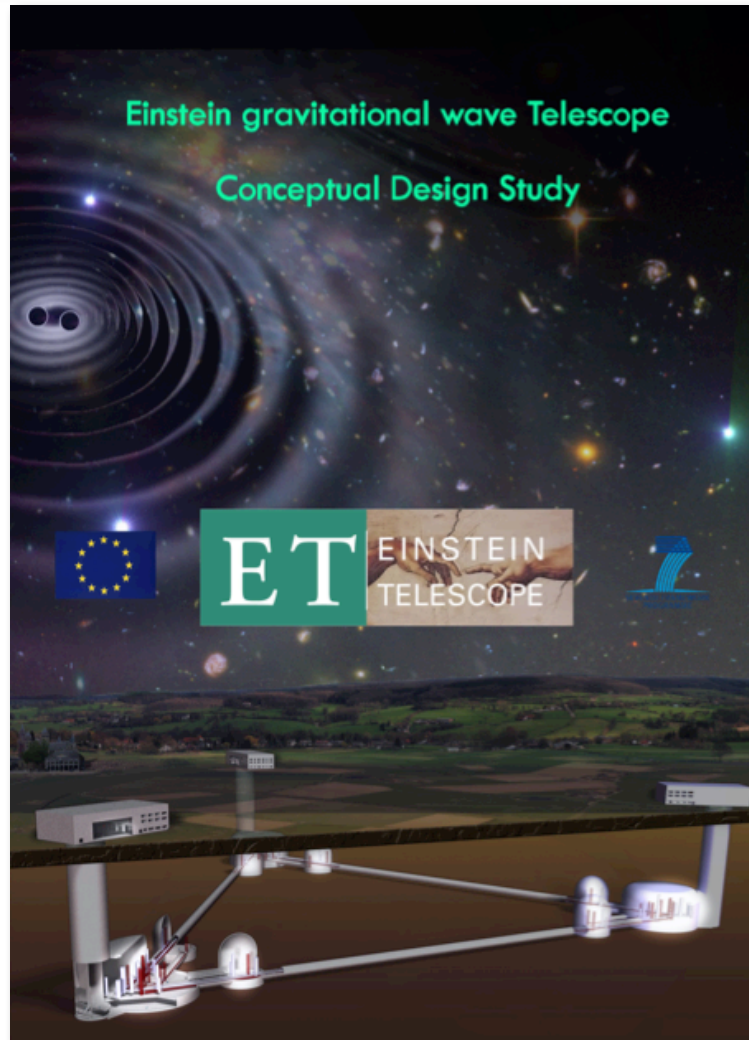
Voyager (2)

- ➔ In contrast to the Einstein Telescope and KAGRA (both operating at 10-20K range) the cooling in Voyager design will mainly be done via radiation (and not via conduction through the fibres).
- ➔ As a result the cryogenic implementation is simpler and higher optical powers can be possible.





ET Design study



Author list: ET Science Team

M Abernathy¹, F Acernese^{2,3}, P Ajith³⁰, B Allen⁴, P Amaro-Seoane^{54,32}, N Andersson⁵, S Aoudia⁵⁴, P Astone^{6,7}, B Krishnan⁴, L Barack⁵, F Barone^{2,3}, B Barr¹, M Barsuglia⁸, M Bassan^{9,10}, R Bassiri¹, M Beker¹¹, N Beveridge¹, M Bizouard¹², C Bond¹³, S Bose¹⁴, L Bosi¹⁵, S Braccini¹⁶, C Bradaschia^{16,17}, M Britzger⁴, F Brueckner¹⁸, T Bulik¹⁹, H J Bulten²⁰, O Burmeister⁴, E Calloni^{21,21}, P Campsie¹, L Carbone¹³, G Cella¹⁶, E Chalkley¹³, E Chassande-Mottin⁸, S Chelkowski¹³, A Chincarini²², A Di Cintio⁶, J Clark²⁶, E Coccia^{9,10}, CN Colacino¹⁶, J Colas¹⁷, A Colla^{6,7}, A Corsi³⁰, A Cumming¹, L Cunningham¹, E Cuoco¹⁷, S Danilishin²³, K Danzmann⁴, E Daw²⁸, R De Salvo²⁵, W Del Pozzo¹¹, T Dent²⁶, R De Rosa^{2,21}, L Di Fiore², M Di Paolo Emilio⁹, A Di Virgilio¹⁶, A Dietz²⁷, M Doets¹¹, J Dueck⁴, M Edwards²⁶, V Fafone^{9,10}, S Fairhurst²⁶, P Falferi^{29,56}, M Favata³⁰, V Ferrari^{6,7}, F Ferrini¹⁷, F Fidecaro^{17,51}, R Flaminio³¹, J Franc³¹, F Frasconi¹⁶, A Freise¹³, D Friedrich⁴, P Fulda¹³, J Gair⁵⁷, M Galimberti³¹, G Gemme²², E Genin¹⁷, A Gennai¹⁶, A Giazotto^{16,17}, K Glampedakis⁴⁰, R Gouaty²⁷, C Graef⁴, W Graham¹, M Granata⁸, H Grote⁴, G Guidi^{33,34}, J Hallam¹³, G Hammond¹, M Hannam²⁶, J Harms³⁰, K Haughian¹, I Hawke⁵, D Heinert¹⁸, M Hendry¹, I Heng¹, E Hennes¹¹, S Hild¹, J Hough¹, D Huet¹⁷, S Husa⁵⁵, S Huttner¹, B Iyer³⁸, I Jones⁵, G Jones¹, I Kamaretsos²⁶, C Kant Mishra³⁸, F Kawazoe⁴, F Khalili³⁹, B Kley¹⁸, K Kokeyama¹³, K Kokkotas⁴⁰, S Kroker¹⁸, R Kumar¹, K Kuroda⁴¹, B Lagrange³¹, N Lastzka⁴, T G FLi¹¹, M Lorenzini³³, G Losurdo^{33,17}, H Lück⁴, E Majorana⁶, V Malvezzi^{9,10}, I Mandel^{42,13}, V Mandic³⁶, S Marka⁵⁰, F Marin³³, F Marion²⁷, J Marque¹⁷, I Martin¹, D McLeod²⁶, D Mckechnan²⁶, M Mehmet⁴, C Michel³¹, Y Minenkov⁹, N Morgado³¹, A Morgia⁹, S Mosca^{2,21}, L Moscatelli⁶, B Mours²⁷, H Müller-Ebhardt⁴, P Murray¹, L Naticchioni^{6,7}, R Nawrodt¹⁸, J Nelson¹, R O'Shaughnessy⁴³, C D Ott³⁰, C Palomba⁶, A Paoli¹⁷, G Parguez¹⁷, A Pasqualetti¹⁷, R Passaquietti¹⁶, D Passuello¹⁶, M Perciballi⁶, F Piergiovanni^{33,34}, L Pinard³¹, M Pitkin¹, W Plastino⁴⁴, M Plissi¹, R Poggiani¹⁶, P Popolizio¹⁷, E Porter⁸, M Prato²², G Prodi^{45,56}, M Punturo^{15,17}, P Puppó⁶, D Rabeling²⁰, I Racca¹⁶, P Rapagnani^{6,7}, V Re⁹, J Read³⁷, T Regimbau⁴⁷, H Rehbein⁴, S Reid¹, L Rezzolla⁵⁴, F Ricci^{6,7}, F Richard¹⁷, A Rocchi⁹, R Romano², S Rowan¹, A Rüdiger⁴, A Sambrowski⁴, L Santamaría³⁰, B Sassolas³¹, B Sathyaprakash²⁶, R Schilling⁴, P Schmidt²⁶, R Schnabel⁴, B Schutz^{26,54}, C Schwarz¹⁸, J Scott¹, P Seidel¹⁸, A M Sintees⁵⁵, K Somiya⁴⁸, C F Sopuerta⁴⁹, B Sorazu¹, F Speirits¹, L Storchio¹⁵, K Strain¹, S Strigin²³, P Sutton²⁶, S Tarabrin⁴, B Taylor⁴, A Thürin⁴, K Tokmakov¹, M Tonelli^{16,51}, H Tournefier²⁷, R Vaccarone¹⁷, H Vahlbruch⁴, J F J van den Brand^{11,20}, C Van Den Broeck¹¹, S van der Putten¹¹, M van Veggel¹, A Vecchio¹³, J Veitch²⁶, F Vettrano^{33,34}, A Vicere^{33,34}, S Vyatchanin²³, P WeRele⁵², R Willeke⁴, W Winkler⁴, C Wopen¹, K Wojcik²⁶, A Woodcraft⁵³, K Yamamoto³⁵

Available at:

<http://www.et-gw.eu/etdsdocument>

² INFN, Sezione di Napoli, Italy

³ Università di Salerno, Fisciano, I-84084 Salerno, Italy

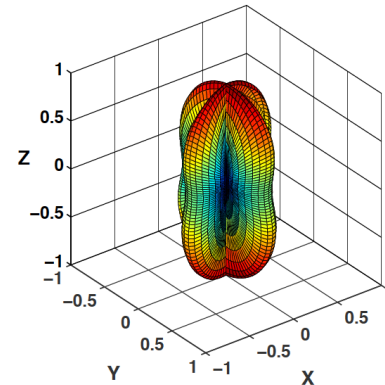
⁴ Max-Planck-Institut für Gravitationsphysik und Leibniz Universität Hannover, D-30167 Hannover, Germany



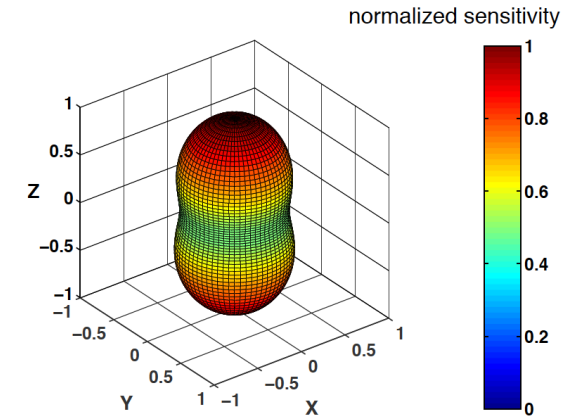
The ET Footprint

- ➔ As ET is a new infrastructure, we can start from scratch.
- ➔ What to see the full sky.
- ➔ Want to resolve both polarisations.
- ➔ Want to have redundancy.
- ➔ 1 Triangle vs 4 Ls:
 - Both have 30km integrated tunnel length
 - Both resolve both polarisations and offer redundancy.
 - Both give equivalent sensitivity.
 - Triangle reduces the number of end stations.
- ➔ **ET will be a triangle.**

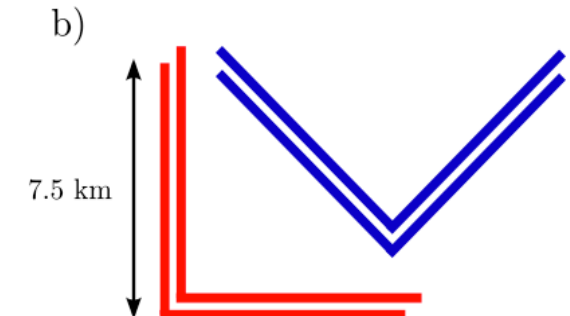
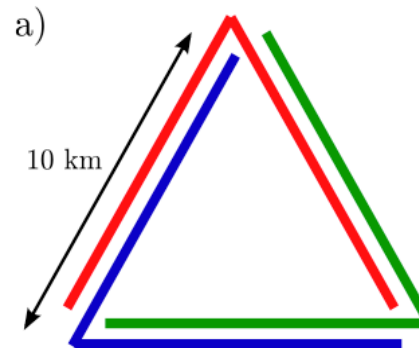
Single L-shaped IFO



Triangle of 3 IFOs



Freise, A.; Chelkowski, S.; Hild, S.; Pozzo, W. D.; Perreca, A. & Vecchio, A. *CQG*, **2009**, 26, 085012 (14pp)



Triangle first proposed: 1985, MPQ-101. W.Winkler, K.Maischberger, A.Rüdiger, R.Schilling, L.Schnupp, D.Shoemaker,: Plans for a Large Gravitational Wave Antenna in Germany



Xylophone Concept

- ➔ As our detectors become more and more complex and at the same time aim increase even further the observation bandwidth the xylophone concept becomes more and more attractive.
- ➔ The xylophone concept was originally suggested for advanced LIGO:

R.DeSalvo, CQG 21 (2004) S1145-S1154

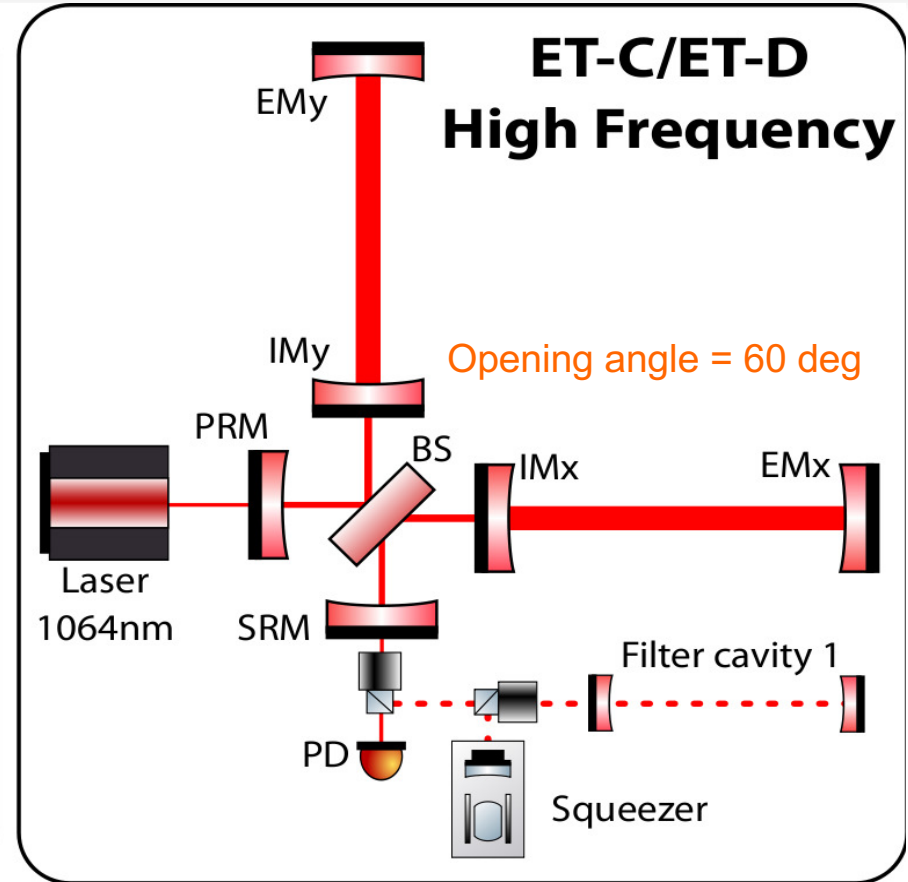
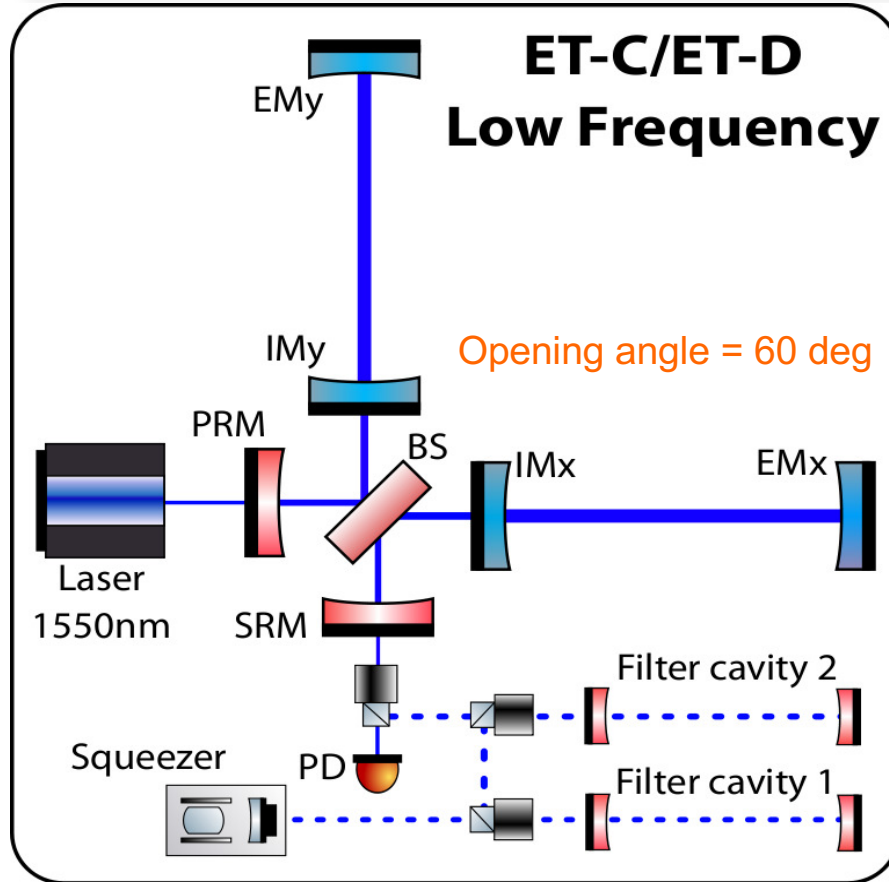
G.Conforto and R.DeSalvo, Nuc. Instruments 518 (2004) 228 - 232






D.Shoemaker, presentation at Aspen meeting (2001), <http://www.ligo.caltech.edu/docs/G/G010026-00.pdf>

- ➔ Allows to overcome 'contradicting' requirements in the technical detector design:
 - To reduce **shot noise** you have to increase the light power, which in turn will reduce the sensitivity at low frequencies due to higher **radiation pressure** noise.
 - Need cryogenic mirrors for low frequency sensitivity. However, due to residual absorption it is hard to combine **cryogenic mirrors** with **high power** interferometers.
- ➔ For ET we choose the conservative approach (designing an infrastructure) and went for a 2-band xylophone: **low-power, cryogenic low-frequency detector** and a **high-power, room-temperature high-frequency detector**.



The ET core interferometers

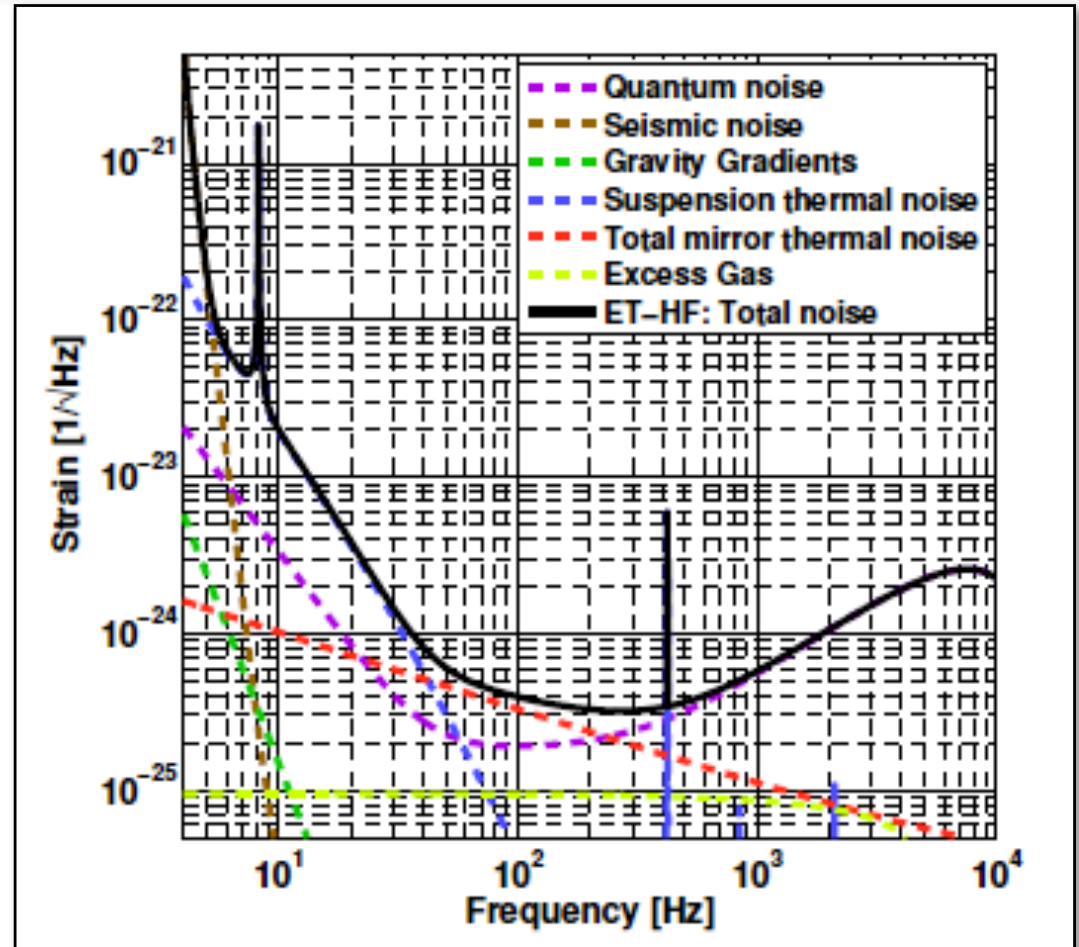


	Optical element, Fused Silica, room temperature		Optical element, Silicon, cryogenic		Laser beam 1550nm
					Laser beam 1064nm
					squeezed light beam



The High-Frequency Detector

- **Quantum noise:** 3MW, tuned Signal-Recycling, 10dB Squeezing, 200kg mirrors.
- **Suspension Thermal and Seismic:** Superattenuator
- **Gravity gradient:** No Subtraction
- **Thermal noise:** 290K, 12cm beam radius, fused Silica, LG33 (reduction factor of 1.6 compared to TEM00).

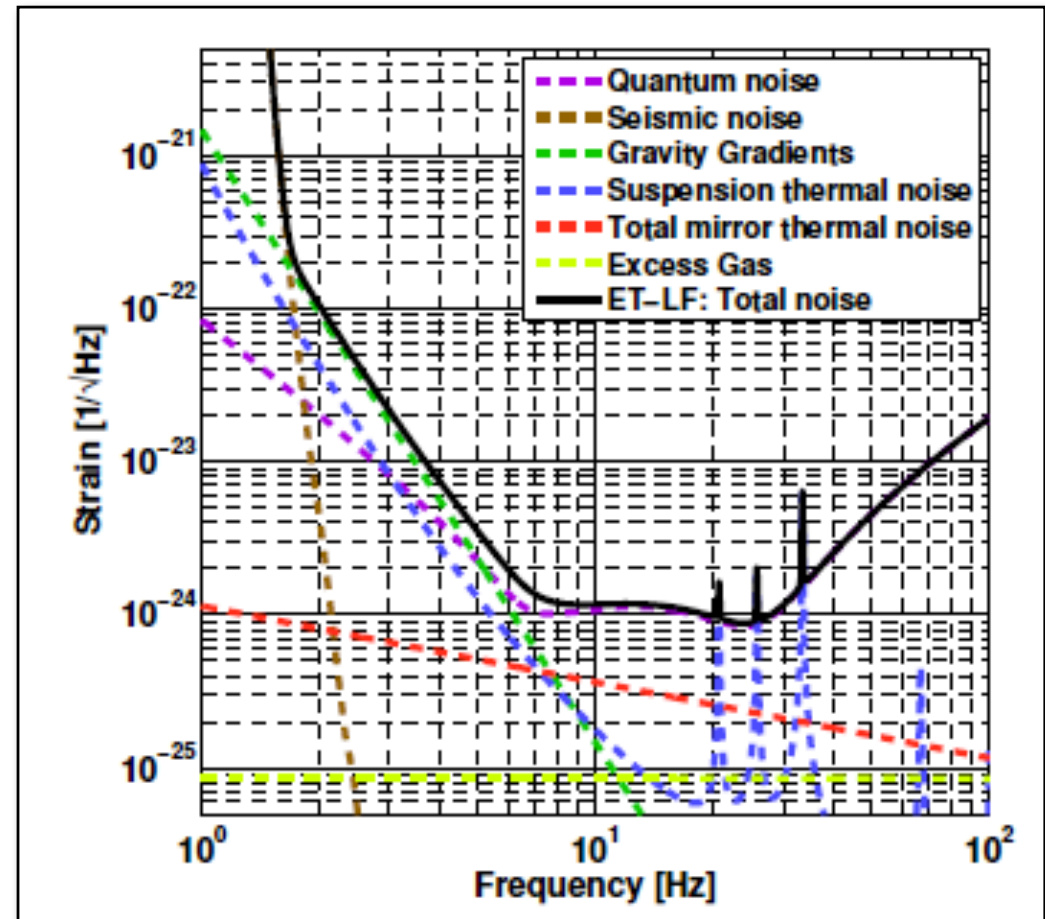


Coating Brownian reduction factors (compared to 2G):
3.3 (arm length), 2 (beam size) and 1.6 (LG33) = 10.5



The Low-Frequency Detector

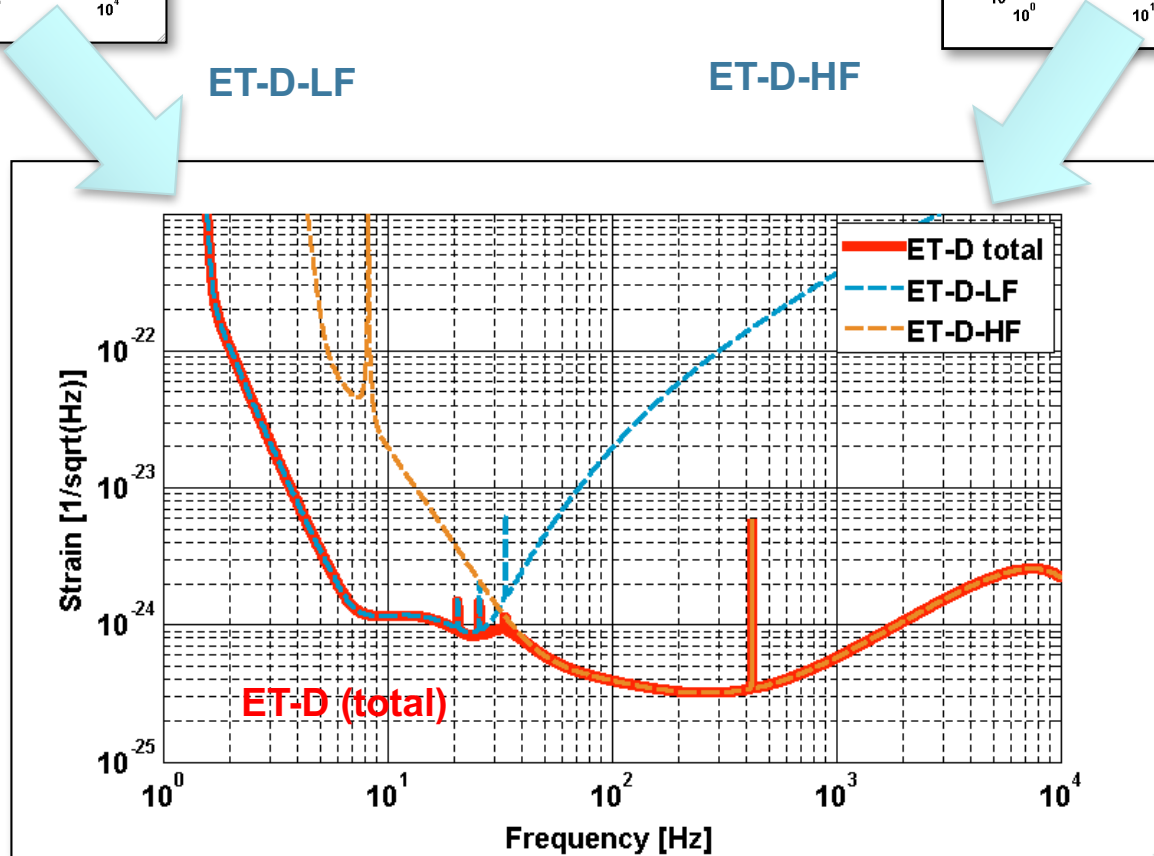
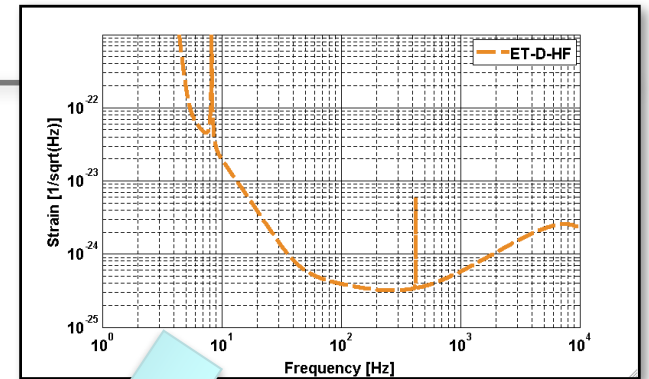
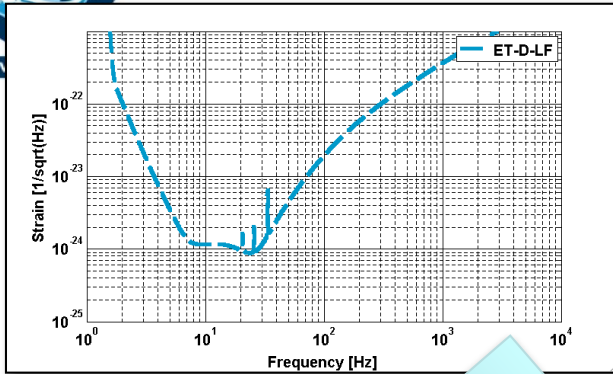
- ➔ **Quantum noise:** 18kW, detuned Signal-Recycling, 10dB frequency dependent squeezing, 211kg mirrors, 1550nm.
- ➔ **Seismic:** 17m Superattenuator
- ➔ **Gravity gradient:** Underground, Black forest location
- ➔ **Thermal noise:** 10K, Silicon, 9cm beam radius, TEM00.
- ➔ **Suspension Thermal:** 3mm Silicon fibres. Penultimate mass at 2K.



As mirror TN is no longer limiting, one can relax the assumptions on the material parameters and the beam size...

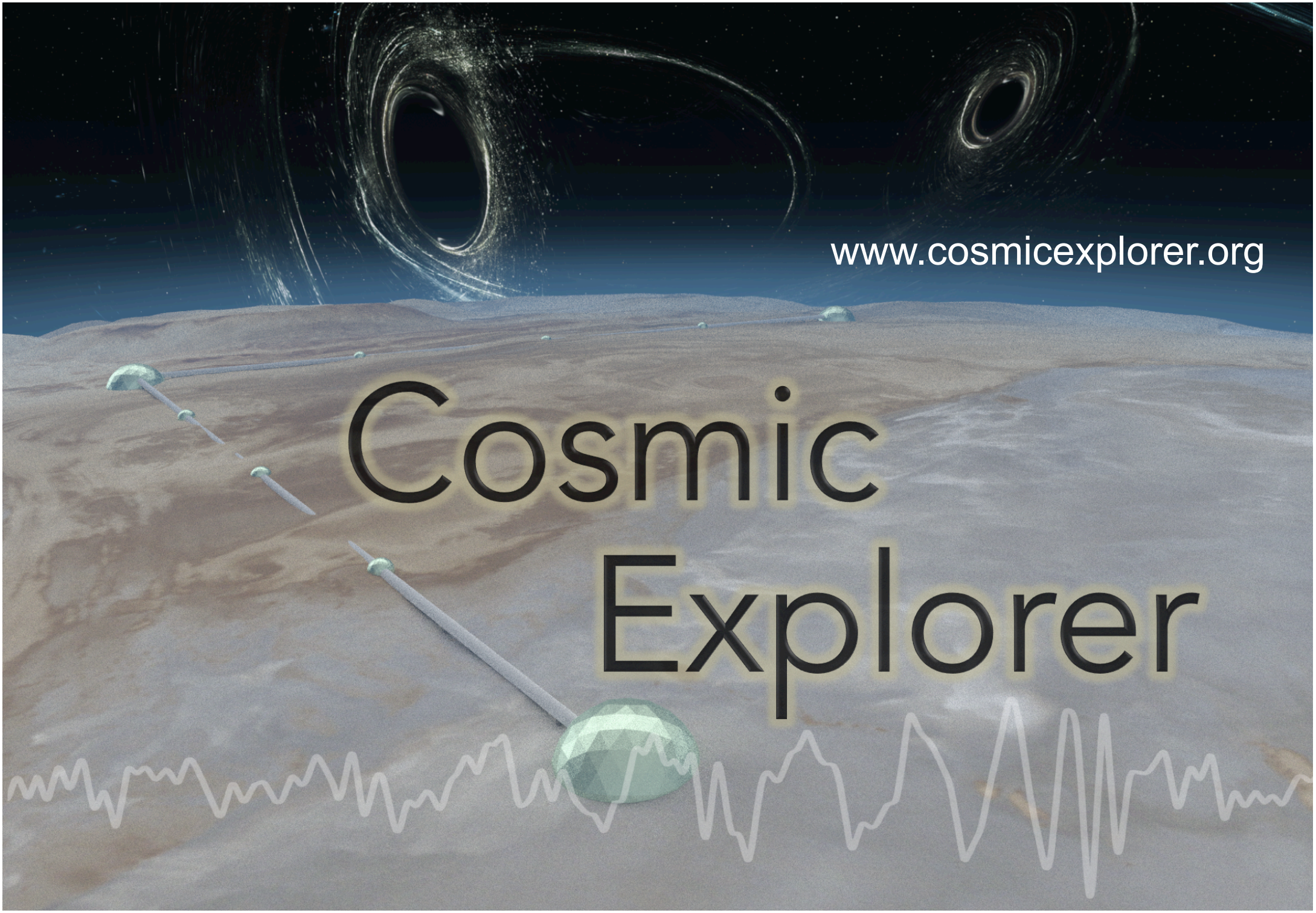


Combining 2 IFOs



www.cosmicexplorer.org

Cosmic Explorer



How do fundamental noises scale?

Shot Noise
while maintaining bandwidth

$$\frac{h_{\text{shot}}}{h_{0 \text{ shot}}} = \sqrt{\frac{2 \text{ MW}}{P_{\text{arm}}}} \sqrt{\frac{\lambda}{1.5 \mu\text{m}}} \left(\frac{3}{r_{\text{sqz}}}\right) \sqrt{\frac{40 \text{ km}}{L_{\text{arm}}}}$$

Radiation Pressure Noise
while maintaining bandwidth

$$\frac{h_{\text{RPN}}}{h_{0 \text{ RPN}}} = \sqrt{\frac{P_{\text{arm}}}{2 \text{ MW}}} \sqrt{\frac{1.5 \mu\text{m}}{\lambda}} \left(\frac{3}{r_{\text{sqz}}}\right) \left(\frac{320 \text{ kg}}{m_{\text{TM}}}\right) \left(\frac{40 \text{ km}}{L_{\text{arm}}}\right)^{3/2}$$

Coating Thermal Noise
constant loss angle...

$$\frac{h_{\text{CTN}}}{h_{0 \text{ CTN}}} = \sqrt{\frac{T}{123 \text{ K}}} \sqrt{\frac{\phi_{\text{eff}}}{5 \times 10^{-5}}} \left(\frac{14 \text{ cm}}{r_{\text{beam}}}\right) \left(\frac{40 \text{ km}}{L_{\text{arm}}}\right)$$

Residual Gas Noise
facility limit...

$$\frac{h_{\text{gas}}}{h_{0 \text{ gas}}} = \sqrt{\frac{P_{\text{gas}}}{4 \times 10^{-7} \text{ Pa}}} \sqrt{\frac{14 \text{ cm}}{r_{\text{beam}}}} \sqrt{\frac{40 \text{ km}}{L_{\text{arm}}}}$$

Where could we put a 40km detector?

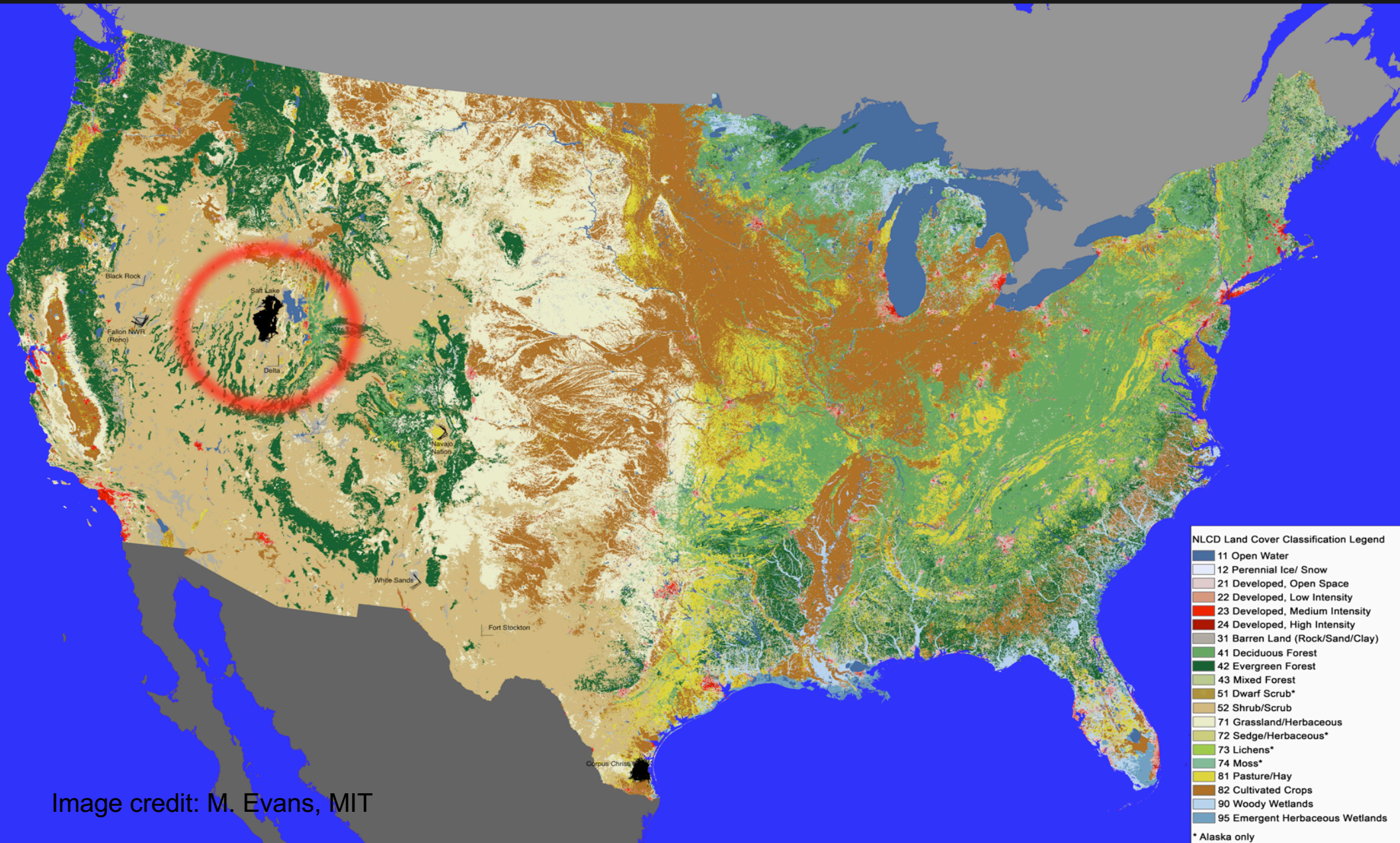
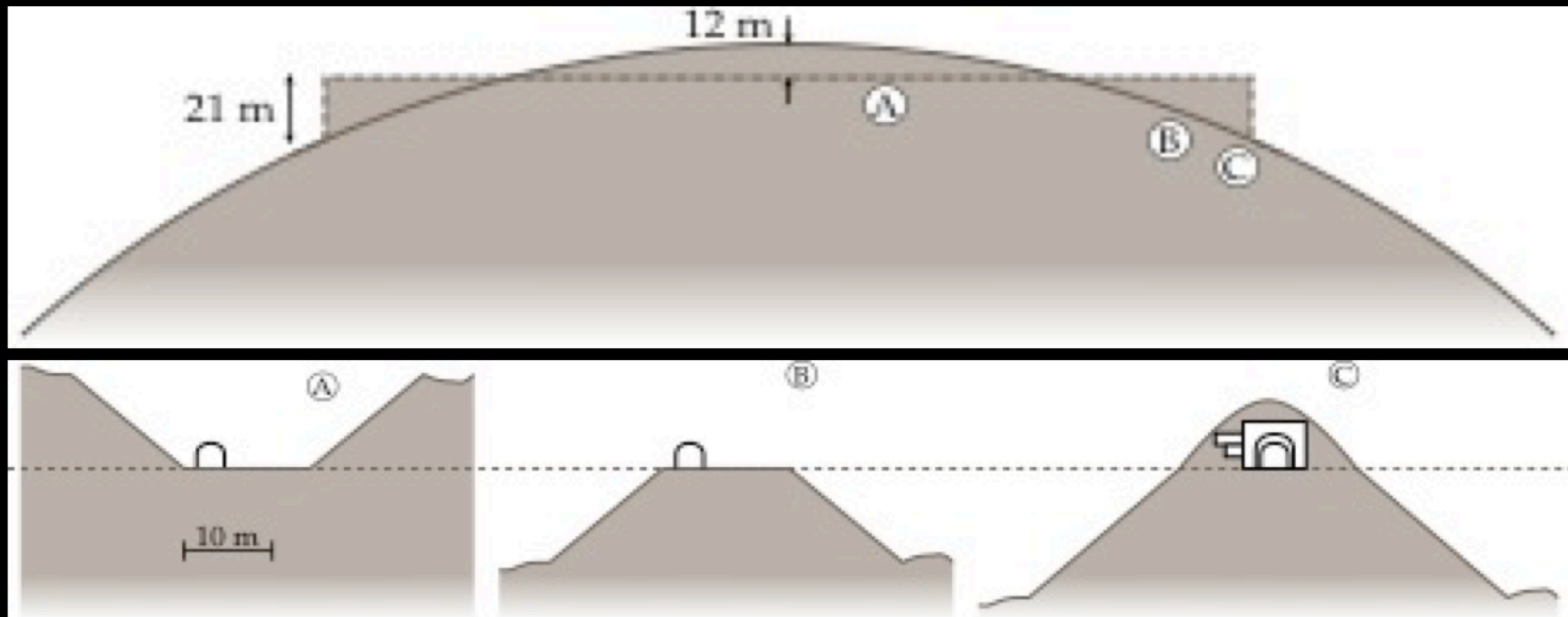


Image credit: M. Evans, MIT

Why 40 km?

- Costs grow quickly with length above ~ 40km
 - surface excavation depth is quadratic in length, and that earth must be moved (presumably to the ends to use as fill)
 - flat or bowl-shaped locations become scarce for longer sites

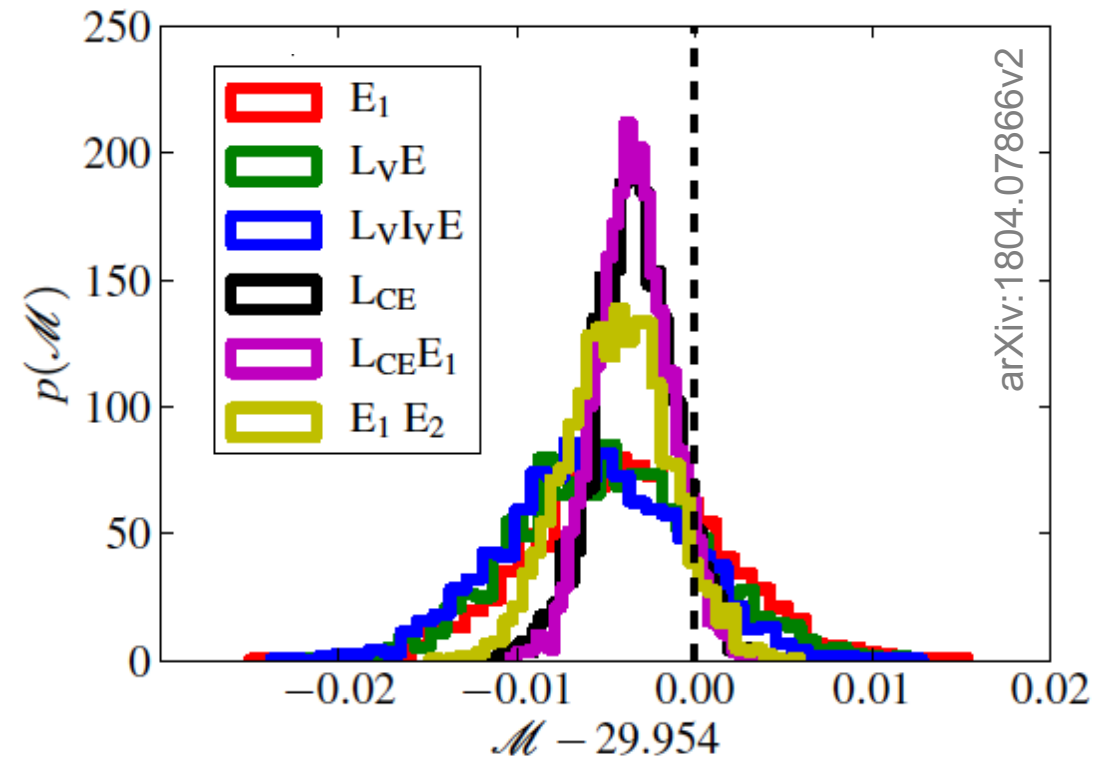
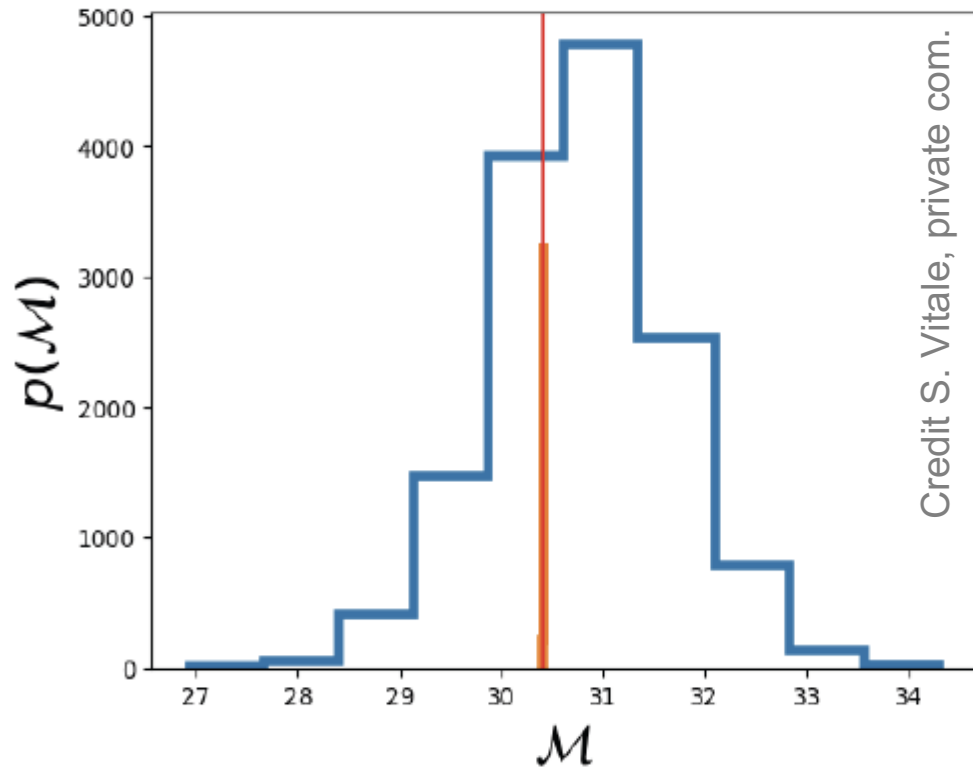


Known Unknowns – Big Mirrors

- Getting big enough substrates for Voyager poses a problem, but apparently one that can be addressed. What about CE?
 - Can we make **silicon** mirrors big enough for CE (~1m diameter)?
 - If, for whatever reason, we end up with the initial version of CE running at room temperature on **silica**, the substrate production may also be challenging, but probably less so.
- Polishing seems doable, but better than aLIGO would be good
- Coating these large optics will be non-trivial
 - for IBS coatings, it is “just a matter of engineering” (easy to say)
 - for crystalline coatings, it may be more challenging

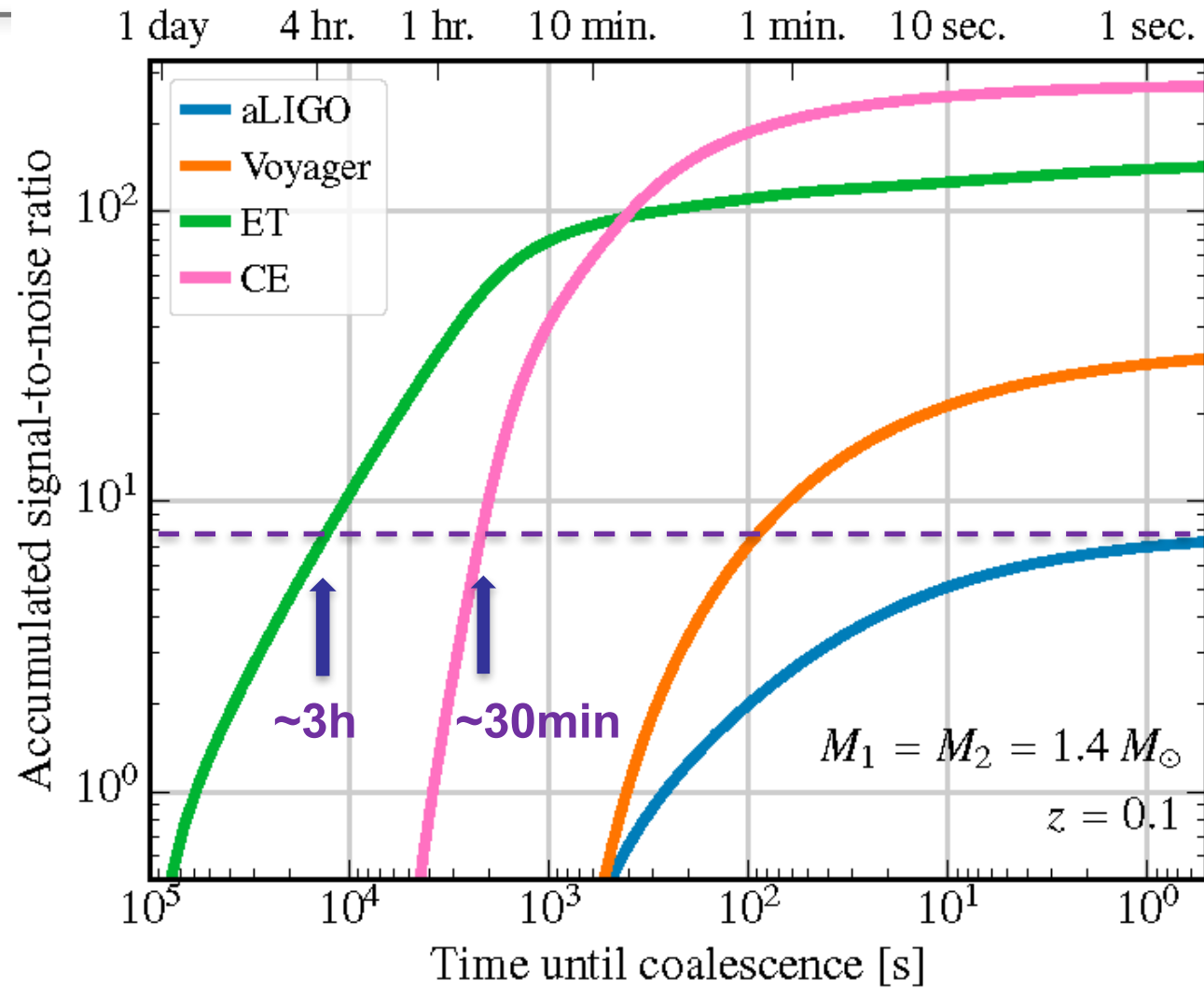


PE of GW150914-like event with 3G



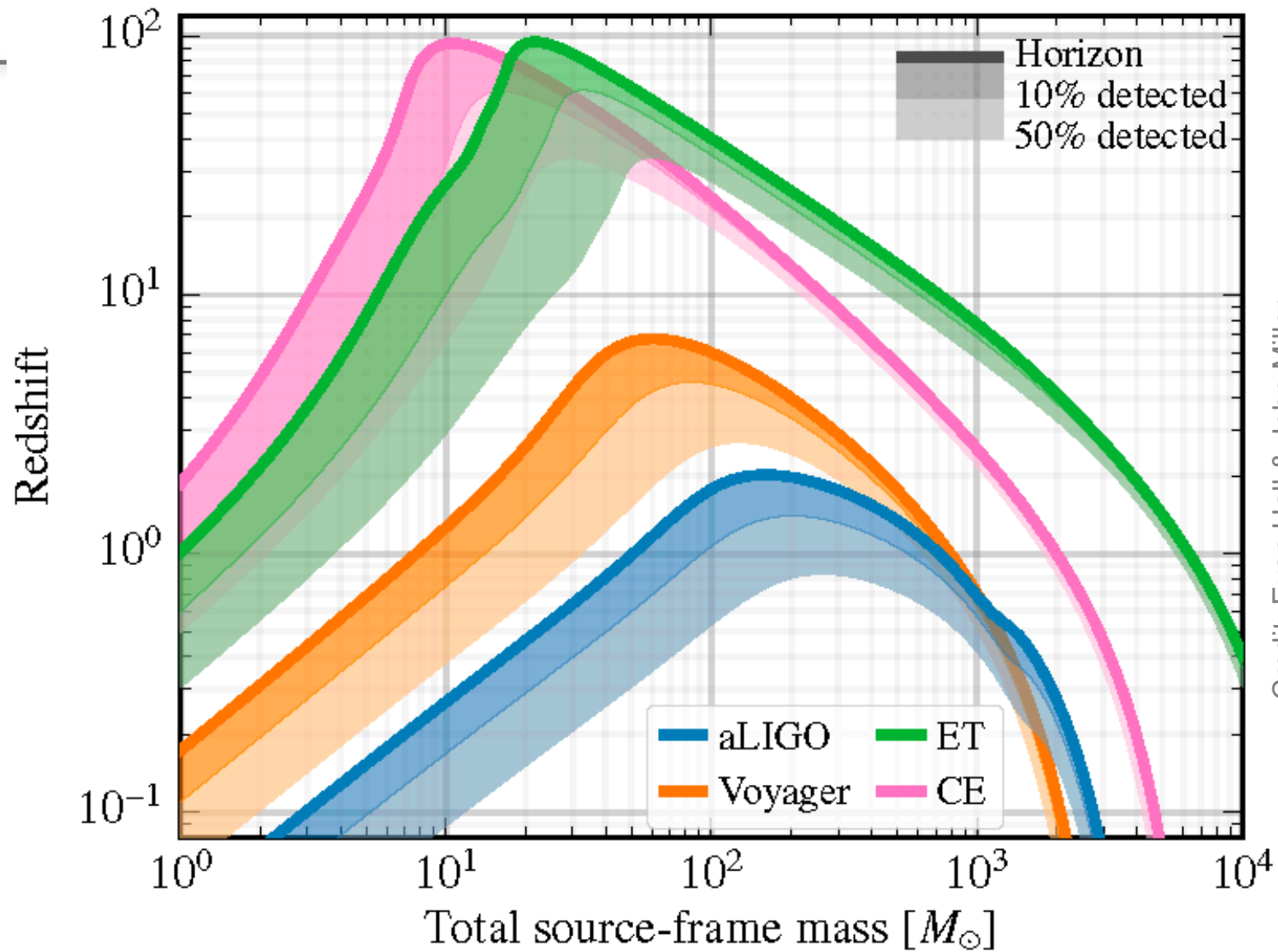


BNS pre-warning time with 3G



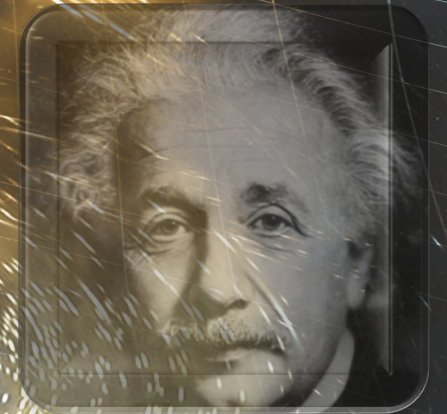


Cosmological reach of 3G



Credit: Evan Hall & John Miller

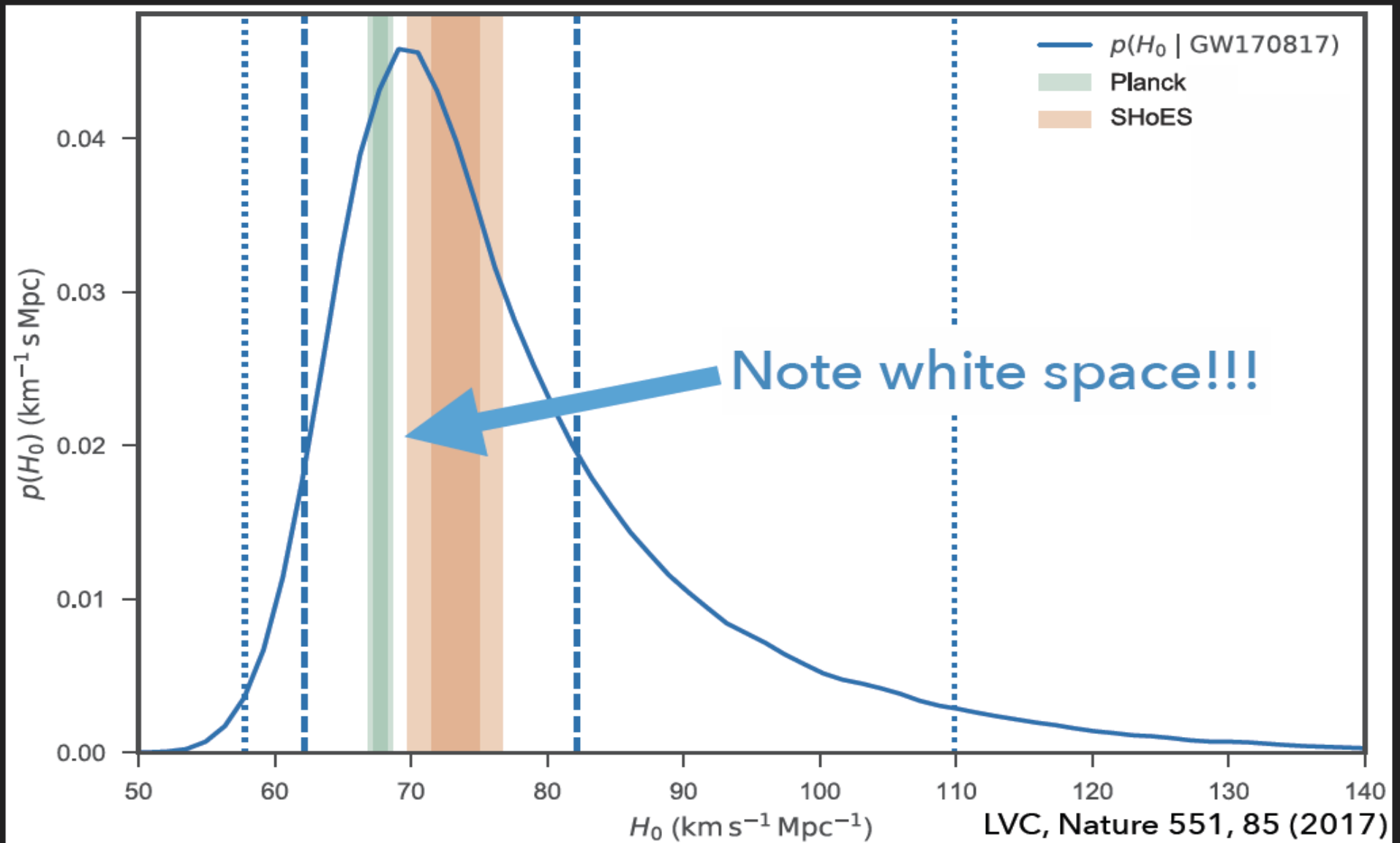
GW Astronomy results to date and pro-spects, Current and future GW detectors – sensitivity they achieve and how they do it, **Astrophysical requirements and benefits of calibration accuracy**



Prof Stefan Hild,
University of Glasgow, UK

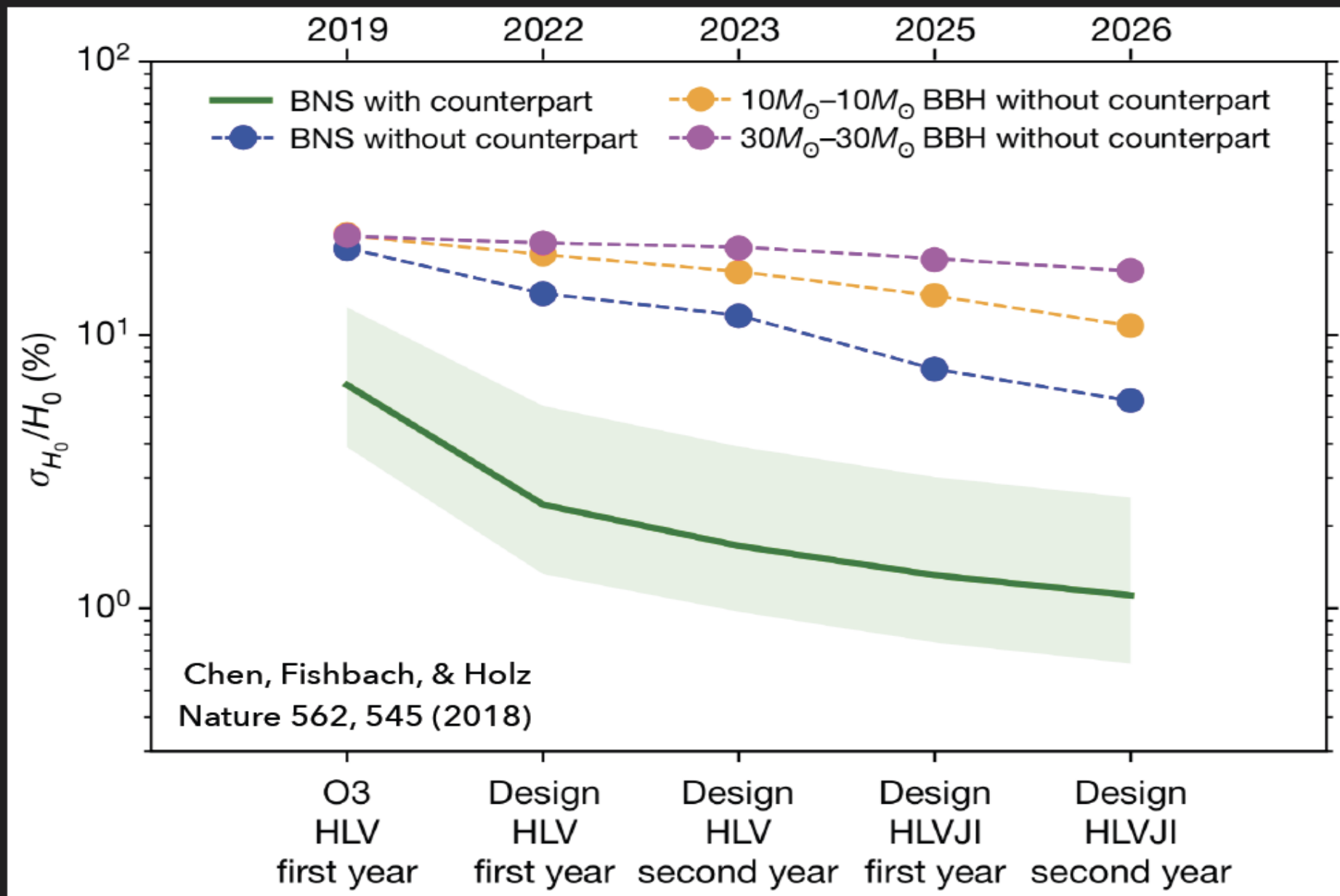


Who cares about standard sirens?



$$H_0 = 70.0_{-8}^{+12} \text{ km s}^{-1} \text{ Mpc}^{-1}$$

We need 1% soon!



Percent-level measurement in ~5 years!

Calibrating gravitational-wave detectors with GW170817

Reed Essick, Daniel E. Holz

(Submitted on 21 Feb 2019)

The waveform of a compact binary coalescence is predicted by general relativity. It is therefore possible to directly constrain the response of a gravitational-wave (GW) detector by analyzing a signal's observed amplitude and phase evolution as a function of frequency. GW signals alone constrain the relative amplitude and phase between different frequencies within the same detector and between different detectors. We analyze GW170817's ability to calibrate the LIGO/Virgo detectors, finding a relative amplitude calibration precision of approximately $\pm 20\%$ and relative phase precision of $\pm 15^\circ$ ($1-\sigma$ uncertainty) between the LIGO Hanford and Livingston detectors. Incorporating additional information about the distance and inclination of the source from electromagnetic observations, the relative amplitude of the LIGO detectors can be tightened to $\sim \pm 15\%$. We investigate the ability of future events to improve astronomical calibration. By simulating the cumulative uncertainties from an ensemble of detections, we find that with several hundred events with electromagnetic counterparts, or several thousand events without counterparts, we reach percent-level astronomical calibration. This corresponds to $\sim 5-10$ years of operation at advanced LIGO and Virgo design sensitivity. It is to be emphasized that direct *in-situ* measurements of detector calibration provide significantly higher precision than astronomical sources, and already constrain the calibration to a few percent in amplitude and a few degrees in phase. In this sense, our astronomical calibrators only corroborate existing calibration measurements. Nonetheless, astrophysical calibration may become an important corroboration of existing calibration methods, providing a completely independent constraint of potential systematics.

Comments: 12 pages, 6 figures

Subjects: **Instrumentation and Methods for Astrophysics (astro-ph.IM)**; General Relativity and Quantum Cosmology (gr-qc)Cite as: [arXiv:1902.08076](#) [astro-ph.IM](or [arXiv:1902.08076v1](#) [astro-ph.IM] for this version)

Submission history

From: Reed Essick [[view email](#)]

[v1] Thu, 21 Feb 2019 14:44:48 UTC (2,966 KB)

[Which authors of this paper are endorsers?](#) | [Disable MathJax](#) ([What is MathJax?](#))[Browse v0.1](#)



We assume additive stationary Gaussian noise (n) in each detector and model the data recorded (d) as a function of frequency as

$$d = n + (1 + \delta A) e^{i\delta\psi} (F_+ h_+ + F_\times h_\times) \quad (1)$$

where δA is the amplitude calibration error, $\delta\psi$ the phase error, $F_{+,\times}$ are the antenna response functions,¹ and $h_{+,\times}$ the astrophysical strain incident on the detectors. The strain incident on the detector can be written as

$$h_+ = \frac{1 + \cos^2 \theta_{\text{jn}}}{2D_L} e^{i\phi_o} h \quad (2)$$

$$h_\times = \frac{\cos \theta_{\text{jn}}}{D_L} e^{i(\phi_o + \pi/2)} h \quad (3)$$

where D_L is the luminosity distance to the source, θ_{jn} the angle between the source's total angular momentum and our line of sight, ϕ_o the orbital phase at coalescence, and h the intrinsic waveform generated by the source. If the recorded data's calibration is correct, then $\delta A = \delta\psi = 0$. Calibration errors are modeled as a



- (GW): GW data alone with loose calibration priors. We assume standard (uninformative) priors for all intrinsic and extrinsic parameters. In particular, we assume sources are uniformly distributed in volume ignoring local cosmological effects: $p(D_L) \propto D_L^2$.
- (GW+ D_L): loose calibration priors and the source's location constrained by the approximate uncertainty in NGC 4993's location. We assume conservative bounds of $D_L \in [32, 50]$ Mpc with $p(D_L) \propto D_L^2$.
- (GW+ $D_L+\theta_{jn}$): loose calibration priors using the EM constraint on the source location as well as approximate constraints on the source's inclination from EM observations. We again use somewhat conservative constraints of $\theta_{jn} \in [10^\circ, 30^\circ] \oplus [150^\circ, 170^\circ]$ while [30] suggests $14^\circ \leq \theta_{jn} \leq 28^\circ$ (see also [30, 31]).
- (*in-situ*): GW data alone but with the directly-measured calibration prior uncertainties [12, 32].

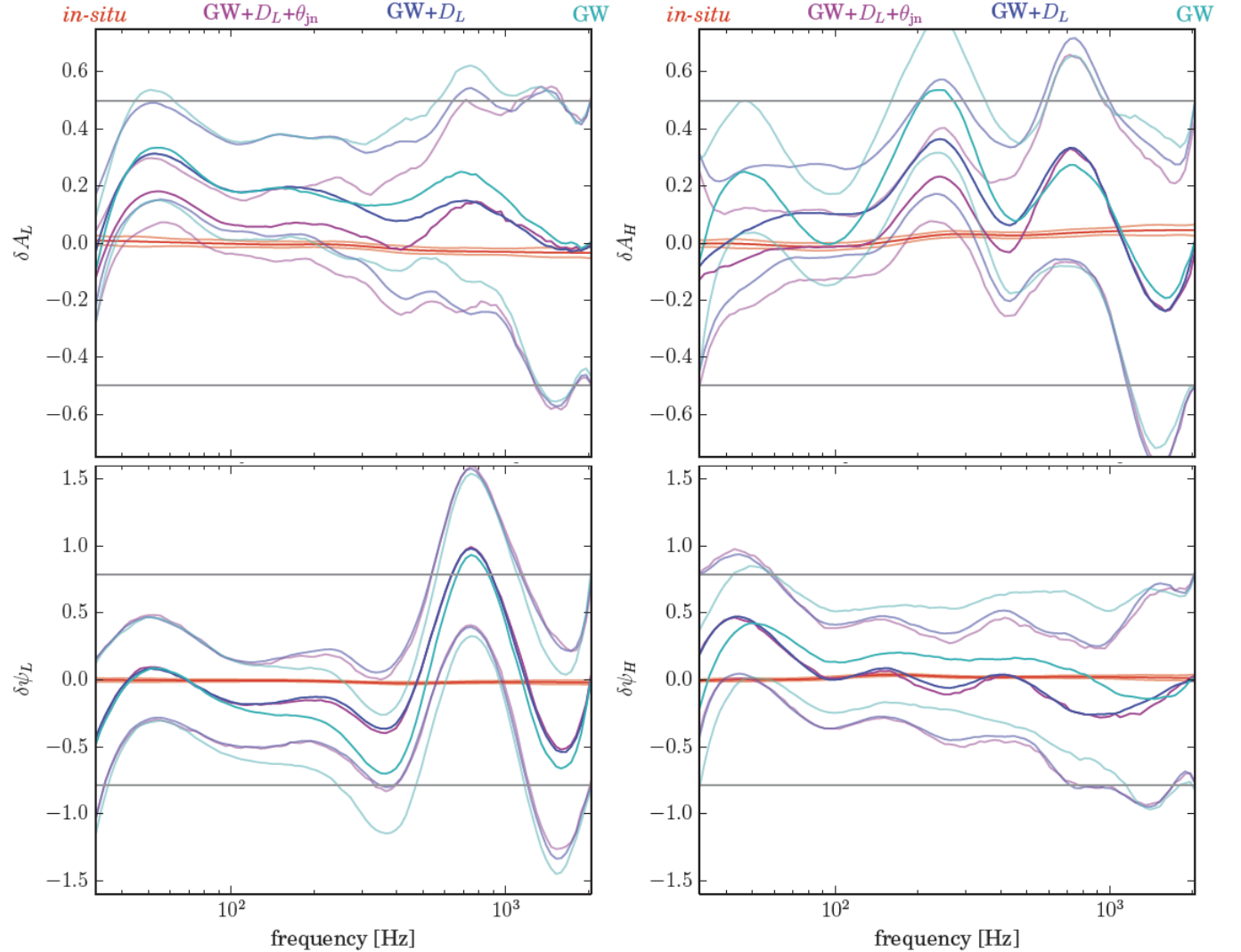
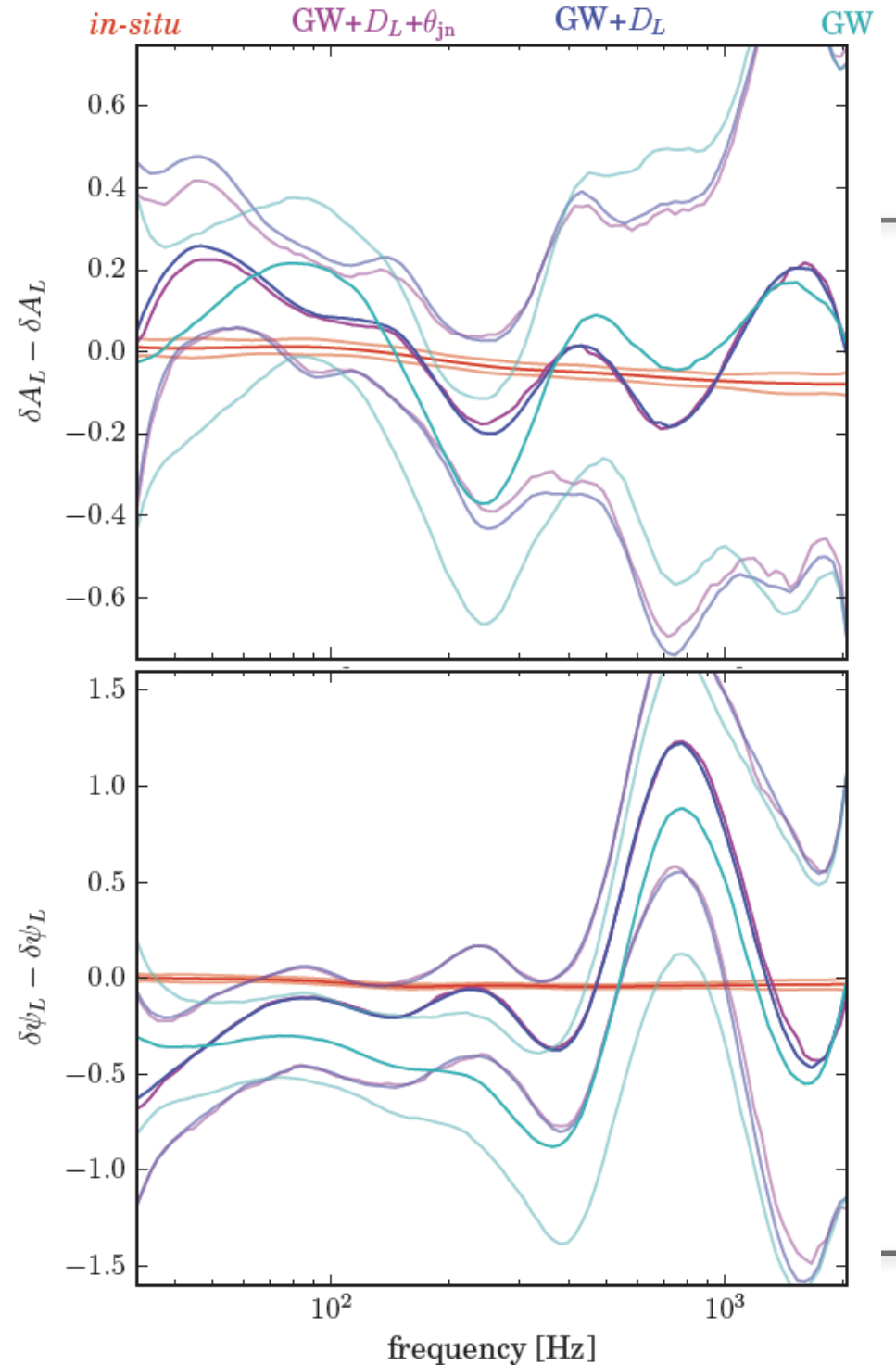


FIG. 2. Posterior processes for both absolute amplitude and phase calibration errors for the LIGO Livingston (*left*) and LIGO Hanford (*right*) detectors. Dark colored lines correspond to the median *a posteriori*; light colored lines correspond to the $1\text{-}\sigma$ *posterior* credible regions; grey lines correspond to $1\text{-}\sigma$ *prior* credible regions. We include results using the directly-measured calibration uncertainties (red: *in-situ*), wide calibration prior uncertainties with only GW data (light blue: GW), wide calibration priors and EM constraints on D_L (dark blue: GW+ D_L), and wide calibration priors and EM constraints on both D_L and θ_{jn} (purple: GW+ $D_L+\theta_{jn}$).



- (GW): GW data alone with loose calibration priors. We assume standard (uninformative) priors for all intrinsic and extrinsic parameters. In particular, we assume sources are uniformly distributed in volume ignoring local cosmological effects: $p(D_L) \propto D_L^2$.
- (GW+ D_L): loose calibration priors and the source's location constrained by the approximate uncertainty in NGC 4993's location. We assume conservative bounds of $D_L \in [32, 50]$ Mpc with $p(D_L) \propto D_L^2$.
- (GW+ $D_L+\theta_{jn}$): loose calibration priors using the EM constraint on the source location as well as approximate constraints on the source's inclination from EM observations. We again use somewhat conservative constraints of $\theta_{jn} \in [10^\circ, 30^\circ] \oplus [150^\circ, 170^\circ]$ while [30] suggests $14^\circ \leq \theta_{jn} \leq 28^\circ$ (see also [30, 31]).
- (*in-situ*): GW data alone but with the directly-measured calibration prior uncertainties [12, 32].

FIG. 3. Relative calibration between the Hanford and Livingston detectors; color schemes and naming conventions are identical to Figure 2. We note that, unlike in Figure 2, additional constraints on D_L and θ_{jn} only marginally impact our ability to measure the relative calibration between detectors.



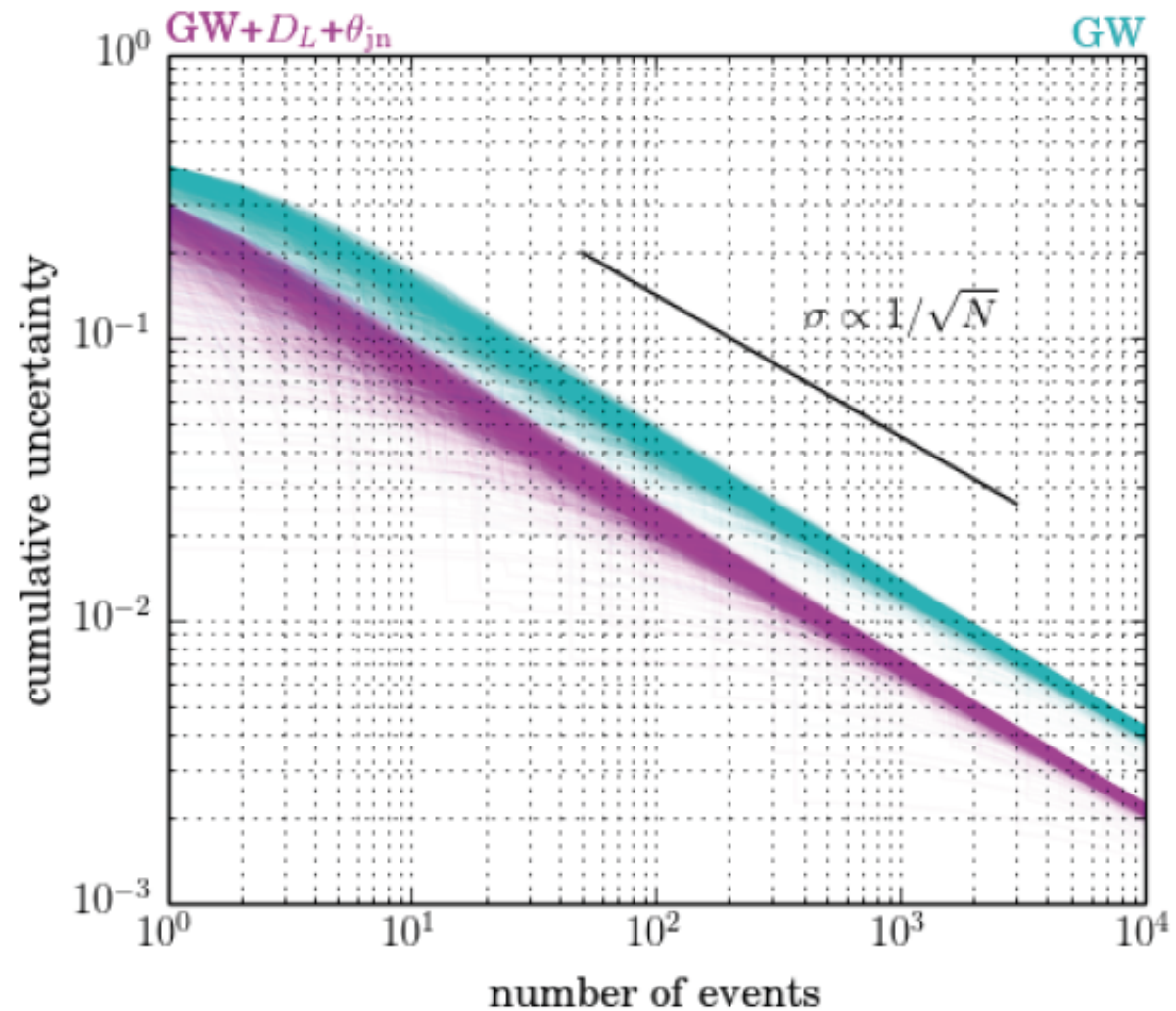
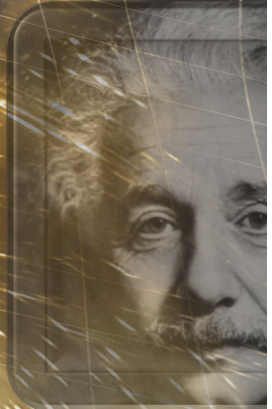


FIG. 6. Expected scaling of the cumulative amplitude uncertainty with a population of events. Each curve shows one realization of our simulation assuming parameters consistent with our wide calibration priors: (*light blue*: GW) relative calibration uncertainty with no EM constraints and (*purple*: GW+ $D_L+\theta_{jn}$) absolute uncertainty with both GW and EM constraints.

**Thank you very much
for your attention!**

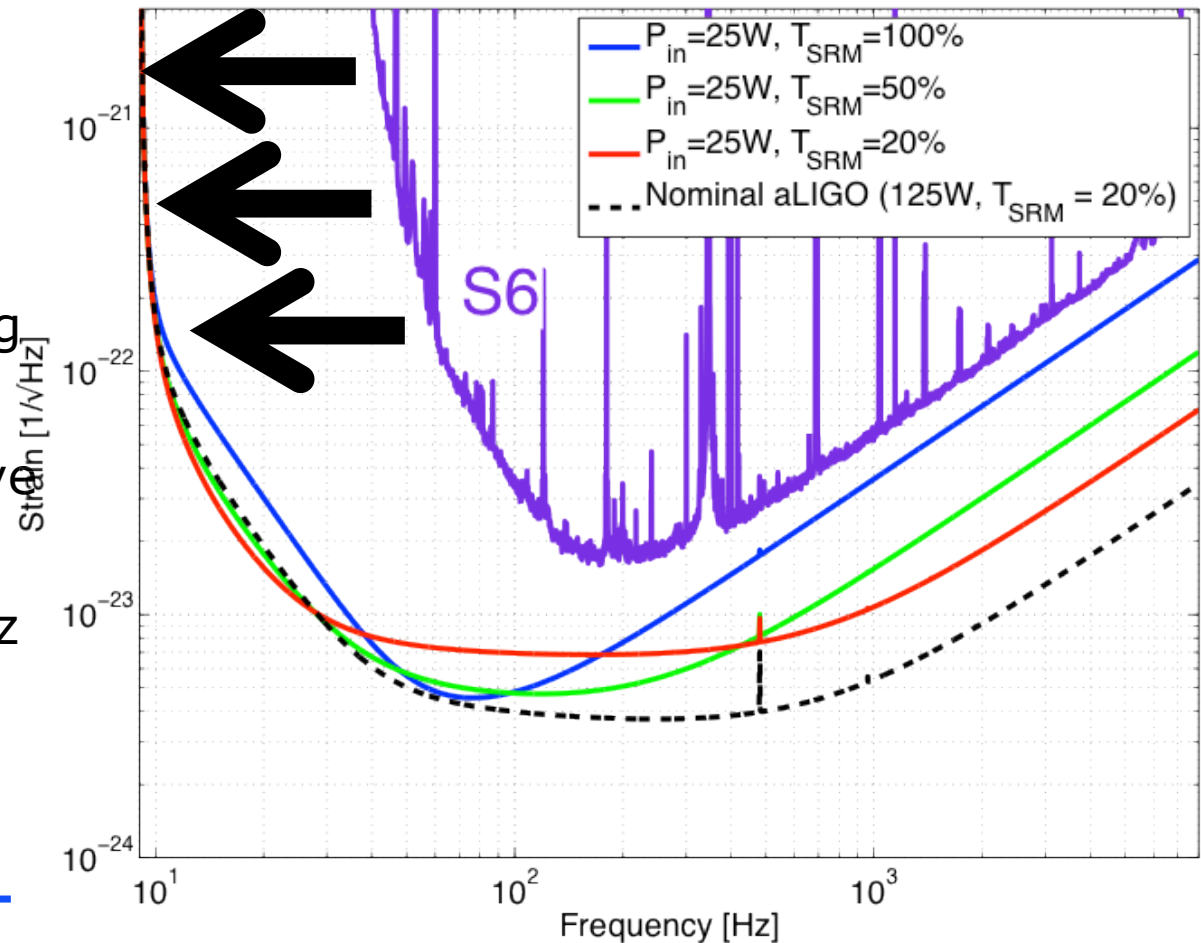




**Thanks very much for your
attention.**

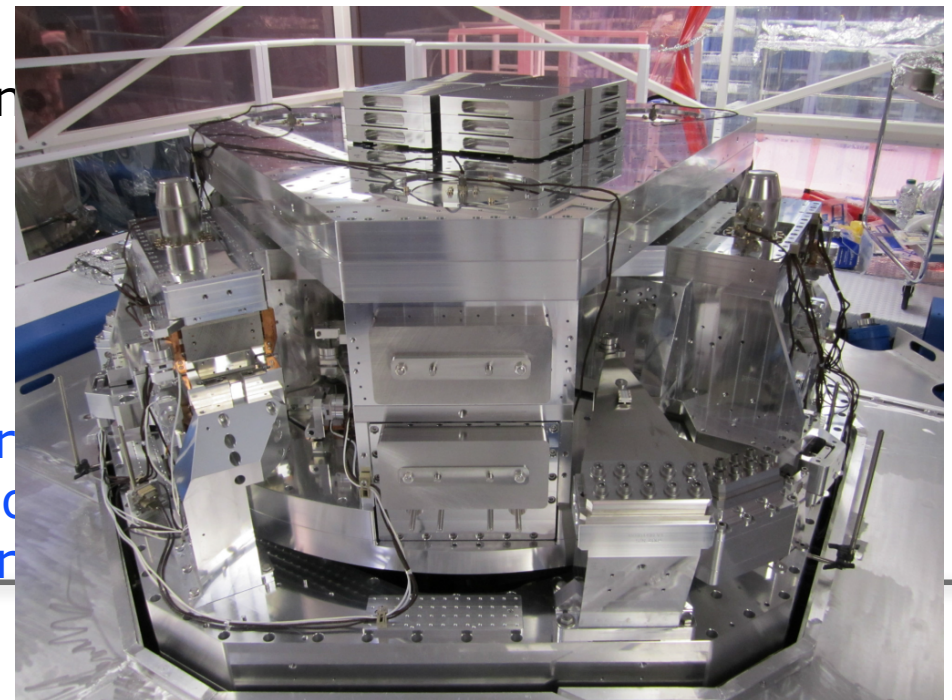
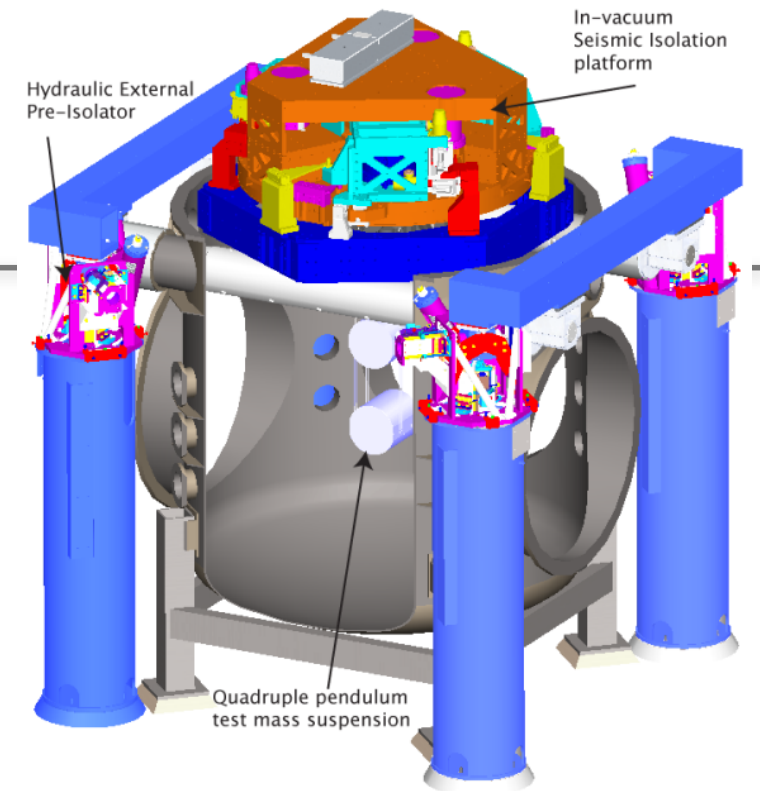
Addressing limits to performance

- **Seismic noise** – must prevent masking of GWs, enable practical control systems
- Motion from waves on coasts...and people moving around
- GW band: 10 Hz and above – direct effect of masking
- Control Band: below 10 Hz – forces needed to hold optics on resonance and aligned
- aLIGO uses **active servo-controlled platforms, multiple pendulums**



Seismic Isolation: Multi-Stage Solution

- Objectives:
 - Render seismic noise a negligible limitation to GW searches
 - Reduce actuation forces on test masses
- Both suspension and seismic isolation systems contribute to attenuation
- Choose an active isolation approach, 3 stages of 6 degrees-of-freedom :
 - 1) Hydraulic External Pre-Isolation
 - 2) Two Active Stages of Internal Seismic Isolation
- Low noise sensors (position, velocity, acceleration) are combined, passed through a servo amplifier, and delivered to the optimal actuator as a function of frequency to hold platform still in inertial space



- ➔ Due to thermal fluctuations the position of the mirror sensed by the laser beam is not necessarily a good representation of the center of mass of the mirror.
- ➔ Various noise terms involved: Brownian, thermo-elastic and thermo-refractive noise of each substrate and coating (or coherent combinations of these, such as thermo-optic noise).
- ➔ For nearly all current and future designs coating Brownian is the dominating noise source:

$$S_x(f) = \frac{4k_B T}{\pi^2 f Y} \frac{d}{r_0^2} \left(\frac{Y'}{Y} \phi_{\parallel} + \frac{Y}{Y'} \phi_{\perp} \right)$$

PSD of displacement
 Boltzmann constant
 Temperature
 Geometrical coating thickness
 Loss angle of coating
 Young's modulus of mirror substrate
 laser beam radius
 Young's modulus of coating

Harry et al, CQG 19, 897–917, 2002



How to reduce Mirror Thermal Noise?

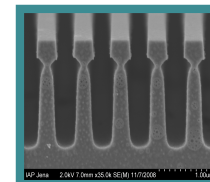


Improved coating materials (e.g. crystalline coatings like AlGaAs, GaPAs)

Cole et al, APL 92, 261108, 2008

Waveguide mirrors

Brueckner et al, Opt. Expr 17, 163, 2009
PhD thesis of D.Friedrich



Cryogenic mirrors (120K)

Cryogenic mirrors (10-20K)

Uchiyama et al, PRL 108, 141101 (2012)

Khalili cavities

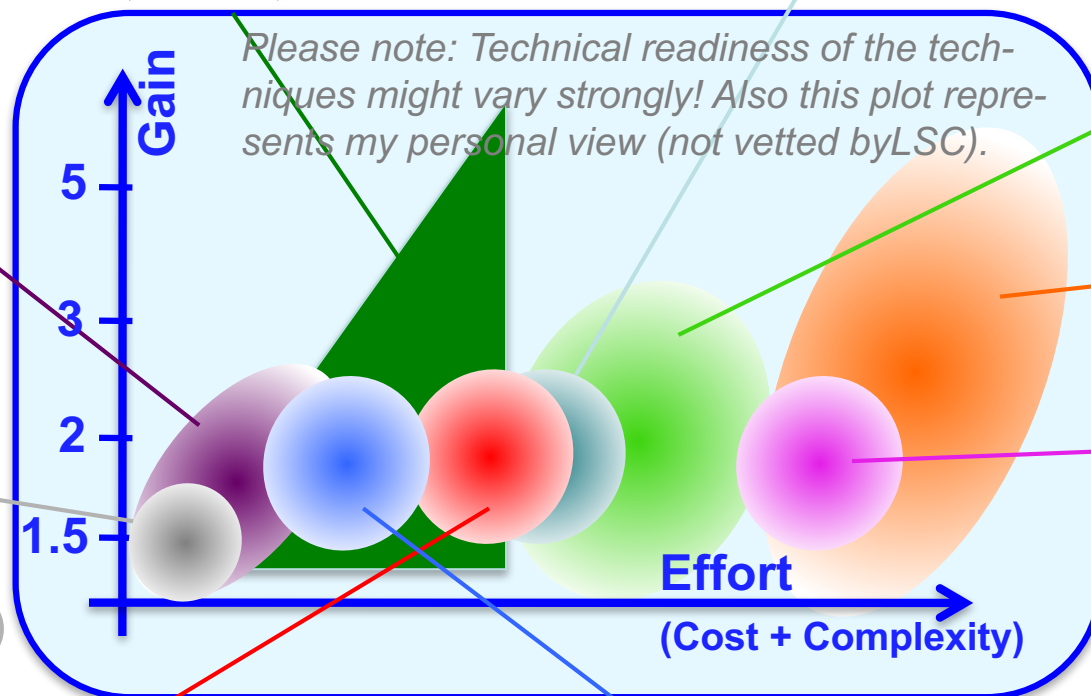
Khalili, PLA 334, 67, 2005
Gurkovsky et al, PLA 375, 4147, 2011

Larger beam size (needs larger mirrors)

Harry et al, CQG 19, 897-917, 2002

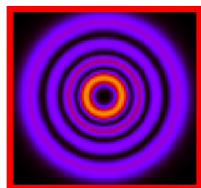
Optimisation

(annealing, layer thickness, doping)



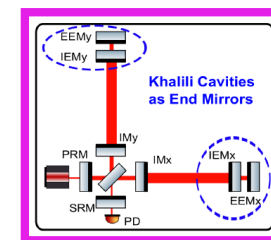
Different beam shape

Mours et al, CQG, 2006, 23, 5777
Chelkowski et al, PRD, 2009, 79, 122002



Amorphous Silicon coatings

Liu et al, PRB 58, 9067, 1998



PSD of displacement

$$x^2(\omega) = \frac{4k_B T \omega_0^2 \phi(\omega)}{\omega m [(\omega_0^2 - \omega^2)^2 + \omega_0^4 \phi^2(\omega)]}$$

Boltzmann constant

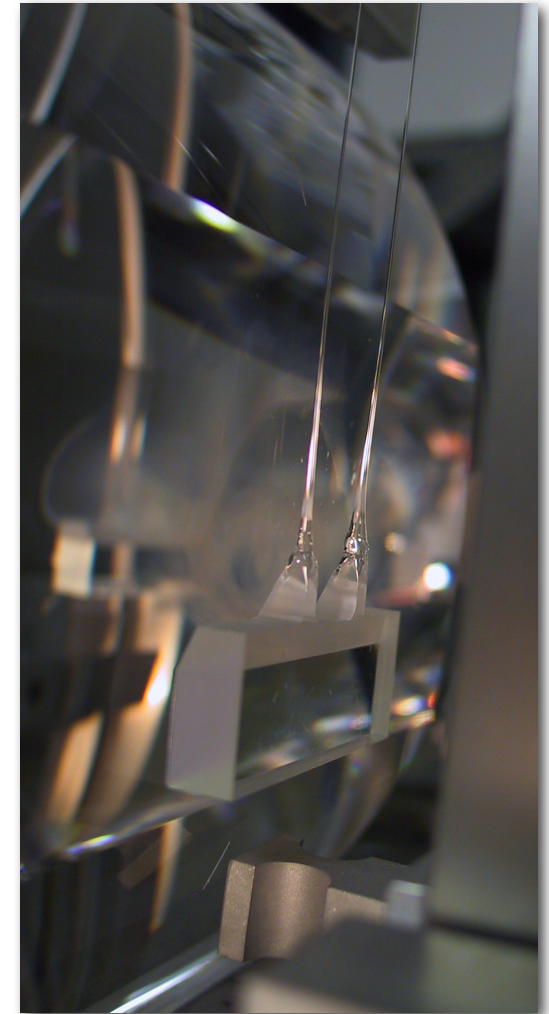
Temperature

Loss angle

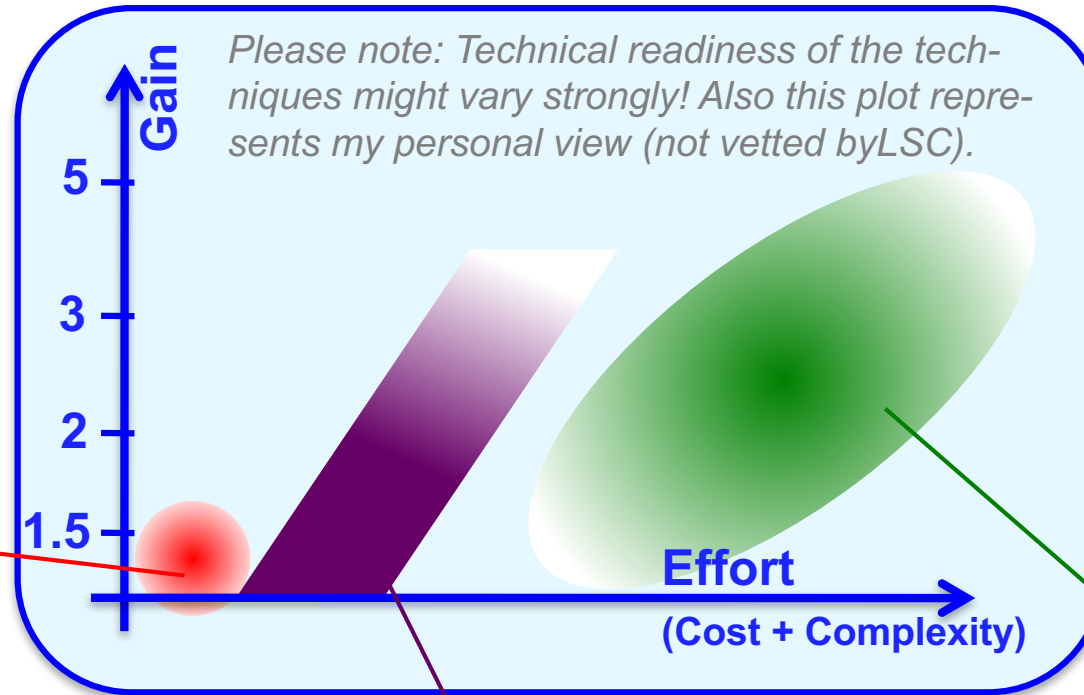
Mirror mass

Resonance frequency

- ➔ Mirrors need to be suspended in order to decouple them from seismic.
- ➔ Thermal noise in metal wires and glass fibres causes horizontal movement of mirror.
- ➔ Relevant loss terms originate from the bulk, surface and thermo-elastic loss of the fibres + bond and weld loss.
- ➔ Thermal noise in blade springs causes vertical movement which couples via imperfections of the suspension into horizontal noise.



How to reduce Suspension Thermal Noise?



Improve fibre geometry/profile

Bending points, energy stored via bending and neck profile can be potentially further optimised.

Increase length of final pendulum stage.

Allows the push suspension thermal noise out detection band.

Cooling of the suspension to cryogenic temperatures.

Usually also requires a change of materials.

Gravity Gradient Noise (also referred to as Newtonian)

- ➔ Seismic causes density changes in the ground and shaking of the mirror environment (walls, buildings, vacuum system).
- ➔ These fluctuations cause a change in the gravitational force acting on the mirror.
- ➔ Cannot shield the mirror from gravity. ☹️

Coupling constant (depends on type of seismic waves, soil properties, etc)

Gravitational constant

Density of ground

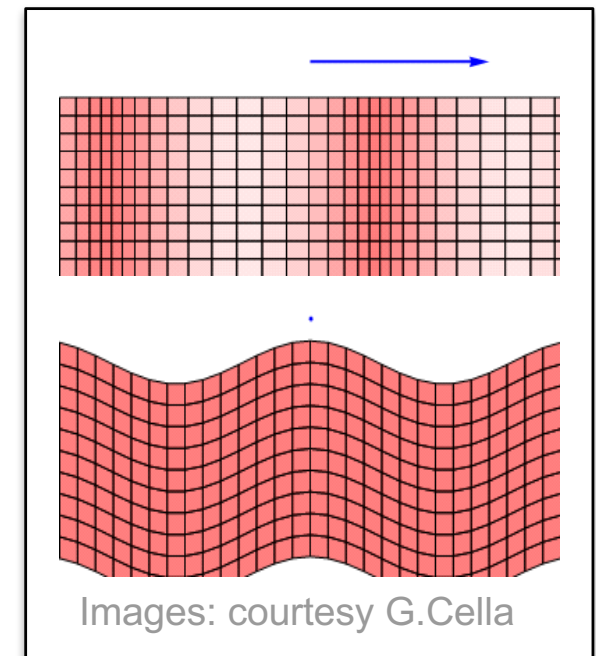
PSD of strain

$$N_{GG}(f)^2 = \frac{4 \cdot \beta^2 \cdot G^2 \cdot \rho_r^2}{L^2 \cdot f^4} \cdot X_{seis}^2$$

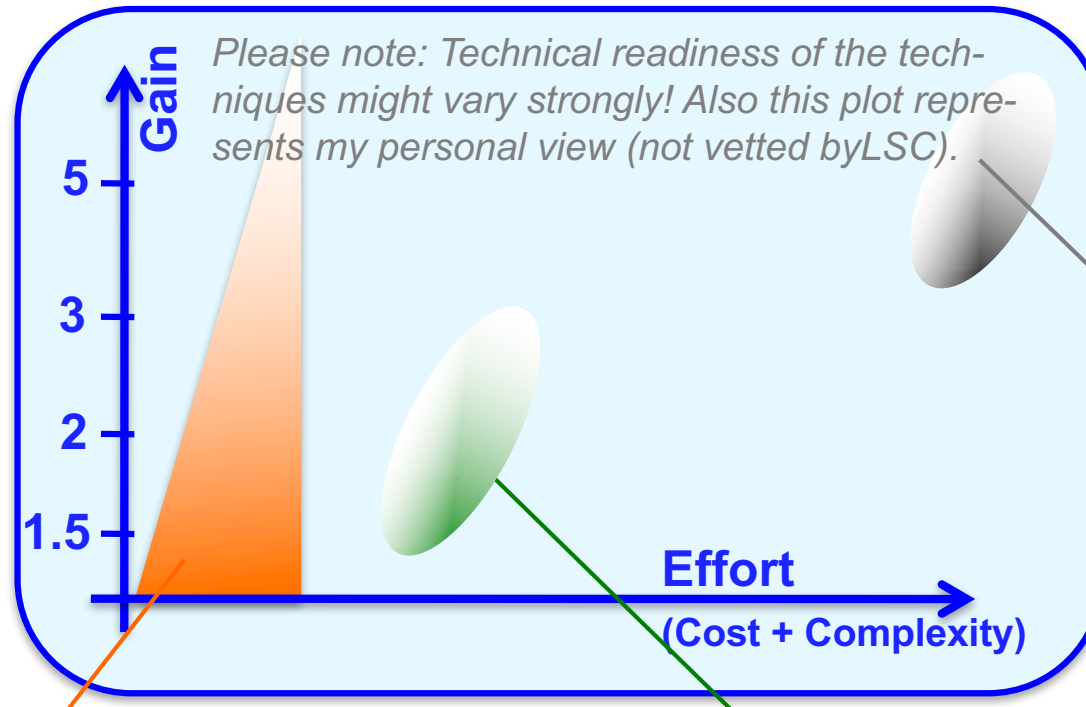
Arm length

frequency

PSD of seismic



How to reduce Gravity Gradient Noise?



Reduce seismic noise at site., i.e. select a quieter site, potentially underground.

Beker et al, Journal of Physics: Conference Series 363 (2012) 012004

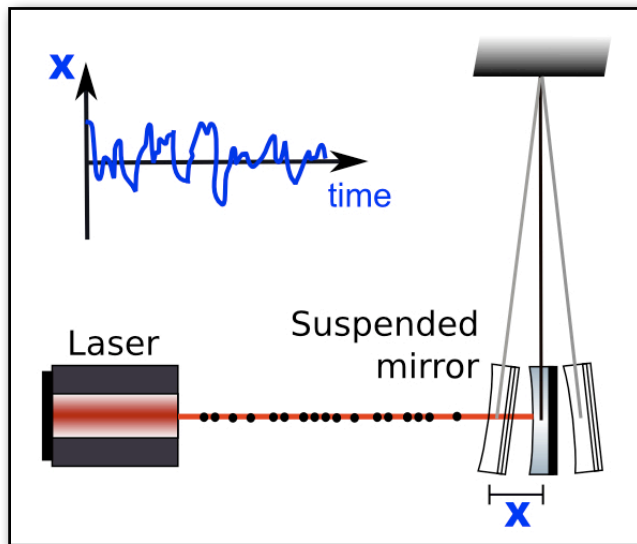
Subtraction of gravity gradient noise using an array of seismometers.

- Beker et al: General Relativity and Gravitation Volume 43, Number 2 (2011), 623-656
- Driggers et al: arXiv:1207.0275v1 [gr-qc]

Shaping local topography

- Harms et al, CQG Volume 31, Number 18, 2014

- ➔ Quantum noise is a direct manifestation of the **Heisenberg Uncertainty Principle**.
- ➔ It is comprised of **photon shot noise (sensing noise)** at high frequencies and **photon radiation pressure noise (back-action noise)** at low frequencies.

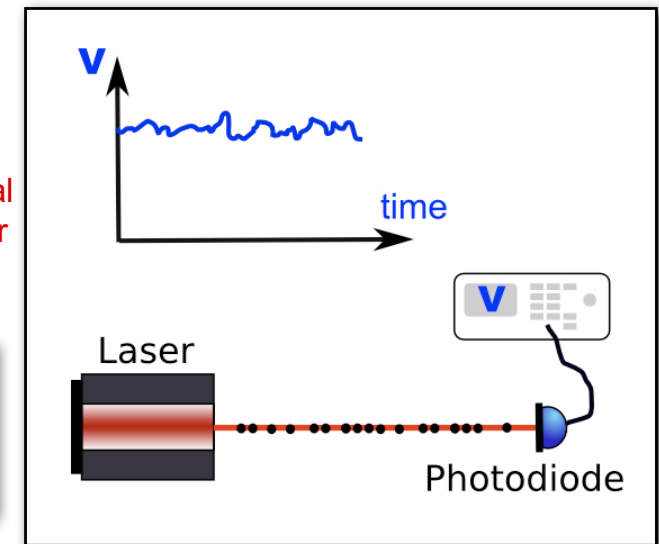


$$h_{\text{sn}}(f) = \frac{1}{L} \sqrt{\frac{\hbar c \lambda}{2\pi P}}$$

wavelength (points to λ)
optical power (points to P)
Arm length (points to L)

$$h_{\text{rp}}(f) = \frac{1}{m f^2 L} \sqrt{\frac{\hbar P}{2\pi^3 c \lambda}}$$

Mirror mass (points to m)



photon radiation pressure noise

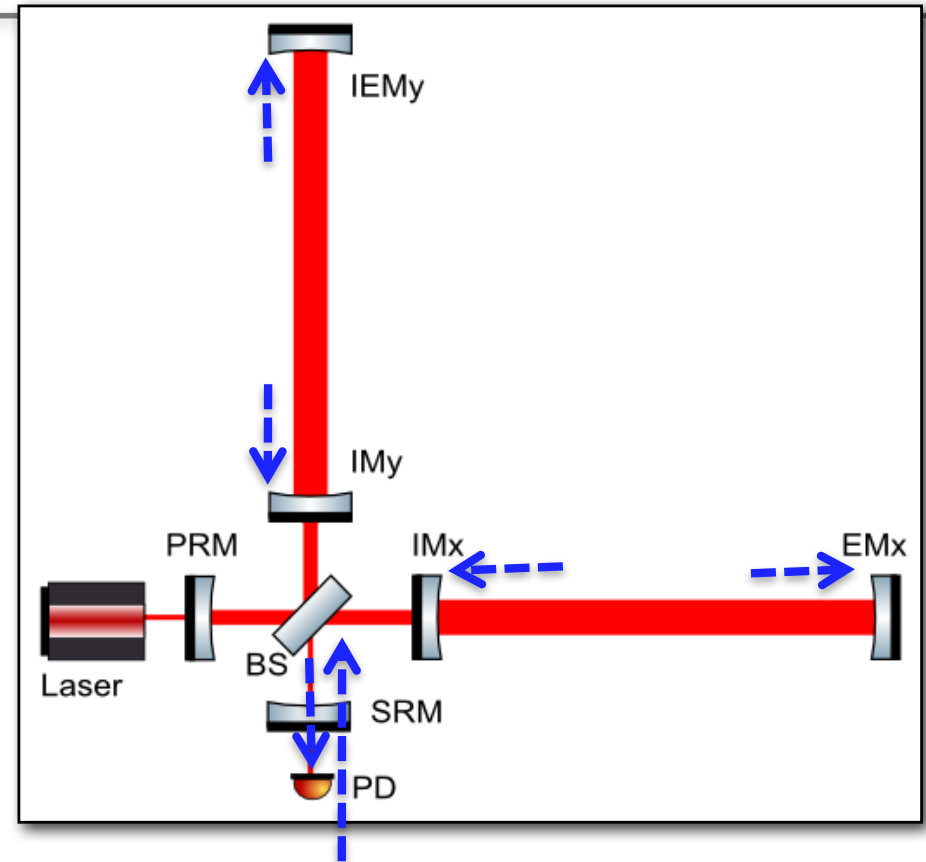
photon shot noise



Vacuum fluctuations

Quantum noise can also be understood as vacuum fluctuations entering the interferometer via any open port:

- ➔ Fluctuations reflected from interferometer detected a photo-detector as shot noise
- ➔ Fluctuations acting on mirrors cause radiation pressure noise



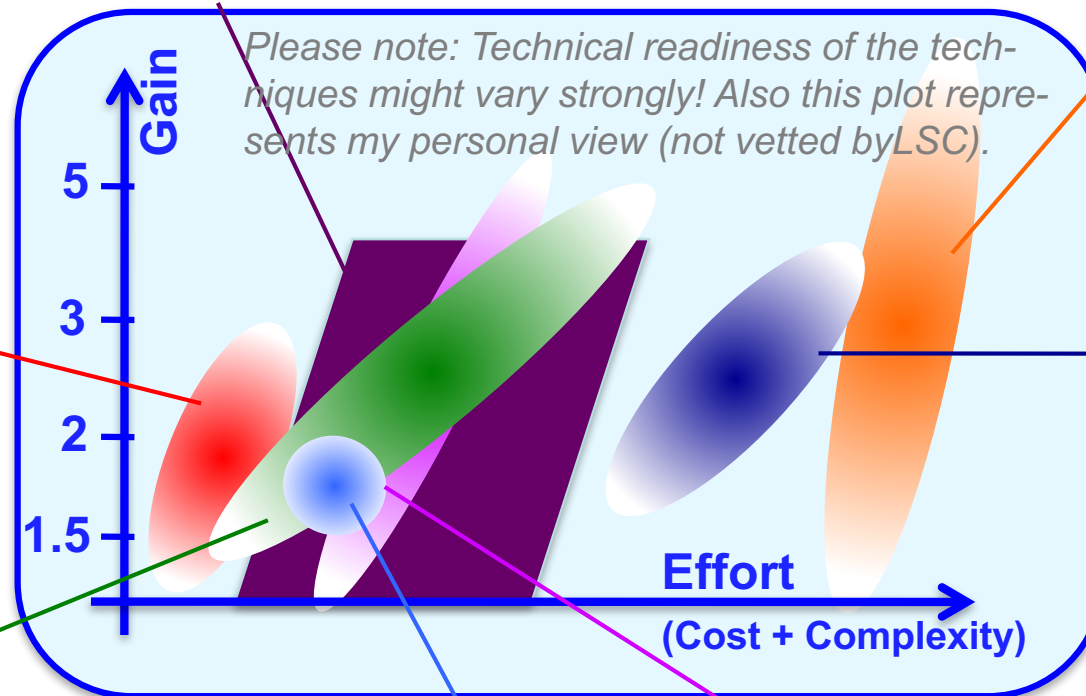
Vacuum fluctuations

Squeezing with frequency dependent squeezing angle

Kimble et al, PRD 65, 2002

Speedmeter

Measures momentum of test masses and is therefore not susceptible to Heisenberg Uncertainty Principle.
Chen, PRD 67, 122004, 2003



Squeezed Light

LIGO Scientific collaboration, Nature Phys. 7 962–65, 2011

Increased Laser Power

Need to deal with thermal problems and instabilities

Local readout

Rehbein et al, PRD 78, 062003, 2008

Increased Mirror Weight

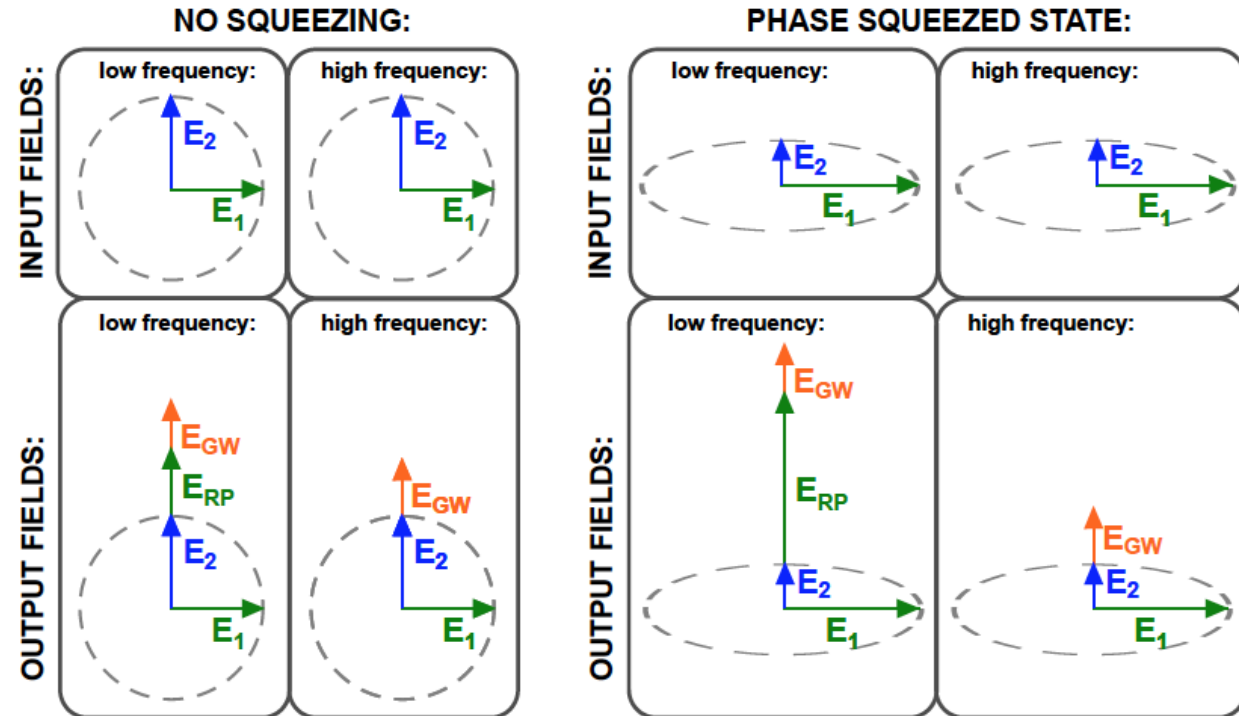
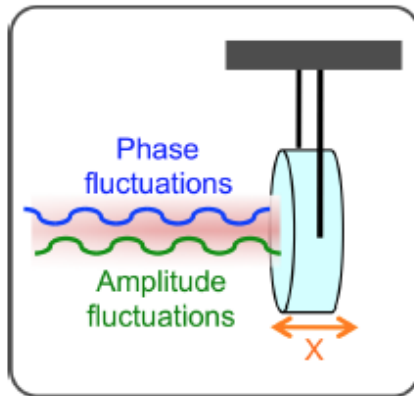
Need to deal with thermal problems and instabilities

Optical Bar + Optical Lever

Khalili, PLA 298, 308-14, 2002



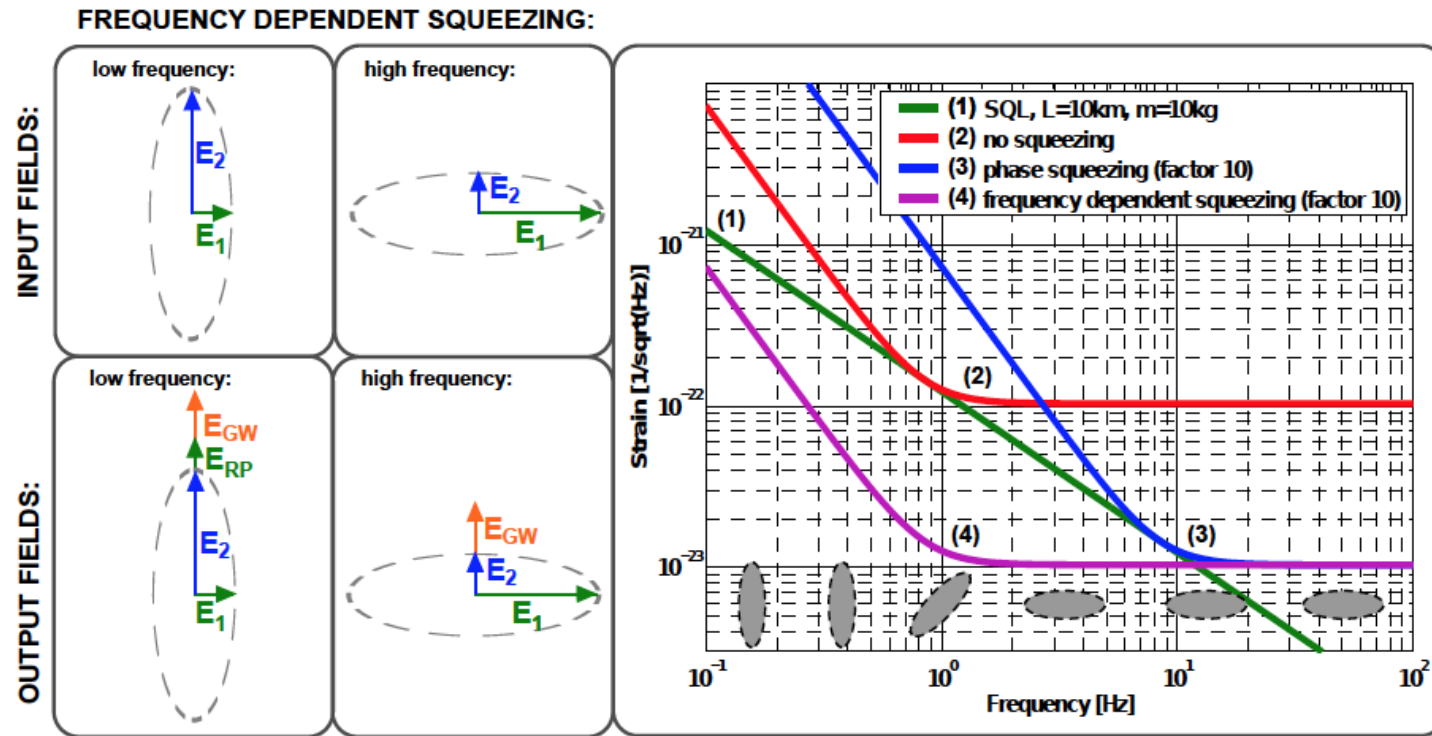
Why do we need a frequency dependent squeezing angle?



- Frequency independent squeezing can only improve sensitivity at one end of the spectrum (phase squeezing improves shot noise, amplitude squeezing improves radiation pressure noise), while it degrades sensitivity at the other end of the spectrum.



Frequency Dependent Squeezing

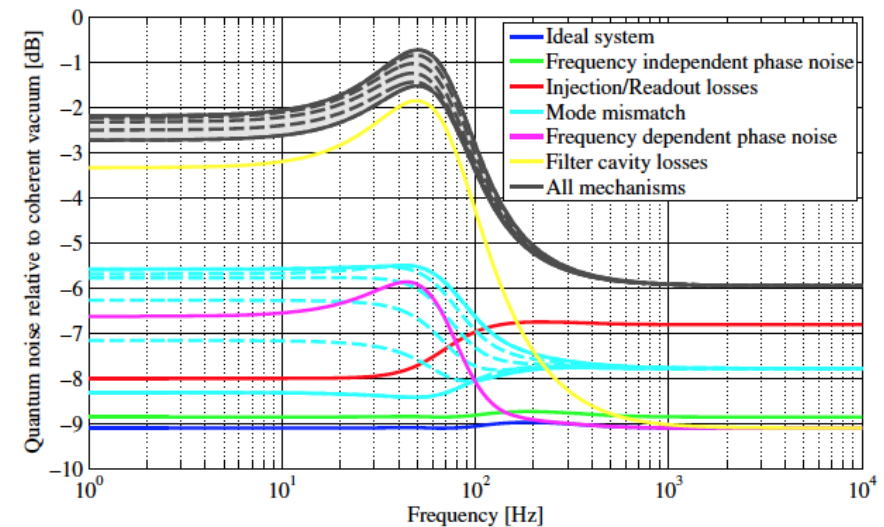
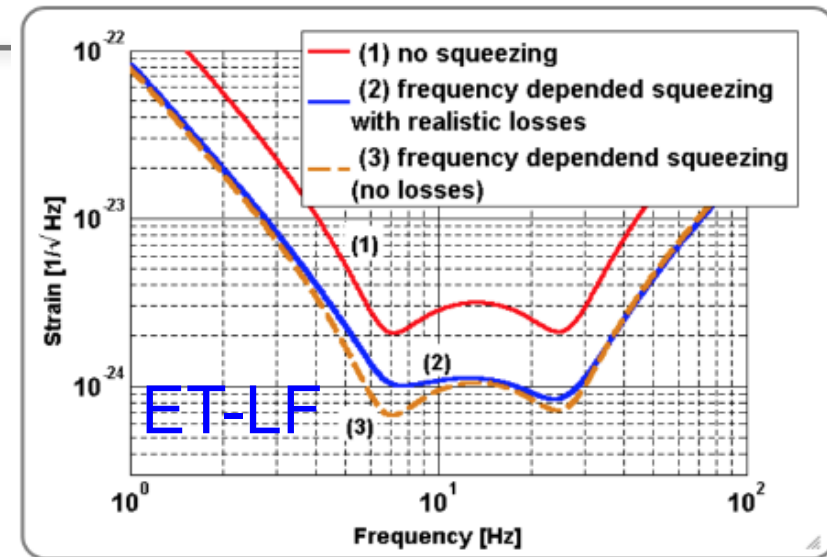


- ➔ Frequency dependent squeezing angle allows to obtain **broadband quantum noise suppression**.
- ➔ Use **dispersion in reflection of a cavity** to realise frequency dependent rotation of squeezing angle. Chelkowski et al. PRA 71, 013806, 2005



Filter Cavity Considerations

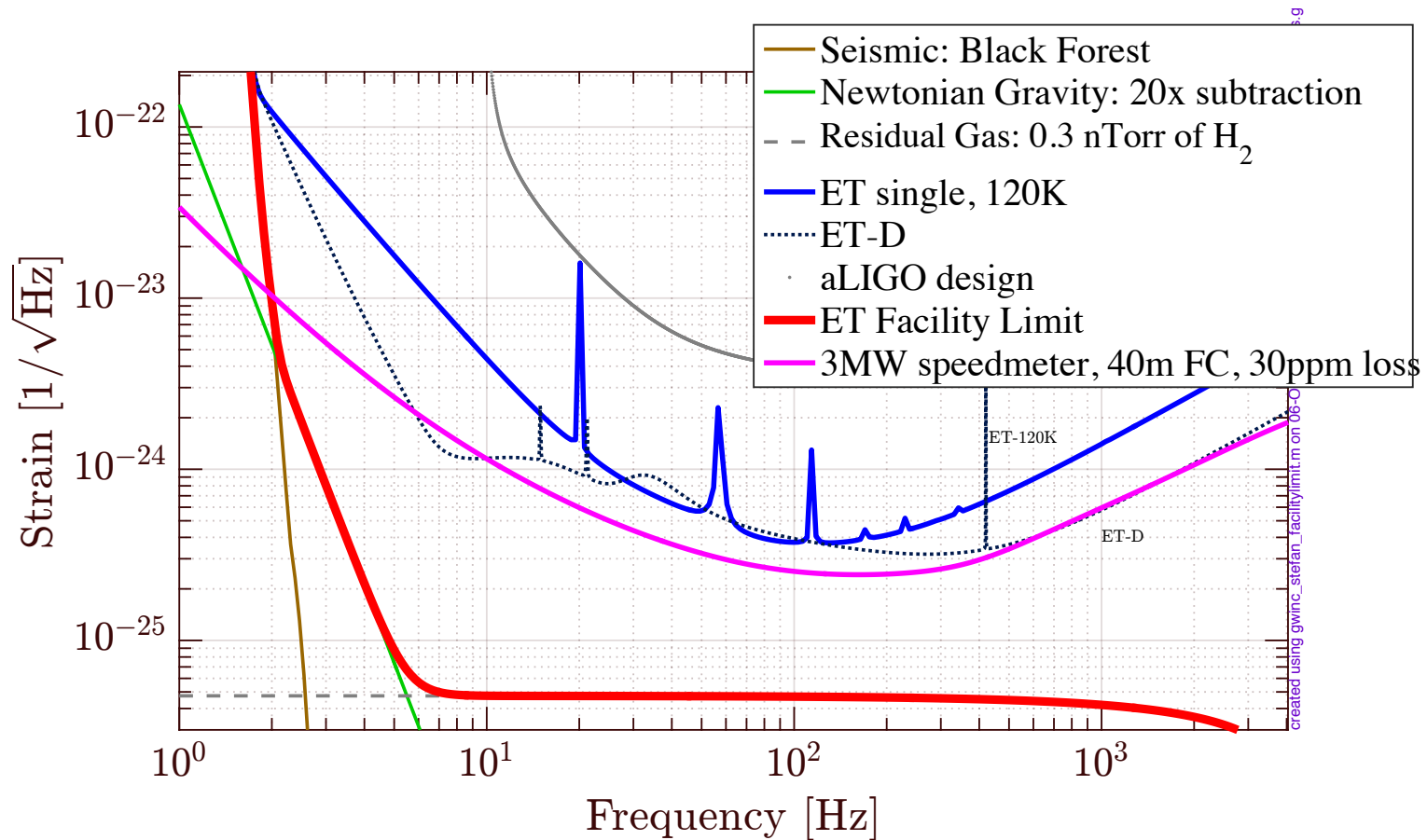
- ➔ Obtainable squeezing factor not limited by squeezing factor of squeezing sources.
- ➔ Achievable quantum noise reduction limited by losses of squeezing encounter in injection path and filter cavity.
- ➔ Extremely low losses in filter cavity are vital.
- ➔ Requires low cavity linewidth (product of cavity length and Finesse needs to be large).
- ➔ For detuned RSE one loses most squeezing on resonance.



Kwee et al.: PRD 90, 062006 (2014)



Example a of a more ambitious single detector sensitivity





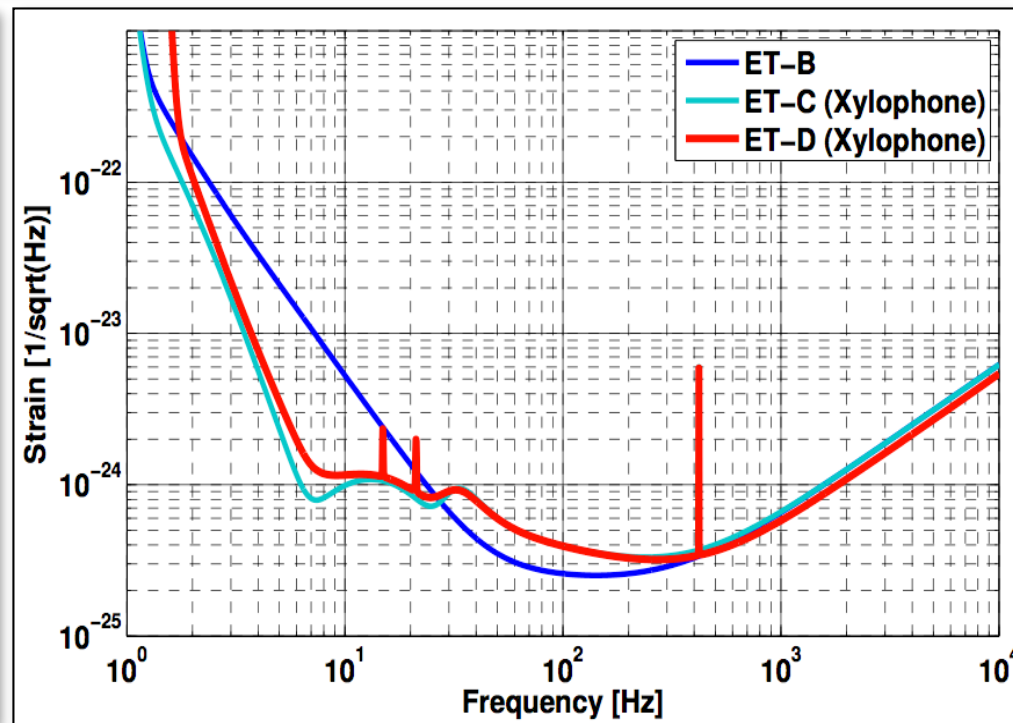
Future Detector Parameters

IFO Cases	aLIGO	A+	Voyager	CE (pess)	CE	ET LF	ET HF
Arm Length [km]	4	4	4	40	40	10	10
Mirror Mass [kg]	40	40	200	320	320	211	200
Mirror Material	Silica	Silica	Silicon	Silica	Silicon	Silicon	Silica
Mirror Temp [K]	295	295	123	295	123	10	290
Sus Fiber	0.6m SiO ₂	0.6m SiO ₂	0.6m Si	1.2m SiO ₂	1.2m Si	2m Si	0.6m SiO ₂
Fiber Type	Fiber	Fiber	Ribbon	Fiber	Ribbon	Fiber	Fiber
Input Power [W]	125	125	140	150	220	3	500
Arm Power [kW]	710	750	3000	1400	2000	18	3000
Wavelength [nm]	1064	1064	2000	1064	1550	1550	1064
NN Suppression	1	1	10	10	10	1	1
Beam Size [cm]	5.5 / 6.2	5.5 / 6.2	5.8 / 8.4	12 / 12	14 / 14	9 / 9	12 / 12
SQZ Factor [dB]	0	6	8	10	10	10	10
F. C. Length [m]	none	300	300	4000	4000	10000	500



ET Sensitivity evolution

Parameter	ET-D-HF	ET-D-LF
Arm length	10 km	10 km
Input power (after IMC)	500 W	3 W
Arm power	3 MW	18 kW
Temperature	290 K	10 K
Mirror material	Fused silica	Silicon
Mirror diameter / thickness	62 cm / 30 cm	min 45 cm/ TBD
Mirror masses	200 kg	211 kg
Laser wavelength	1064 nm	1550 nm
SR-phase	tuned (0.0)	detuned (0.6)
SR transmittance	10 %	20 %
Quantum noise suppression	freq. dep. squeez.	freq. dep. squeez.
Filter cavities	1 × 10 km	2 × 10 km
Squeezing level	10 dB (effective)	10 dB (effective)
Beam shape	LG ₃₃	TEM ₀₀
Beam radius	7.25 cm	9 cm
Scatter loss per surface	37.5 ppm	37.5 ppm
Partial pressure for H ₂ O, H ₂ , N ₂	10 ⁻⁸ , 5 · 10 ⁻⁸ , 10 ⁻⁹ Pa	10 ⁻⁸ , 5 · 10 ⁻⁸ , 10 ⁻⁹ Pa
Seismic isolation	SA, 8 m tall	mod SA, 17 m tall
Seismic (for $f > 1$ Hz)	5 · 10 ⁻¹⁰ m/f ²	5 · 10 ⁻¹⁰ m/f ²
Gravity gradient subtraction	none	none



- ➔ Data from ET-LF and ET-HF can be coherently or incoherently be added, depending on the requirements of the analysis.
- ➔ Sensitivity data available for download at: <http://www.et-gw.eu/etsensitivities>
- ➔ For more details please see S.Hild et al: 'A Xylophone Configuration for a third Generation Gravitational Wave Detector', CQG 2010, 27, 015003 and S.Hild et al: 'Sensitivity Studies for Third-Generation Gravitational Wave Observatories', CQG 2011, 28 094013.